NOTICE

The quality of this microform is heavily dependent upon the quality of the original thesis submitted for microfilming. Every effort has been made to ensure the highest quality of reproduction possible.

If pages are missing, contact the university which granted the degree.

Some pages may have indistinct print especially if the original pages were typed with a poor typewriter ribbon or if the university sent us an inferior photocopy.

Previously copyrighted materials (journal articles, published tests, etc.) are not filmed.

Reproduction in full or in part of this microform is governed by the Canadian Copyright Act, R.S.C. 1970, c. C-30.

AVIS

La qualité de cette microforme dépend grandement de la qualité de la thèse soumise au microfilmage. Nous avons tout fait pour assurer une qualité supérieure de reproduction.

S'il manque des pages, veuillez communiquer avec l'université qui a conféré le grade.

La qualité d'impression de certaines pages peut laisser à désirer, surtout si les pages originales ont été dactylographiées à l'aide d'un ruban usé ou si l'université nous a fait parvenir une photocopie de qualité inférieure.

Les documents qui font déjà l'objet d'un droit d'auteur (articles de revue, tests publiés, etc.) ne sont pas microfilmés.

La reproduction, même partielle, de cette microforme est soumise à la Loi canadienne sur le droit d'auteur, SRC 1970, c. C-30.

Canada

ISBN 0-315-40750-6

UNIVERSITÉ D'OTTAWA
UNIVERSITY OF OTTAWA

ACKNOWLEDGEMENTS

I would like to thank Professor Brian Conway for his patience during the sometimes difficult times that were encountered over these years.

I would also like to thank David Tessier, Viola Birss, Brian Barnett, Erol Ayranci, Carl Tripp, David Wilkinson and Richard MacFarlane for their productive conversations during my tenure in Ottawa; their willingness to discuss various topics led to a better understanding of my project. The conversations with Professors Durst, Milne and Detellier, and with Professor Woolley in the Physics Department were also very helpful, thank you.

A debt of gratitude is owed to the faculty and staff of the Chemistry department of Brandeis University (Waltham, MA). Without their having thrown their doors open to me this work would never have been completed. In particular I would like to express my gratitude to Professors Colin Steel, Ernest Grunwald and Bruce Foxman who provided me with facilities, discussion and motivation. Thanks also to Professors Stuhl and Stolzenberg for their helpful discussions.

I would like to express my gratitude to Cliff Watkins, Matt Stershic, Sandy Burr, Leo Martin, Stanley Richter and to my sister Julie and her husband, Richard for changing my attitude about this project.

Last, but not least, I would like to express my deepest gratitude to my Canadian "family", the vanEs family of Regina, whose patience, understanding and support have helped to transform my life.

ABSTRACT

The general aims of the work reported in this thesis were to examine the relationship between charge-transfer and mass-transport at two similar intercalating interfaces, TiS_2 and $TiSe_2$. In addition, the role of the solvent/solute on the interfacial process was to be discussed in comparison with other works. The solvent — 2-methyl-tetrahydrofuran — was chosen because of its low reactivity and because of the observed cycling efficiencies of both the lithium and TiS_2 electrodes in electrolytes based upon this solvent. $TiSe_2$ was also used as a host material. $TiSe_2$ has a similar ionicity to TiS_2, but has a larger van der Waals gap between the layers and larger octahedral sites for the guest species to occupy. Much attention was paid to the preparation of components and to the properties of the electrolyte solution. Preparative methods for both the electrolyte solution and for the host materials is discussed in detail.

Results of the electrolytic conductance measurements are discussed in terms of both ion-pairing and triple-ion formation. The results for the ^7Li-NMR chemical shift measurements are discussed in terms of ion-pairing only.

Chronoamperometry was used to investigate the nature of the charge-transfer/mass-transport processes at the solution/host interface for these systems. The mechanisms and limitations of the interfacial reaction are discussed in terms of a particulate electrode model.

The opportunity also existed to utilize a new non-linear least-squares program which more realistically accounts for the uncertainty of measurement than most programs of this type.

TABLE OF CONTENTS

LIST OF FIGURES

LIST OF TABLES

CONTRIBUTIONS TO ORIGINAL RESEARCH

1. The methods of solvent and electrolyte preparation and analysis have been thoroughly reviewed. I believe that the methods outlined herein represent the most rigorous techniques reported for electrolytes based upon 2MeTHF.
2. For low dielectric constant solvents, where the solvent correction may be as high as the electrolytic conductance, the measurement of conductance at low concentrations (e.g., $<10^{-4}$ M) is not practical and mathematical analysis by techniques that are based solely upon ion-pairing is shown to be meaningless and incorrect.
3. The ionic interaction term that is used in the Fuoss-Kraus equation was found to be inadequate. A new term should be developed which accounts for viscosity changes, dielectric constant changes and ion-pair activity in the relatively concentrated solutions that are used.
4. The diffusion coefficients and heterogeneous rate constants for Li^+ intercalation into TiS_2 and $TiSe_2$ from $LiCF_3SO_3$/2MeTHF solutions have been determined by chronoamperometry. The values obtained for D_{Li^+} in TiS_2 appear to be solvent dependent.
5. Very little co-intercalation of 2MeTHF was observed for either system. This is in contrast to the observed results when DMF and DME are used as solvents. The

lesser role of 2MeTHF in the intercalation process is attributed to a difference in the donicities of the solvents used (solvents which either solvate Li^+ strongly or have a large base-strength will tend to co-intercalate). The longer cycle-life observed for Li^+ intercalation cells based upon 2MeTHF was attributed to the lack of solvent involvement at this interface.

6. A computer program was developed (with others) that performs a non-linear least-squares fit and more realistically accounts for experimental uncertainty in the parameters that are obtained in the fit.

INTRODUCTION

The reaction of intercalation of Li^+ into layer-lattice compounds offers a new source of solid-state materials and electrochemical devices to the market. The reaction can be performed chemically, or with more control, electrochemically. The nature of the interface of layer-lattice compounds is much different from that of other types of solid electrodes, and the properties of the electrode during the reaction are a hybrid of the behavior of other electrode types. For example, the electrode has some of the properties of a membrane electrode in that mobile charge carriers, both positive and negative, are active on both sides of the interface; the electrode also behaves in a manner similar to a metal deposition electrode in that as a new phase is formed, the activity of the electrode and its surface area change.

Several authors have worked on the interfacial properties and intercalation mechanisms with mixed results. For these systems there are *no standard methods* of electrode preparation - a situation which precludes the unambiguous investigation of the interface. Chronoamperometry measurements bypass some of these difficulties to give a quantitative measure of the rate of charge-transfer with respect to solid-state diffusion. This method does not critically depend upon the method that is used to prepare the electrode (preparation of

the electrode material itself is another matter) but this "advantage" does not allow for a complete mechanistic study which really requires a well defined (e.g., single-crystal) electrode surface.

In these systems, the role of the solvent cannot be underestimated. Lewis base incorporation by layered host structures is well known and the intercalation of large solvated species is known to occur with certain solvents.

The first chapter investigates the electrolyte solution. A detailed explanation for the choice of each component is presented. Then, a rigorous regime of purification and preparation is outlined. The properties of the electrolyte solution are characterized through electrolytic conductance and NMR chemical shift measurements. The data are analyzed in terms of ion-association.

The second chapter examines the host materials from both a synthetic and structural viewpoint. The procedures for consistently producing "electrochemically active" host materials are developed.

In the final chapter the problem of putting these two systems together to form an electrochemical cell and the subsequent evaluation of the charge-transfer/mass-transport processes in the chosen systems, is examined.

THE ELECTROLYTE SOLUTION

INTRODUCTION

Classical investigations of chemical reactions and physical properties in solution have taken place primarily in aqueous solutions. As a result of this predominance of aqueous-based studies, the physicochemical data available in the literature for aqueous electrolyte solutions have been much more precise; witness the treatises and monographs that have been devoted to water. Solvents other than water are certainly not new to chemistry and in the last two decades both fundamental research and practical applications involving non-aqueous media have experienced rapid growth. One index of this activity is the large body of physicochemical data determined in non-aqueous solvents such as that compiled in the two-volume handbook by Janz and Tomkins (1), and discussed, for example, by Coetzee and Ritchie (2), Covington and Dickinson (3), Kolthoff and Elving (4), Popovych and Tomkins (5), Mann and Barnes (6), Riddick and Bunger, (7), Lagowski (8), Gordon (9), and Mamantov (10) in their respective monographs.

In the context of this work, the term "non-aqueous" will refer specifically to organic solvents. When "non-aqueous" is referenced in the literature, however, the discussion may include not only the pure liquids, but also any one of their

mixtures with each other or with water. In addition, inorganic solvents and molten salts are also considered to be "non-aqueous" solvents.

The first part of this chapter will be concerned with the choice of solvent and solute that are to be used in the associated electrochemical system. Here, the pertinent physicochemical data are presented. Next, the methods of purification of both the solvent and solute will be discussed. The third part of this chapter will deal with electrolyte preparation and analysis (primarily for water and organic impurities).

The fourth part of this chapter will describe the experimental techniques that will be used to investigate the dynamic properties of the electrolyte solution, with a stress on the conductivity results. The properties of the solution as determined by spectroscopic measurements and as inferred from conductivities and thermodynamic properties will also be discussed.

1. THE CHOICE OF ELECTROLYTE COMPONENTS

1.1 THE CHOICE OF SOLVENT

It is widely recognized that the cycling behavior of the lithium electrode is the key technical problem preventing the realization of ambient temperature secondary lithium batter-

ies. The cycling efficiency of the electrode is visibly affected and largely determined by the properties of the electrolyte solution (11-17): while lithium deposition may occur with an efficiency of nearly 100% (11-13), the subsequent process of anodic dissolution is invariably less than 100% efficient (11-17).

Although the study that is the focus of this work concerns the interfacial processes at the cathode material (as opposed to lithium being the anode in a cell), the choice of a solvent (or solvents) and solute (or solutes), and the subsequent formation of an electrolyte solution takes importance if the chosen system is to represent a serious contribution and, hopefully, practical alternative for use in a secondary lithium battery system.

In the development of an electrolyte one must first choose solvents which manifest low reactivity towards metallic lithium. The system must then be refined via stringent procedures for purification and qualitative/quantitative analysis. Of course, the electrolyte system so chosen must have other desirable properties such as (a) being sufficiently inert toward the cathode material to prevent cell degradation, (b) being thermally stable (w.r.t. reaction with other cell components) in the projected long-lifetime of practical lithium cells, and (c) being able to maintain appreciable conductivity and Li^+ ion transport capability at low temperatures (e.g., 260 to 270 K).

The question of solvent and/or solute reactivity with lithium or any of the other cell components is an important one since the presence of significant amounts of impurities that result from oxidative or reductive processes, or direct chemical reaction, could interfere with the safe operation of an experimental cell, not to mention casting doubt upon the validity of the results so obtained.

Protic solvents must immediately be eliminated from consideration because of the reactivity of labile protons with metallic lithium. (Even slow reaction of labile protons with lithium cannot be tolerated when the product is a gas such as hydrogen.) This limits the investigation to the use of aprotic solvents which must be further limited to the investigation of dipolar-aprotic solvents since the presence of a dipole moment in the molecule can lead to substantial solvation energies for the electrolyte salts and therefore to dissolution of such salts. There is a loose correlation between dipole moments and dielectric constants, and a higher dielectric constant tends to aid ionic dissociation thus increasing the electrical conductivity for the solution.

Selim and Bro (11) established some guidelines that may be of some use in selecting a solvent. They pointed out that many polar solvents are intrinsically reactive towards metallic lithium due to the presence of the molecular dipole. For organic solvents this dipole is often the result of an unequal distribution of electron density about a carbon-

heteroatom bond which facilitates electron transfer from lithium to the bond.

Since it is probably true that there is no solvent which is thermodynamically stable to both lithium and the cathode material (that is to say it is possible to write a reaction for the solvent with either lithium or the cathode material corresponding to a negative free energy change; cf., the reactions between ethylene carbonate (EC) and lithium (18) and between EC and MnO_2 (19)) one must rely on kinetic inhibition of these thermodynamically favored reactions as an approach to solvent selection. A analysis of the thermodynamics for reactivity between metallic lithium and a variety of organic solvents demonstrated that all are susceptible to reduction by lithium (20).

The subject of solvent reactivities with reducing agents (e.g., Li) and oxidizing agents (cathode material, e.g., MoS_2, TiS_2) is also a subtle one: some applications can require the presence of protective films on the lithium which are usually formed by a limited reaction with the solvent (e.g., $Li/SOCl_2$). Peled's explanation (21) attributes specific properties to a non-metallic surface film on the lithium which he calls the solid electrolyte interphase (SEI). For non-aqueous systems he suggested that alkali metals will always be covered by a surface layer at least 1.5 - 2.5 nm thick. This layer is formed "instantly" upon contact of the metal with the solution with the thickness determined

by the electron tunneling range. The layer consists of some insoluble products from the reaction between the metal and the solution and acts as an interphase between them. Ideally this layer will have the properties of a solid electrolyte. Hence the name "solid electrolyte interphase". For many systems the rate-determining step was found to be ionic migration through the SEI.

Beyond the basic considerations of thermodynamic and kinetic stability there are several other aspects of solvent properties that should be considered: in non-aqueous systems the resistivity contributes a major part of the overall ohmic loss of the cell because of the low conductivity of these solutions compared with aqueous electrolytes. In addition, because of the differences in transport of the anion and cation in an electric field, the concentration gradient between the electrodes is amplified beyond purely diffusive effects. This results in an increase in the diffusion overpotential. These two effects are interrelated because conductivity, diffusion coefficients and transference numbers depend upon concentration and there *is* a concentration gradient present. An exact analysis of the electrolyte behavior is impossible because of this complex relationship and because of the lack of an adequate theory of transport properties in concentrated electrolyte solutions. Most workers, in recognition of these effects, seek electrolyte solutions with as high a conductivity as possible.

Other properties may be important as well, but are not as obvious. A low viscosity may be important to the operation of the cell because of a net volume decrease of the solid materials when the reactants are changed into products. When this happens, a void volume is created and in order for operation to continue the electrolyte must be able to flow easily into regions where it is required. A low solution viscosity facilitates this bulk flow requirement. Also, the ability of the solution to wet the electrode materials (and separator) may play a role in this aspect of cell operation but the precise effect of this property is very difficult to define. These and other complications may cause the solution of choice for a given system to be other than the one with the highest concentration.

A number of approaches have been taken to modify the lithium/solution interface and its reactivity (22):

(a) the use of surface-active additives to modify the morphology of the deposit and its reactivity;
(b) the use of alloy anodes (e.g., LiAl);
(c) the use of an internally generated scavenger to remove lithium dendrites and to conserve active mass of lithium;
(d) rigorous purification of the electrolyte; and
(e) control of the solvent structure.

Reviews have been published on the first three items (23-27); however, none of these has yet found application. The value of rigorous electrolyte purification cannot be overemphasized, and this, coupled with structural control of the

electrolyte components, allows for prudent investigation of the interface.

Two approaches to structural control of the electrolyte were taken (22): the group at Exxon investigated a wide range of solvents for stability towards attack by alkali metals. EIC (Norwood, MA) proceeded in the opposite direction to that of the Exxon group. At EIC the electrolyte salt was chosen first before a non-reactive solvent was sought.

At Exxon, several ethers were found to be stable and 1,3-dioxolane (Diox) was preferred because it dissolves lithium salts well enough to produce concentrated and highly conductive solutions.

EIC recognized the superior performance of $LiAsF_6$ (vs $LiClO_4$) in several solvents (14,28,29) all of which appeared to be highly reactive with lithium. The main emphasis was then to find non-reactive solvents.

Koch, et al. (16) suspected that cyclic ethers would have the best chance of retarding Li/solvent reactivity since the C-O bond is less polar than the C=O bond (e.g., in methyl acetate and propylene carbonate), or S=O bonds (e.g., in dimethyl sulfoxide), which are found in other solvents in which the lithium electrode has been cycled.

With this in mind, Koch investigated tetrahydrofuran (THF) reactivity with lithium (17,30). It was observed that $LiAsF_6$/THF electrolytes outperformed electrolytes that were based upon $LiAsF_6$ in either propylene carbonate (PC) or

methyl acetate (12,14,28) in terms of lithium electrode cycling efficiency. In spite of this, the THF media were judged to be too reactive for further use.

With evidence obtained by isolating reaction products (from cycling studies at a lithium electrode) and from earlier mechanistic work, Koch postulated a reduction mechanism involving an initial transfer of an electron from Li to the lowest unfilled molecular orbital (LUMO) centered on the oxygen atom of THF (30). It was observed that this led to ring-opened products. Assuming that this accurately accounts for the rate-determining step in the reduction of THF by metallic lithium, then one can possibly modify the reaction kinetics by raising the activation energy of this slow step (16). Perturbing the LUMO of the solvent molecule upward would accomplish this. Koch felt that placing an electron donating group in the 2-position (adjacent to the oxygen atom) would localize additional electron density on the O-atom and thus raise the activation energy required to form the anion radical. Koch also showed (16,31,32) that 2-methyltetrahydrofuran (2MeTHF) and 2,5-dimethyltetrahydrofuran (2,5-diMeTHF) were less reactive toward lithium than THF itself.

Independently, the reactivity of 2MeTHF toward lithium and TiS_2 (one of the cathodes used in this study) was examined and no significant degradation of solvent and/or depolarizer was observed (17,33).

Other cyclic ethers, e.g., Diox, have been examined as solvents for systems where transition metal chalcogenides are used as cathode material (34,35) and were found to be reactive in that solvent degradation (polymerization) was observed. However, the mechanism has been attributed to several factors and is not well understood. A methylated 1,3-dioxolane would be expected to be an improvement over 1,3-dioxolane, but none was found to be commercially available.

Electrolytes that are based upon diethyl ether (DEE) and blends of DEE with cyclic ethers have shown promise and exhibit a high degree of kinetic stability toward lithium which was attributed to the formation of a protective film of lithium ethoxide. If the LUMO argument is correct, then DEE should be easier to reduce than the tetrahydrofurans (36) and if DEE is in fact reduced more rapidly than THF then one would expect an <u>increase</u> in stability since the reductions would yield the relatively insoluble lithium ethoxide from DEE and the relatively soluble lithium butoxides from the THF. The protective film of lithium ethoxide appears to be electronically insulating, but Li^+-ion conducting (i.e., an SEI) (36).

By virtue of its stability w.r.t. the cell components, the solvent chosen for use in this study is 2MeTHF. The reactivity of this solvent with lithium has been well studied, likewise its performance (and reactivity) in systems where

transition metal chalcogenides are used. The solvent is readily available (Aldrich) and its methods of purification have been well documented. It must be reemphasized that although a study of the processes at the lithium electrode are not a part of this work, a solvent with kinetic stability towards metallic lithium is deemed necessary in cases where either metallic lithium is used as a reference electrode or metallic lithium is generated (inadvertently or otherwise) in an experimental cell. Hopefully, this will reduce the amount of degradation products that could potentially interfere with studies at the chalcogenide interface.

The dielectric constant of 2MeTHF is only 6.26 at 298 K; however, solutions of several electrolytes in excess of 2 molar have been prepared. No reference was found for a measured dipole moment; however, the dipole moment should be similar to, but somewhat less than, that of THF (1.75 D @ 298 K). The viscosity of 2MeTHF is low (0.457 cP @ 298 K) and this should be a help to the conductivity of an electrolyte solution. The boiling point of 2MeTHF is 353 K (80 °C) which is slightly higher than that for most of the solvents that have been otherwise considered. Since the presence of metallic lithium will be minimized in the experimental design, the need for stabilizing co-solvents such as DEE does not seem to exist.

In spite of its excellent performance, 2MeTHF still has some problems: in Li/TiS_2 cells, where the electrolyte has

been $LiAsF_6$/2MeTHF, there has been an observed formation of a brown film on the lithium electrode and an impedance increase at this electrode during cycling (16,17,37,38). Some of this degradation may depend upon the anion of the solute (38, refer to section 1.2 of this work). All of this suggests that in spite of in spite of much effort the system will still be quite reactive.

Some of the properties of 2MeTHF are summarized in Table 1 along with those of some of the other solvents that have been of interest in the study of secondary lithium systems. A few comments on the virtues and problems associated with some of these solvents is in order:

Propylene Carbonate - The nature of the reactivity of PC with metallic lithium is an issue which is still under debate (13,22,26). Anhydrous PC is very difficult to produce with the result that, in lithium systems, the researchers may actually be observing a ring opening of the PC at the metallic surface which is catalyzed by H_2O. PC's high viscosity is reflected in the low conductivity of most salts in PC; the specific conductance of $LiCF_3SO_3$ shows a maximum of $2.1 \times 10^{-3} \Omega^{-1} cm^{-1}$ at a concentration of 0.5 M. In spite of these (and other) problems, PC is still widely used for ambient-temperature lithium battery studies.

Dimethoxyethane (DME) and 1,3-Dioxolane (Diox) - Although there is a reported solubility of 2.0 M for $LiCF_3SO_3$ (and other Li salts) in DME (39), there is still some question as

References 1,3,7

TABLE 1

PHYSICAL PROPERTIES OF SELECTED SOLVENTS AT 298 K

Solvent	m.p. °C	b.p. °C	dielectric constant	viscosity cP	density g/cm^3	dipole moment Debyes	DN	AN
PC	-49	241	64.4	2.53	1.19	5.21	15.1	18.3
1,2 DME	-58	83	7.2	0.455	0.859	1.07	20	
1,3 Dioxolane	-95	78	7.13	0.589	1.06			
Diethylether	-116.2	34.6	4.265	0.224	0.708	1.18	19.2	3.9
DMF	-61	153	36.71	0.944	0.796	3.86	30.9	
THF	-108.5	65	7.39	0.46	0.88	1.75	20	8
2MeTHF		80	6.26	0.457	0.808			

to the stability of DME (as with Diox) in contact with metallic lithium.

The Tetrahydrofurans - As previously discussed, tetrahydrofurans methylated in the α-position manifest remarkable chemical and electrochemical stability towards lithium metal. While THF distilled off benzophenone ketyl and stored with Li at 344 K (71 °C) reacts in two days (16), 2MeTHF treated similarly was stable for over 10 months. Unlike the alpha methylated THFs, 3-methyl-THF was as reactive toward lithium as THF itself. Thus, the position of the methyl substituent with respect to the cyclic ether's oxygen atom seems to be critically important (16). The good cycling efficiency exhibited by 2MeTHF electrolytes is desirable not only for the lithium electrode, but also for the cathode since the electrodes will probably be cycled many times in both directions. The low conductivity of $LiAsF_6$ solutions in the substituted THFs is a bit distressing with the conductivity of 1.5 M solutions in 2MeTHF being only one-quarter of that in THF itself but for solutions in 2,5-diMeTHF (also non-reactive with metallic lithium) the conductivity is about 100 times less than in THF (16).

One last and very important property that must be considered is the stability limits of the solvent to anodic and cathodic polarization. Ethers are oxidized with relative ease (40) and this can be a problem with very oxidizing cathode materials such as Cr_3O_8 or anodically-charged

polyacetylene. The anodic oxidation limits have been determined for all of the cyclic ethers mentioned here (and a few others) (16). In each case the anodic limit was reached at a potential in excess of 4.0 V vs Li/Li^+ in 1 M $LiAsF_6$ (the experimental particulars are in reference 16). The anodic limits have been determined independently within the body of the present work. Cathodically, the $LiAsF_6$ solutions do not show appreciable reduction on $C_{graphite}$ or on $TiS_2 + C_{graphite}$ down to 1.4 V vs Li/Li^+ (22). In the context of this work the small trade-off in anodic stability (100 to 150 mV for methylated ethers versus unsubstituted ones) is a great bargain considering the gain in cathodic stability (versus that with unsubstituted ethers). The stability of the solvent towards oxidizing anions will be addressed in the next section.

1.2 THE CHOICE OF SOLUTE

The electrochemical reaction that is under study is the intercalation of Li^+-ions by $TiCh_2$ (Ch = chalcogen). The processes occurring in the double-layer for this type of reaction are quite different from most electrode reactions and there must be some control and understanding of the nature of the electrolyte solution as lithium ions are discharged from the solution into the host structure (cathodic process at $TiCh_2$). Since some relationship certainly

exists between the structure of the solution and the electrode process, the presence of ions that could interfere with this [Li^+,A^-,Solvent] structure should be avoided. Sodium and potassium will enter the host lattice readily as will substituted ammonium cations of virtually any size (41). The presence of any of these ions in the double-layer would interfere with the local "structure" of the solvated lithium ions and indeed they may themselves intercalate under the ambient conditions (a thermodynamic stability problem). Therefore, the presence of cations other than lithium may alter in an unpredictable way the transients for the electrode reaction - they could in fact change the reaction that is being studied and make the subsequent analysis difficult if not impossible.

The solutes to be used (including any that might be considered for supporting electrolytes) must be <u>restricted to lithium salts</u>. This ensures that the only cations that are available for intercalation by the host structure will be Li^+, $Li(S_n)^+$ (where S is a solvent molecule) and other positively charged aggregates made up of Li^+, A^- and S. The result is that any influence that the electrolyte solution has on the cathodic polarization will be due to the rate at which these lithium-containing species reach the discharging sites.

The choice of a suitable anion (or anions) for this work is not as obvious. Several properties must be evaluated for

a particular anion before it can be considered as suitable for this study:

(a) solubility of the lithium salt in a given solvent;
(b) dissociation tendency in a given solvent;
(c) stability towards oxidation by the cathode material;
(d) stability towards reduction by the anode material (Li);
(e) stabiity towards reduction by the solvent; and
(f) ability of the anion's salt to be easily purified and dried.

In general, a good solute will have a low crystal lattice energy and a large solvation energy. This favors ionization. The simple halide and chalcogen ions (which are stable towards reduction) are not sufficiently soluble in most non-aqueous solvents and result in solutions with inadequate conductivity for practical use. One is then forced to consider large, complex, monovalent anions which have good charge separation from the cation. Anions of this type are necessarily large (In non-aqueous solvents the lithium ion will be solvated and the anion usually will not. Ion transport is therefore predominantly anionic since the unsolvated anion is smaller than the solvated lithium.) and are usually composed of a central metal or non-metal atom in a high oxidation state and surrounded by four to six groups (halide, oxide, alkyl, or aryl) that are strongly bonded to the central atom. Examples would include perchlorate (ClO_4^-), hexafluoroarsenate (AsF_6^-),tetrafluoroborate (BF_4^-), tetraalkylborates (BR_4^-) and hexafluorophosphate (PF_6^-). Since the central atom of these ions is in a high

oxidation state and the ions are thus intrinsically reducible, one must rely (as with the solvents) on kinetic rather than thermodynamic stability. ***NOTE:*** The ion size and lattice energy argument is a generality (ClO_4^- is smaller than I^- yet ClO_4^- is much more soluble than I^-). There must be an entropy gain by the polyatomic ion when it goes into solution. The solubility data that are needed for lithium salts in many of the solvents that have been discussed are not widely available even in some of the major compilations of data; authors, including this one, must often determine the solubility of a given solute in a given solvent themselves.

The solubility of $LiClO_4$ in a number of organic solvents was determined by Markowitz et al. (42). These authors concluded that simple criteria such as the dielectric constant and dipole moment of the solvent are not particularly useful in correlating solubilities, but that a more comprehensive view of the solvents' properties such as steric hinderance, electron delocalization, degree of hydrogen bonding and other specific interactions in addition to the former properties, must be taken into account to explain their results (2,3,42,43).

Early workers in this field utilized the superior solubility of $LiClO_4$ in many solvents with high base-strength (a relative measure of this is a high donor number "DN"). Much of this work was carried out in PC because it was one of the few solvents for which there was any significant compilation

of lithium salt solubility data (44). Further work utilized $LiClO_4$ in a variety of other solvents that were more stable to metallic lithium than PC. The cycling efficiencies of the lithium electrode in several solutions e.g., $LiClO_4$/Diox were reported to be excellent (45). Work with this electrolyte has been curtailed, however, because of a series of explosions during cycling experiments. It was shown that the $LiClO_4$/Diox solutions are shock-sensitive and that the solute was to blame (34). It was also shown that the anodic polarization of $LiClO_4$/Diox solutions on a platinum electrode resulted in the polymerization of Diox at 3.25 V vs Li/Li^+ (34).

Lithium hexafluorophosphate ($LiPF_6$) could not be used with ~~diox~~ because it also initiated polymerization of the solvent and was found to be reactive with the lithium metal itself (45).

Several lithium tetraborates (including $LiBF_4$ and $LiBR_4$) have been investigated (40,46-49). The reasoning behind the study of these compounds was that a desirable set of electrolyte properties was intimately related to the fundamental properties of the anion (i.e., shape, ion-pairing tendencies, charge-to-size-ratio, charge delocalization, cathodic stability, etc.). With adequate synthetic freedom to modify anion structure one could affect these properties and a proper balance of bulk electrolyte properties could be achieved by design (46). Systematic structural modifications

of organoborate anions have shown that lithium tris-alkyl (or aryl) borate salts are somewhat satisfactory as electrolytes in Li/TiS_2 cells where continuous cycling at discharge rates of 5 mA cm^{-2} has been demonstrated (47). However, the oxidation potential of the BR_4^- anion (with small R groups and with R ≡ F) renders it reactive toward TiS_2 and prolonged contact with this cathode material produces BR_3, RH, and RR (40,46-49). (BEt_3 has been shown to cause a reductive cleavage of THF to nBuOH and of 2MeTHF to 2-pentanol (50).)

A family of anions that are <u>not</u> structurally based upon a central atom and radically bound groups are the closoboranes. Closoborane anions are closed polyhedra of boron atoms with terminal hydrogen or halogen atoms (51). A typical example would be $B_{10}Cl_{10}^{2-}$. The salts of closoborane anions exhibit a greater degree of kinetic stability to oxidation, reduction, and thermal decomposition than do organoborates or fluoroborates (52-54). The salts are insoluble in DME and Diox alone, but are soluble in Diox solution up to about 1 M if 4 to 6 equivalents of DME are present. Presumably the DME forms a solvate with the lithium cations (52). At concentrations below 0.3 M the solution separates into two phases. The performance of lithium closoborane electrolytes ($B_{10}Cl_{10}^{2-}$ and $B_{12}Cl_{12}^{2-}$) was examined (52) in Li/TiS_2 cells. Even at low discharge rates (1 mA cm^{-2}) the ambient temperature performance offered only 30% cathode utilization. This could be due to the low solubility and conductivity at room

temperature. Much time, effort, and money is necessary to produce these salts and there is every indication that their performance is most suited for study at higher than ambient temperature (54).

Lithium hexafluoroarsenate ($LiAsF_6$) is probably the most widely studied of the solutes for secondary lithium systems. This is largely due to the work of Koch, et al. (previous citations) in THF and 2MeTHF. The AsF_6^- anion is reduced by lithium to AsF_3. In the tetrahydrofurans, AsF_3 further reacts with lithium butoxides (from a ring-opening of the solvent) to form a brown film on the lithium. The brown film appears to be composed of a $(-As-O-As-)_n$ polymer and LiF (30). When other solvents are used, AsF_5, As_2O_3, organic carboxylates, alkyl fluorides and lithium fluorosilicates have been detected (33,55). ESCA studies on a lithium electrode after cycling in a 1.5 M $LiAsF_6$/2MeTHF electrolyte also showed the presence of magnesium (Mg and Si are reported impurities in $LiAsF_6$) (33).

The role of the film on the lithium is still a matter of debate. In any case the film must act as a SEI that is conductive to lithium ions or else the lithium electrode would not work in electrolytes containing this anion. The interaction of the AsF_6^- anion with $TiCh_2$ has *not* been the subject of a major investigation. Because of the reactivity of AsF_6^- with both lithium and with the solvent, another anion was sought for this work.

In other studies, lithium hexafluoroantimonate ($LiSbF_6$) and lithium hexafluorotungstate ($LiWF_6$) were examined (1 M in 2MeTHF) as electrolytes in lithium cycling tests and were rejected for poor performance (56). The SbF_6^- anion has been used to initiate polymerization of tetrahydrofurans (57).

Lithium trifluoromethanesulfonate has also been examined and the results of its use are a matter of debate (56-58). The anodic stability of this salt is comparable to that of $LiClO_4$ and $LiAsF_6$ in acetonitrile (56). $LiCF_3SO_3$ dissolved in a mixture of DME, Diox and 3-methyl-2-oxazolidone has been used as an electrolyte in studies of Li/FeS_2 (58) with the solubility of the solute reported to be at least 2.0 M. The solubility of $LiCF_3SO_3$ in 2MeTHF has been reported to be low (<0.4 M) (55); however, solutions in excess of 2.0 M have been prepared in this laboratory. No previous studies of $TiCh_2$ stability with this solute have been reported.

The anion that will be used in the present study will be $CF_3SO_3^-$. The ion is highly polarized due to the presence of the CF_3 moiety and appears to be kinetically stable to lithium (58); however, this is also a debated point (56). Solutions of $LiAsF_6$ in 2MeTHF (with or without co-solvents) are very promising and have been extensively studied, yet the desire to minimize the presence of degradation products (from cathode, solvent or solute) via oxidative or reductive mechanisms is largely behind the choice of $LiCF_3SO_3$. For experiments in which lithium metal is not used as an elec-

trode it is possible that $LiAsF_6$ could be employed. An independent study, correlating the intercalation of the lithium ion with the structure of the solute anion, will *not* be a part of this work.

2. THE PREPARATION OF COMPONENTS

There are several schools of thought concerning the preparation of materials for use in an experimental program as well as the relevance of stringent procedures when applied to an industrially important system. The presence of certain impurities inherent to the manufacture of a material may actually be beneficial to the system that one is studying in a fundamental way. The study of processes in lithium power sources is a case in point. Certain impurities are known to be detrimental to the favorable reactions in a cell (e.g., the presence of "large" amounts of sodium or potassium in metallic lithium) while the effect of other impurities may not have been qualified or quantified in many of the industrial laboratories where this work is being carried out (e.g., the role, if any, of trace organic impurities in film formation at a lithium electrode) (59).

In this setting, one is trying to elucidate mechanisms of an industrially important process: the surface processes associated with intercalation. The observation of the solvated lithium ion losing its solvation sheath and moving

into the host lattice is the only concern here. To accomplish this task, the materials should be prepared in their purest (within practicality) form and the presence of impurities would be qualified and quantified. This will allow the process under study to be controlled by the experimenter rather than affected incidentally by the impurities. Some of the discrepant results that have been obtained in the study of these systems underscore the importance of controlled preparative methods.

The next sections will describe the methods of preparation of the solvents and solvents that will be used in the electrolyte.

2.1 THE PREPARATION OF 2-METHYLTETRAHYDROFURAN

2-Methyltetrahydrofuran (I) was purchased from Aldrich Chemical Company. The solvent contained 1% butylated hydroxytoluene (BHT, 2,3 Di-tert-butyl-4-methyl-toluene, b.p. 265 °C) as an inhibitor to peroxide formation.

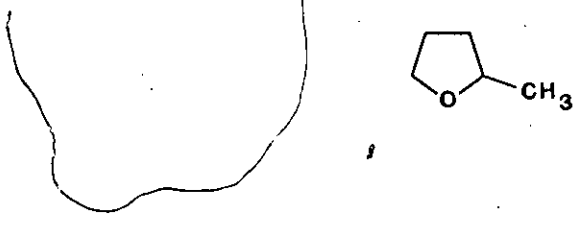

(I)

Peroxides. An intrinsic danger in the use of ethers is the presence of peroxides. When ethers are stored in the

presence of oxygen, a free-radical oxidation of the ether can occur. This process, referred to as autooxidation, may be initiated by hν. The α-position in ethers is autooxidized readily to give hydroperoxides that are usually very explosive. Significant amounts of such peroxides can build up in ether samples that have been exposed to atmospheric oxygen. The hydroperoxides are less volatile than the ethers and would be concentrated by a distillation process thus increasing the risk of explosion. Without precaution, extended storage of ethers that have been exposed to atmospheric oxygen is extremely dangerous.

BHT inhibits the reaction by undergoing hydrogen-atom transfer with peroxy radicals in preference to hydrocarbons. The resulting radicals are relatively stable and do not propagate a chain process but dimerize instead or react in other ways to cause chain termination.

The presence of peroxides in the solvent is indicated by the formation of a red color when the ether is shaken in the presence of Fe^{3+}-ion with aqueous thiocyanate. The peroxide oxidizes the iron (II) to iron (III), which then reacts with thiocyanate ion to give the red complex (60):

$$\text{peroxide} + Fe^{2+} \longrightarrow Fe^{3+} \xrightarrow{SCN^-} \underset{\text{red}}{[Fe(SCN)_n]^{-(3-n)}} \quad (n = 1 \text{ to } 6)$$

The principal peroxide that is present, 2-hydroperoxy-2-methyltetrahydrofuran, is reduced to γ-butryolactone and methanol (61).

Peroxides can be removed from the solvent in this way before distillation, but this would unnecessarily introduce water into the solvent, thus complicating the purification process. Instead, prior to distillation, peroxides are removed by passing the ether through a column of activated alumina whose volume is equal or greater than the volume of ether that is eluted. The peroxides adsorbed by the alumina must be reduced (e.g., by iron (II)) before the alumina can be disposed of or re-activated.

Impurities intrinsic to the manufacture of 2MeTHF. Several methods are currently used for the industrial production of 2MeTHF and each method would give a variety of impurities that would be present in small amounts. There is no way to determine which process was used in producing 2MeTHF for Aldrich - though some methods can be ruled out.

Methylfuran (MeF, b.p., 65 °C) (II) was found to be the major impurity in the "purified" solvent (section 2.2). Thus, a mechanism utilizing MeF is likely for the synthesis of 2MeTHF. Furans can be produced from the cyclization of 1,4 diketones (62).:

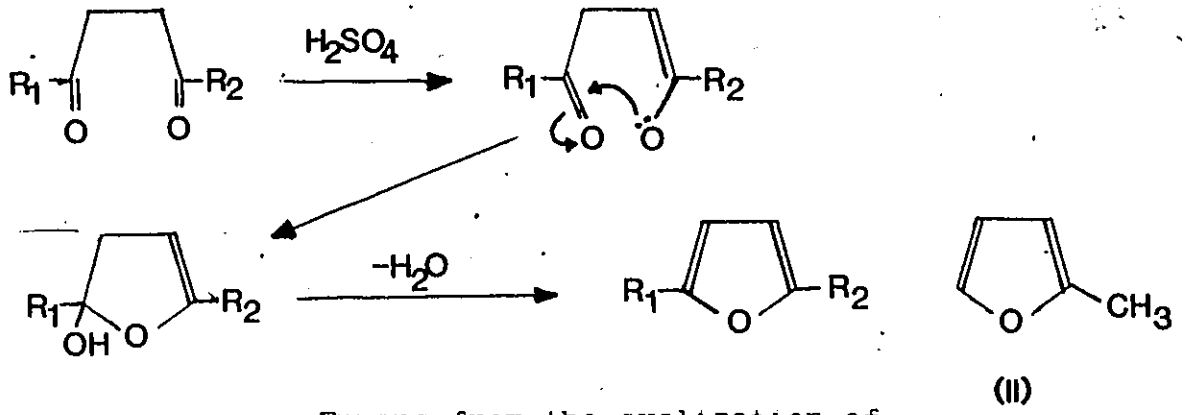

(II)

Furans from the cyclization of 1,4 diketones

Methylfuran can then be hydrogenated in the vapor phase in the presence of a reduced nickel catalyst yielding 2MeTHF in >95% yield (63).

THF's are also produced by the oxidation of primary and secondary alcohols by lead(IV)acetate or the oxidation of enols by mercury(II)acetate, both in refluxing benzene (62). Aldehydes (from a competing oxidation) and benzene would be impurities here but no impurities of this kind were observed (section 2.3).

Distillation of 2MeTHF. Three methods of distillation were used in the preparation of 2MeTHF. Early distillations were performed in a solvent still of a design that is commonly used for the preparation of anhydrous THF for organic synthesis (Figure 1). Distillation with a spinning-band column and a bubble-cap column were performed in the latter stages of this work as this equipment became available. The advantage of these latter methods was the improved

removal of volatile organics from the ether. Each method produced anhydrous 2MeTHF.

Solvent Still (Figure 1). A three-neck flask (2 L) allowed for the allowed for the introduction of benzophenone, sodium and potassium during reflux. The column length was approximately 20 cm and its diameter was 2 cm. No column packing was initially used. The still was operated on total reflux until the characteristic blue of the benzophenone ketyl appeared. The solvent was then allowed to collect in the solvent trap before delivery into the collecting flasks. A rotating receiver allowed for the collection of solvent fractions without opening the system. A small overpressure of argon was maintained throughout the system during the distillation. The pressure was regulated at a gas cylinder and monitored via an oil-bubbler. Heat was provided by a fiberglass heating mantle and controlled by a Variac. Exposed areas of the flask were covered with fiberglass insulation. The column was warmed with a fiberglass heating strip. The number of theoretical plates was not determined and the reflux ratio was not controlled.

The solvent still was modified (Figure 2) so that an additional length of column was between the boiling flask and the solvent trap. This increased the effective column length to about 50 cm. The column was packed with Raschig rings (8 mm) to increase the column efficiency. The number of theoretical plates was not determined and the reflux ratio

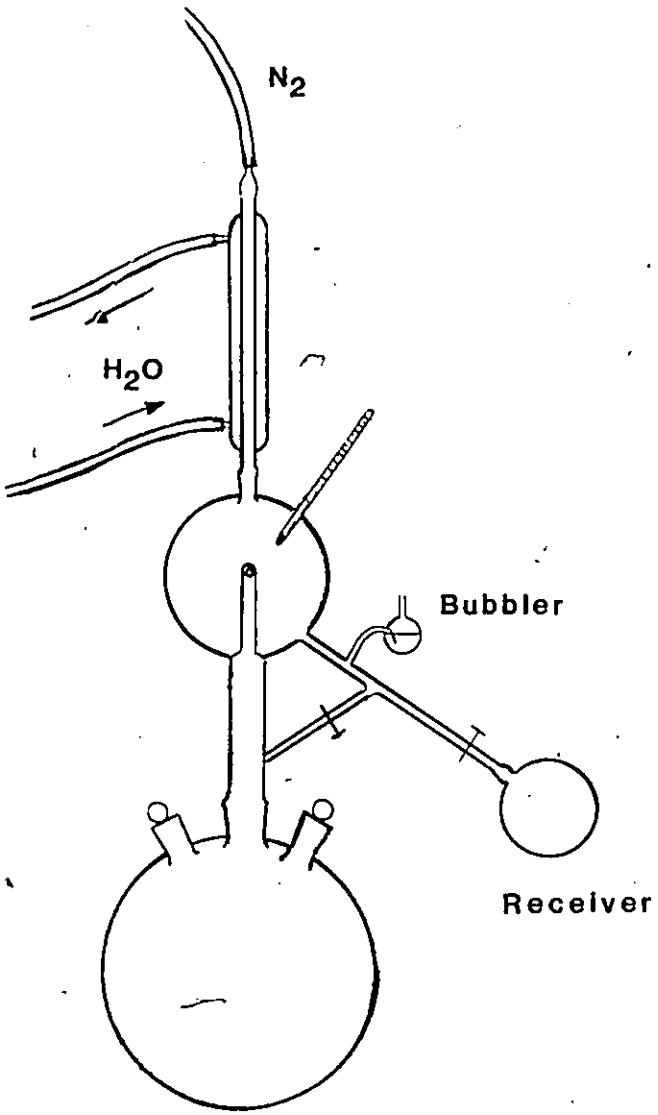

FIGURE 1

SOLVENT STILL FOR THE PURIFICATION OF 2MeTHF

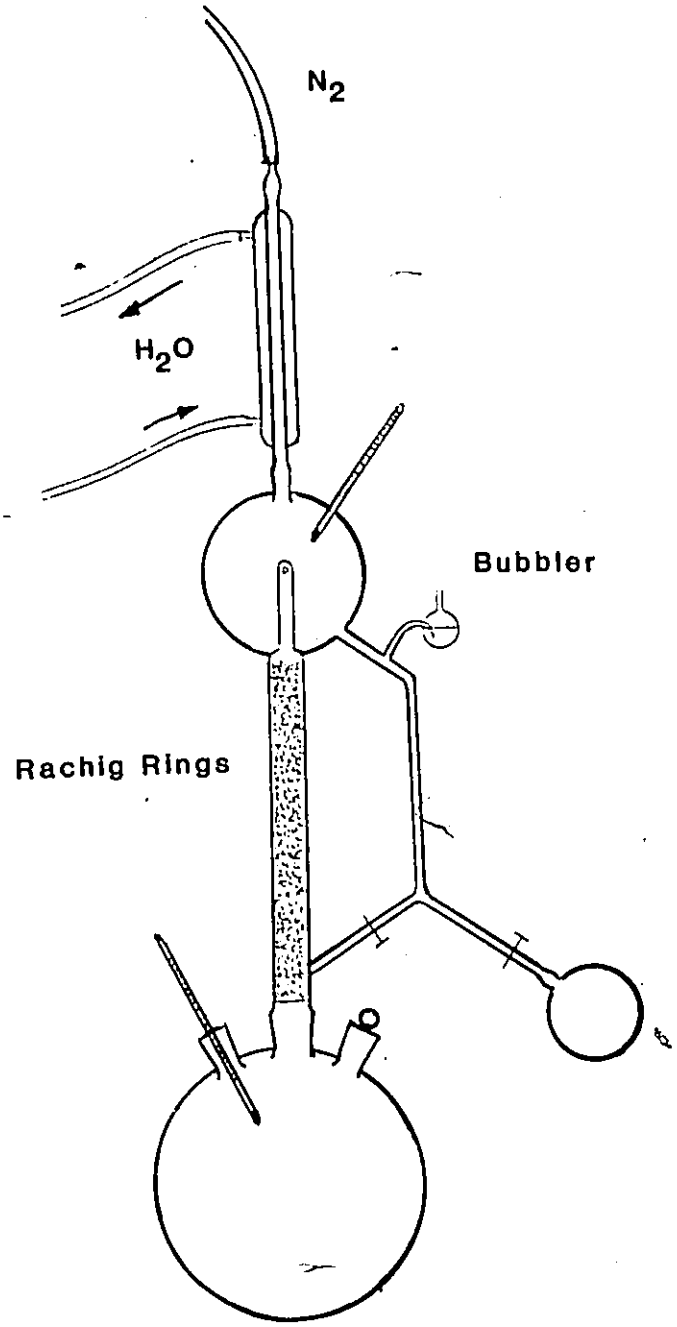

FIGURE 2

MODIFIED SOLVENT STILL WITH INCREASED COLUMN LENGTH AND RACHIG RINGS FOR IMPROVED DISTILLATION EFFICIENCY

was not controlled. In all other respects this still was operated in the same manner as the unmodified solvent still.

A bubble-cap column (Figure 3) was utilized to improve the removal of low-boiling impurities (60 to 80 °C). The column had an inside diameter of 5 cm and a length of 120 cm. The outer jacket of the column was evacuated and silvered, eliminating the need for column heating and allowing the interior of the column to operate at optimum thermal equilibrium. A 2 L three-neck flask served as the boiling vessel. The still was allowed to operate under total reflux until the blue of the benzophenone ketyl appeared. Using an electromagnet in conjunction with a timing device, the reflux ratio was set to about 15:1. Heating of the boiling flask was by means of a fiberglass heating mantle controlled by a Variac. Exposed areas of the flask were covered with fiberglass insulation. The boil-up rate was maintained during the distillation. The temperature was monitored both in the boiling flask and at the still head. Under the set of operating conditions that was used the still provided approximately 15 theoretical plates.

A spinning-band column was use to further separate organic impurities from the ether. The still used was a Perkin-Elmer Adiabatic Mesh column with a length of 90 cm. The band material was stainless steel (#316). The outer jacket of the column was evacuated and silvered. A 200 mL flask served as the boiling vessel. Heat was provided by a fiberglass

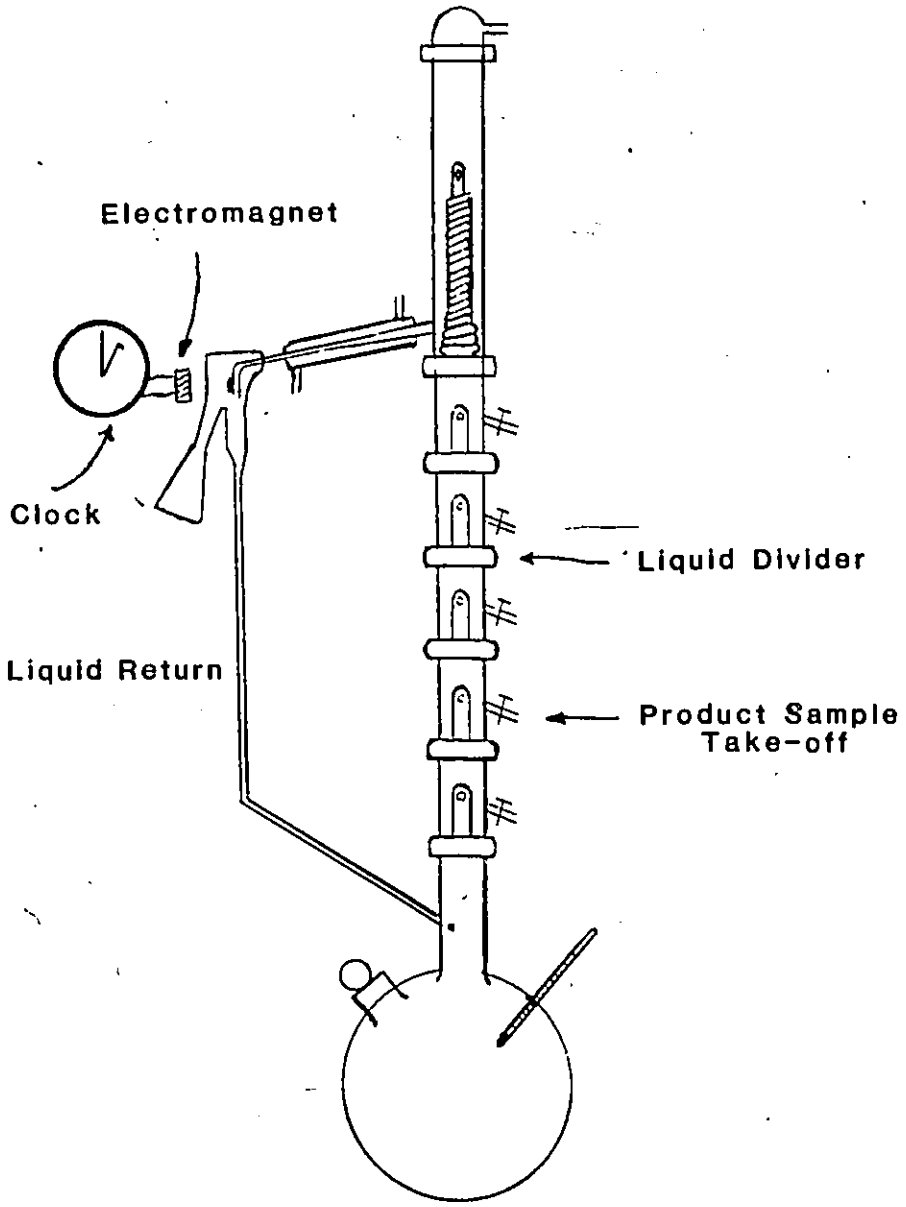

FIGURE 3

BUBBLE-CAP DISTILLATION COLUMN

heating mantle that covered all exposed areas of the flask. The heating mantle was controlled via the "temperature console". The still was operated under total reflux until the blue of the benzophenone ketyl was observed. The boil-up rate was adjusted to about 50 mL/hr. The band speed was set to about 2000 rpm. The reflux ratio was set to about 25:1. The temperature was monitored in the boiling flask and at the still head. Under these operating conditions the still provided about 40 theoretical plates. The middle 1/3 fraction of the ether was collected and stored after dry argon was bubbled through it for five minutes.

PROCEDURES

The importance of utilizing highly purified solvents and solutes in the present work cannot be overemphasized. Hence the preparation and testing procedures used will be described here in some detail.

Peroxide detection and removal

1. 5 mL of the stock ether was shaken with 1 mL of 2 M (aq) Fe^{2+} (ferrous ammonium sulfate or ferrous sulfate). To this several drops of 1 M (aq) KSCN was added. The observation of a red color was taken as an indication of the presence of peroxides. A positive indication (red complex) meant that the treatment of the alumina (step 4) should be performed with dilute ferrous solution.
2. ***NOTE:*** Step 2 is performed even if step 1 gave a negative (visual observation) indication of peroxides. A dry

column of activated alumina (neutral, 150 mesh) was prepared. The bulk volume of the alumina used was about equal to the total volume of ether to be eluted. This helps to inhibit thermal runaway should large amounts of peroxide be present.

3. After elution, the ether was further treated by bubbling dry nitrogen or argon through a frit for several minutes. The ether was distilled immediately.

4. For each litre of ether that was passed through the column, 20 mL of the ferrous solution was passed through in order to reduce peroxides so that the alumina could be safely washed and reactivated. If a positive peroxide indication was obtained in step 1, then the ferrous solution was diluted 10:1 before being passed on the column.

Distillation with the solvent still

1. The boiling flask was charged with 1.5 L of "peroxide-free" 2MeTHF (Aldrich). Four or five small pieces of sodium were prepared by washing the petroleum off with "peroxide-free" ether and they were added to the boiling flask. A small amount (1/2 g) of benzophenone was also added to the flask. Teflon sleeves were used in the glass joints of the still and boiling flask instead of any grease so that no unnecessary contamination would occur.

2. The condenser was turned on. The heating mantles for the boiling flask and the column were turned on. The argon flow was started and adjusted so that about 1 bubble appeared each second at the oil bubbler.
3. The temperature was slowly raised until the system was refluxing. By adjusting the stopcock so that all the solvent returned to the boiling flask (i.e. none remained in the solvent trap), the system was able to operate on total reflux.
4. After about two hours it was usually necessary to add two or three more pieces of prepared sodium and one piece of similarly prepared potassium to the boiling flask. While adding these pieces of metal the flow of argon was increased in order to keep a positive pressure within the still.
5. The introduction of extra sodium and/or potassium was usually sufficient to produce the blue color of the benzophenone ketyl indicating that the system was anhydrous and oxygen-free. The still was allowed to remain on total reflux for about one-half hour beyond the onset of the blue color in order to make sure that it persisted.
6. The solvent was then allowed to collect in the solvent trap. The temperature was monitored at the still head. A first fraction of between 300 and 400 mL was collected

until the head temperature reached 78 °C. This fraction was transferred to the receiver to be discarded.

7. The receiver was rotated into position to collect the main run of the distillation. The main run of the distillation (about 600 mL) was stored in the solvent trap before transfer to the receiver.

8. The final fraction, taken off in a similar manner, was also discarded with care being taken not to distill to dryness.

9. Argon was bubbled via a frit into the main run of the ether for several minutes. The ether was stored in a Teflon (FEP) bottle, sealed with Teflon tape and stored in a dark place.

The production of 600 mL of ether in this manner took about 15 hours. The residue in the boiling flask included bits of sodium and potassium. The pieces of metal and indeed most of the flask were covered with a brown "sludge" which could only be removed by dissolution in a chlorinated solvent. The brown material was not analyzed.

Distillation with the modified solvent still

Distillation with the modified solvent still (Figure 2) followed a procedure identical to that with the regular solvent still. A longer time was necessary for the system to come to thermal equilibrium due to the increased column length and crude heating and insulation for the column. The production of 600 mL of ether in this manner took about 18

hours. The same brown sludge material was observed in the spent boiling flask.

Distillation with the bubble-cap column

1. The boiling flask was charged with 1 L of the "peroxide-free" 2MeTHF, 6 to 8 small pieces of sodium and about 1/2 gram of benzophenone.
2. The heating mantle was turned on as was the condenser. The argon flow was initiated. The temperature was monitored at the still head and in the boiling flask.
3. The temperature was slowly raised until the system was refluxing. The still was operated on total reflux until the blue benzophenone ketyl appeared (The still was initially charged with a large amount of sodium so that the system would not have to be reopened to introduce more sodium and/or potassium to obtain the blue color. In no case was extra metal needed in order to dry the ether and produce the ketyl.)
4. One half hour after the appearance of the ketyl the reflux ratio was set. This was done by setting an electromagnet to allow for solvent collection or solvent return to the column. A timer was utilized for controlling the electromagnet. The timer was set so that a condensate was collected for every 7.5 seconds and all other condensate was returned to the column for 112.5 seconds. (total = 2 minutes). This gave an effective reflux ratio of 15:1 (112.5 : 7.5).

5. The temperature at the still head was always 79 °C and in the boiling flask it was typically 83-86 °C.
6. A first fraction of 200 mL was collected and discarded.
7. The Steps 7 to 9 of the solvent still operation were followed, except that the main distillate typically had a volume of 400 mL.

The production of 400 mL of ether in this manner took about 18 hours. A brown sludge similar to the previous methods was observed in the boiling flask.

Distillation with the spinning-band column

1. The boiling flask was charged with 150 mL of "peroxide-free" 2MeTHF, 2 small pieces of prepared sodium and about 50 mg of benzophenone.
2. The reflux control valve was adjusted to the "total reflux" position. The heating mantle was turned on at the temperature console and heating was increased until 20 to 100 drops per minute are observed from the drip tip.
3. The spinning-band was engaged and the rotor speed was adjusted to about 2000 rpm.
4. When the desired boil-up rate was re-attained the still was allowed to equilibrate for about two hours. If the ketyl was not observed by this time the still was shut off and the entire process was repeated with more sodium.

5. The reflux ratio was set. This was done by counting the total number of drops falling from the condenser drip tip and (after adjusting the reflux control valve) the total number of drops from the take-off drip tip. The ratio of the former to the latter was typically 25:1.
6. The observed temperature at the still head was 78-80 °C and the temperature in the boiling flask was typically 85 °C.
7. Solvent fractions were collected and stored in a manner similar to that which has been described above.

The main fraction was about 60 mL. Argon was bubbled through for a longer period (10 minutes) since this was not done during the distillation. The familiar brown sludge was observed in the boiling flask residue. The distillation typically took 10 hours.

This preparation is more rigorous than the methods that have been previously reported (1,14-17,30,31,36,54,55,59,64). These preparations have included distillations similar to that with the regular solvent still, distillations over calcium hydride, and distillations over sodium and benzophenone under reduced pressure. No pretreatments of the solvent for peroxides were previously reported.

2.2 THE PREPARATION OF LITHIUM TRIFLUOROMETHANESULFONATE

Lithium trifluoromethanesulfonate ($LiCF_3SO_3$, lithium "triflate") was obtained from 3M Corporation. The compound is listed as "Fluorad™ Fluorochemical Acid Salt FC-124".

No indication is given as to the method of preparation of the salt though it is clearly derived from trifluoromethanesulfonic acid. The presence of metal impurities is in question here and the reported metal impurities are listed in Table 2 (39). The presence of these metals must be minimized to prevent their participation in or interference with the interfacial study of Li^+ intercalation (refer to the third chapter of this work). For example, significant amounts of copper may present a problem; copper is known to form intercalates readily with layered hosts (65). The quantity of metal impurities (<100 ppm) is probably insignificant but a procedure for their removal was performed nevertheless.

TABLE 2

LITHIUM TRIFLUOROMETHANESULFONATE (3M); TRACE METAL CONTENT

Metal	ppm	Metal	ppm
Fe	<25	Ni	5-10
Ba	<25	Cu	3-5
Sn	10-15	Zn	3-5

The following procedure was performed routinely on the lithium triflate with samples typically of 2 to 5 grams weight:

1. The salt was taken neat from its bottle, weighed and shaken with 100 mL of hot aqueous 0.01 M disodium EDTA (for removal of trace metals). The solution was filtered twice and the mother liquor was dehydrated and dried in a vacuum oven at 150 °C for two days.
2. The oven was cooled slowly and flushed with dry argon. The salt was then removed from the oven and recrystallized by evaporation from purified 2MeTHF in a glovebox. The salt was then dried again in the vacuum oven for two days as before.
3. The recrystallization from 2MeTHF was repeated. This time, however, the salt was removed from the hot oven and allowed to cool in a vacuum desiccator prior to use.

A more rigorous regime was performed on several samples, particularly those that were used in the conductivity study. Steps 1 to 3 were performed but, before step 2, the salt was fused as described below.

1a. The dried salt was fused in an atmosphere of dry argon at 450 °C (m.p. 423 °C). The fused salt was cooled under argon and pulverized in an agate mortar in a glovebox.

2.3 ANALYSIS FOR IMPURITIES

The preparation of any material in a "pure" form will be limited in part by the methods used and also by the properties of the material and impurities that are present at the start of the procedure. In order to qualify and properly quantify results, some measure of the identity and quantity of impurities is necessary. This is true for both the solvent and solute as well as for their combined form: the electrolyte (section 3). An analysis was *always* performed on the purified solvent or solute, but not always for the unpurified material. Because of this, the *published* levels of the metallic impurities in the as received lithium triflate could not be verified. In addition, the effectiveness of the removal of these metals by EDTA could not be determined. Only the final result was known.

This section will outline the methods that were used to analyze the solvent and solute. Guidelines were also established for "acceptable" impurity levels. These guidelines, which are somewhat arbitrary, are based upon purity levels that were consistently attainable in the early runs. When the impurity levels rose above these guideline figures, the preparation was rejected and the material was subjected to reprocessing. Representative spectra, etc. are included here. Instrumentation used in the analysis changed as the site of the experimentation changed.

2.3.1 THE ANALYSIS OF 2MeTHF

The concern in the analysis of 2MeTHF is the qualification and quantification of organic impurities and the quantification of water. Several methods have been utilized toward this end: ^{13}C NMR, Infrared spectroscopy, UV-spectroscopy, Gas Chromatography, and GC/Mass spectrometry.

Characterization - ^{13}C NMR. Both the undistilled and distilled solvent were characterized by ^{13}C NMR. Quantitative detection of impurities was not possible. The measurements were made at 75.429 MHz in the pulsed Fourier transform mode on a VARIAN XL-300 Nuclear Magnetic Resonance Spectrometer. The field was locked (±1 Hz) on $CDCl_3$ with an external probe. All of the ^{13}C chemical shift measurements are referenced externally to TMS. All measurements were made at 23.0 ± 0.1 °C in 5 mm tubes. The assigned chemical shifts are δ = 21.1, 26.3, 33.6, 67.6, and 75.2 ppm. Figure 4 shows the assignment of the peaks for a sample distilled using the spinning-band column. With respect to organic impurities the solvent is quite pure, i.e., no peak assignments could be made that would correspond to any recognizable organic impurities. Quantitative measurements of impurity levels using ^{13}C NMR were not found to be practical due to the low levels of impurities that would be present and the scanning times that would be required for their detection.

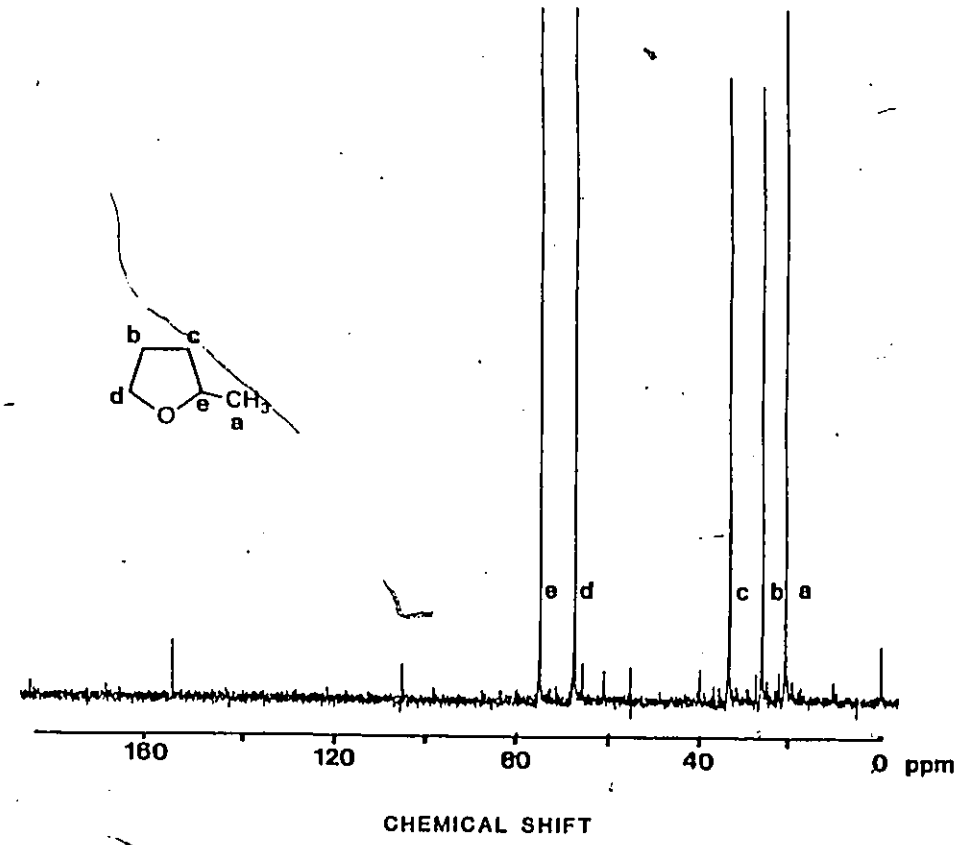

FIGURE 4

^{13}C NMR SPECTRUM OF 2-METHYL-TETRAHYDROFURAN
SHOWING THE ASSIGNMENT OF THE RESONANCES

Characterization - Infrared Spectroscopy. Both the undistilled and distilled solvent were further characterized by infrared spectroscopy. The measurements were made on a Perkin-Elmer 683 Infrared Spectrometer and recorded on magnetic media using a Perkin-Elmer Data Station. The solvent was analyzed neat in a silver chloride cell with a path length 0.01 mm between 2.5 and 15.4μ (4000 - 650 cm^{-1}). The spectrum of the empty cell was subtracted from the spectrum of the 2MeTHF. The resulting spectrum was smoothed using a Savitsky-Golay smoothing function. The smoothing function improves the readability of the spectrum by removing the irregularities in a sequence of points that may be due to errors in measurement. When the spectrum of the cell is subtracted from the spectrum of the sample these irregularities will be amplified; smoothing the spectrum tends to alleviate this problem (refer to the appendix of this work).

The infrared spectrum of the *unpurified* solvent can be seen in Figure 5. In the fundamental region, characteristic absorption peaks were observed at 3.38, 3.48, 6.85, 7.24, and 7.40μ. A small band was observed at 2.85μ. This is the O-H stretch region and the broad nature of the absorbance (the spectrum in Figure 5 has been compressed for publication) is indicative of the presence of a small amount of H-bonded O-H, probably in the form of water. This band was used in the subsequent quantitative analysis for water. A small absorbance was also observed at 5.8μ which can possibly be attribu-

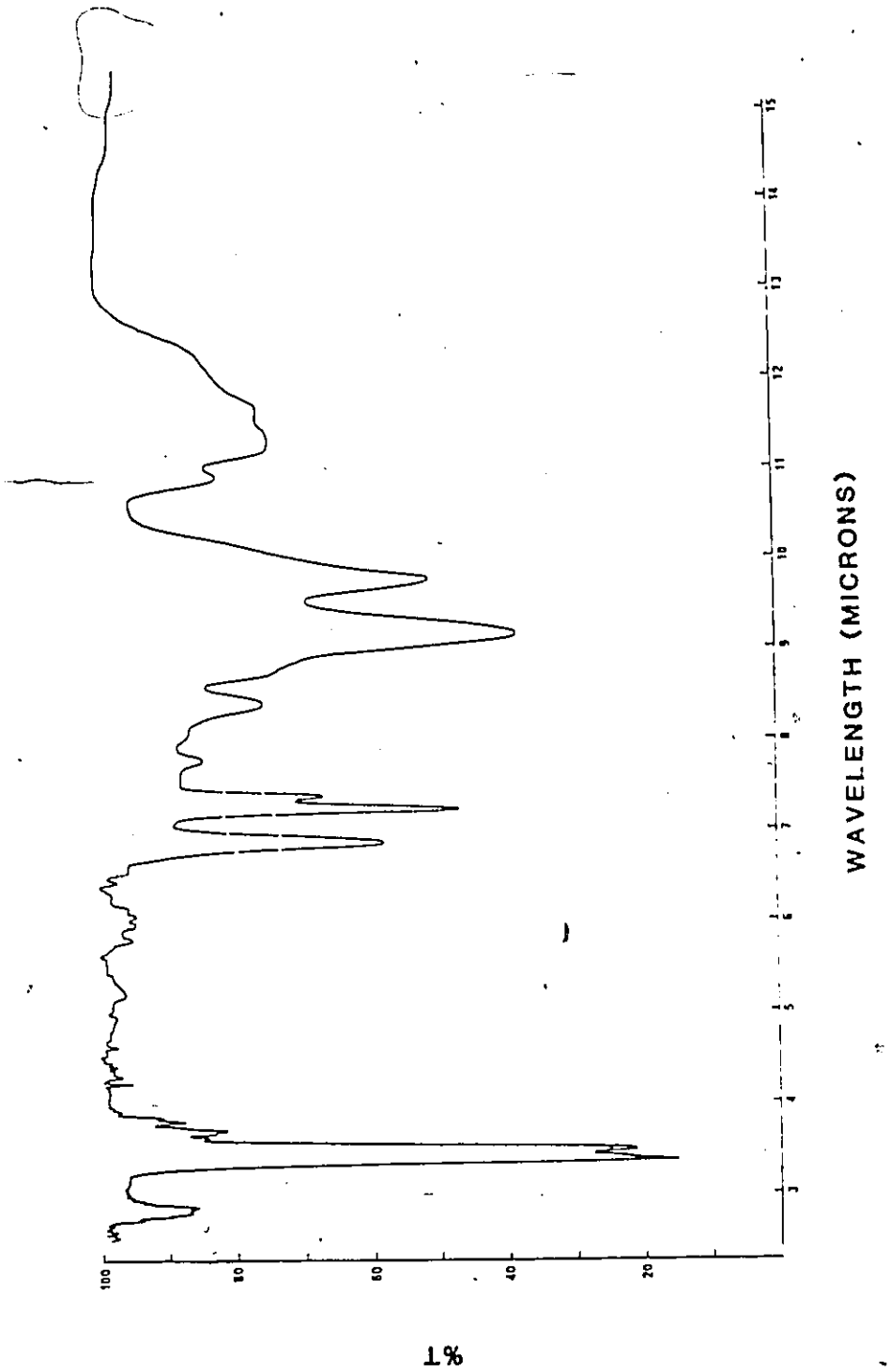

FIGURE 5

INFRARED SPECTRUM OF 2-METHYL-TETRAHYDROFURAN
2.5 TO 15.4 MICRONS

ted to a carbonyl bond from some remaining starting material. The "fingerprint" region from 8 to 15μ shows peaks and bands characteristic of 2MeTHF.

Qualitative Analysis - UV-Vis Spectroscopy. The solvent was qualitatively analyzed by UV-Visible spectroscopy in an attempt to detect benzene or aldehydes as impurities (from the manufacture of 2MeTHF, see pp. 28-29) (64). The spectra were generated by means of a Perkin-Elmer 552A UV-Vis Spectrophotometer and recorded on a Perkin-Elmer 561 Recorder. The slit was set at 0.25 nm and the scan was recorded at 20 nm/minute between 425 and 190 nm. The path length in the matched quartz cells was 10 mm.

In covalently saturated compounds containing heteroatoms unshared p-electrons are present in addition to σ-electrons. Excitation promotes a p-electron to an antibonding σ-orbit (an $n \rightarrow \sigma^*$ transition). In unsaturated and aromatic compounds the absorption results from the displacement of π-electrons. Both the ether (ϵ_{max} = 1000) and benzene (ϵ_{max} = 46,700) will exhibit a λ_{max} at 185 nm; the aldehyde chromophore should exhibit a "strong" absorption at about 210 nm (66). In addition, benzene will absorb at 202 nm (ϵ_{max} = 6900) and at 255 nm (ϵ_{max} = 170). While it was impossible to detect the presence of aldehydes at these wavelengths, the presence of benzene (an impurity in one method of 2MeTHF manufacture) would be indicated by the absorbance at the higher wavelength (with the large absorptivities for the benzene peaks, even

the smallest quantities should be detectable). No such absorbance was observed in either the "as received" or purified solvent. A control solution of the purified solvent containing a small amount of benzene was examined for comparative purposes.

Qualitative Analysis/Characterization - GC-Mass Spectroscopy The distilled and undistilled solvent were characterized by GC-Mass spectroscopy on a Hewlett Packard 5985 Mass Spectrometer fed by a Hewlett Packard 5840 Gas Chromatograph. A 10 meter capillary column served for the separation of volatile organics. The column was packed with Chromasorb-W as a stationary phase. The inject temperature was 40 °C. Helium with a head pressure of 22 psi and a flow rate of 15 mL/minute was the carrier gas. The retention time was 1.48 minutes. The mass-spectrum of a typical sample of "purified" 2MeTHF is given in Figure 6. Gas chromatography of the sample yielded 99.98% 2MeTHF and 0.02% (200 ppm) of one other component (exclusive of water, which could not be detected with the flame ionization detector). Chromasorb-W is a relatively non-polar stationary phase and the separation is largely by boiling point. The impurity appeared first at the detector indicating a lower boiling point. This, coupled with a rough mass-spectrum of the impurity (the detection limits of this particular instrument were being pushed) were

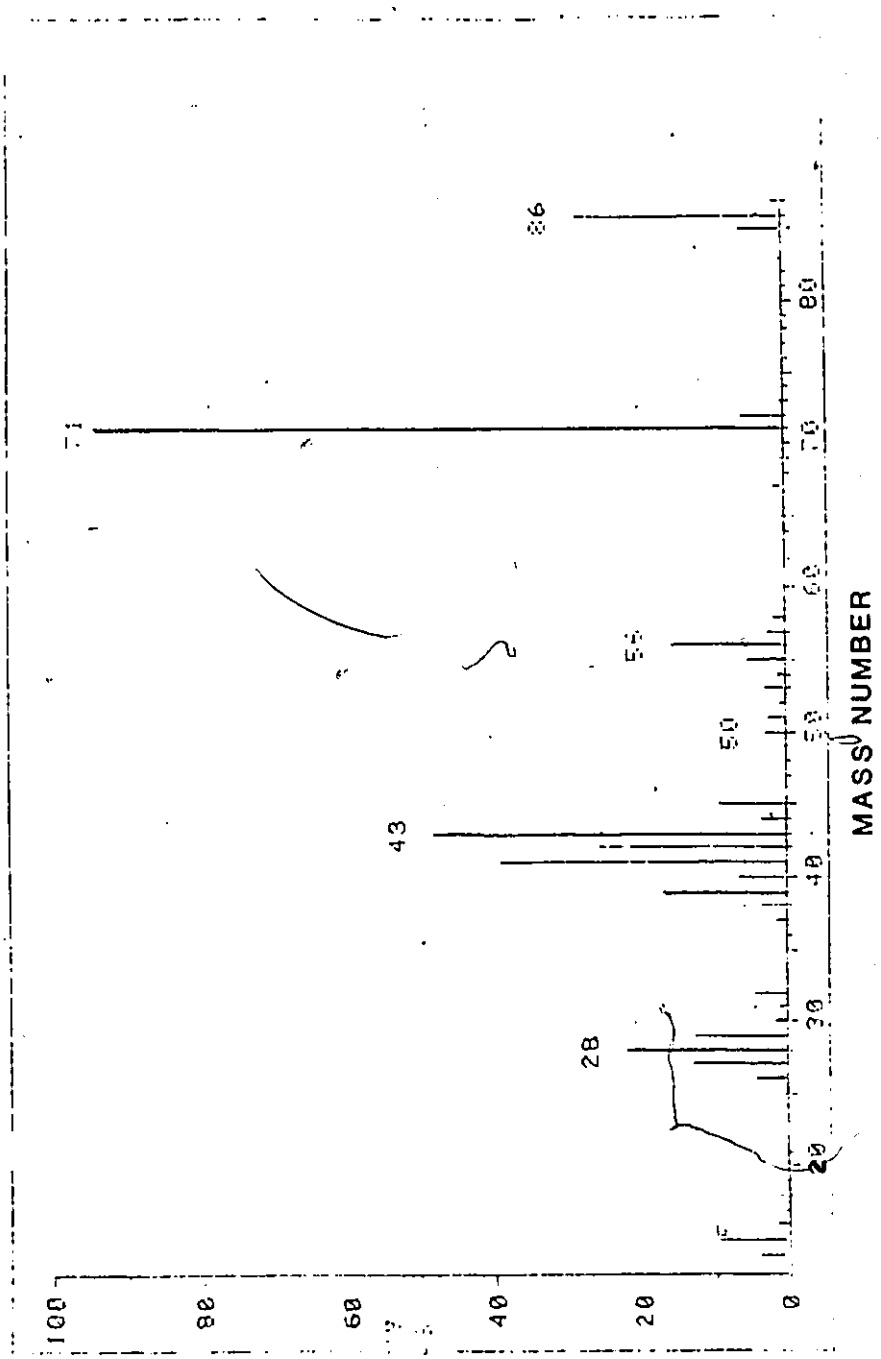

FIGURE 6

MASS SPECTRUM OF 2-METHYL-TETRAHYDROFURAN

indicative of 2-methylfuran (b.p. 66 °C), an impurity that was not unexpected.

Qualitative/Quantitative Analysis - Gas Chromatography

Each preparation of 2MeTHF was analyzed for impurities by gas chromatography. The instrument used was a Hewlett Packard 5890A Gas Chromatograph and the data analyzed on a Hewlett Packard 3392A Integrator. The stationary phase was Chromasorb-W HP (Alltech) 80/100 mesh on a 10 meter stainless steel substrate. The oven temperature was 200 °C. Nitrogen with a head pressure of 22 psi and a flow rate of 15 mL/minute was the carrier gas bringing the sample to a flame ionization detector. The retention time under these conditions was 2.53 ± 0.05 minutes.

The gas chromatography (and mass spectroscopy) showed that each of the methods of distillation was effective in removing all organic components except 2-methylfuran. The relative effectiveness of the separations became evident from the GC results: the solvent still yielded a product that was typically 400 to 600 ppm in 2-methylfuran; both the bubble-cap column and spinning-band column yielded a product that was 180 to 240 ppm in 2-methylfuran. Analysis of samples that were double and/or triple distilled were slightly lower in 2-methylfuran for the solvent still and virtually no different for the latter ~~stills~~.

Quantitative Analysis - Infrared Spectroscopy Several methods have been outlined for the infrared detection of ppm

levels of water in various liquid substances (67-70). Some of these methods utilize the near-infrared to observe the overtone band of water at 1.90μ (67,68). Other methods involve the observation of species in the fundamental region (2.5 to 7μ) (69,70). Direct observation of water at 1.90μ is possible (if one has an instrument capable of operating at this wavelength); however the absorptivity is very small (ϵ = 1.0 L mol^{-1} cm^{-1}) and cells with a path length of 1 to 10 cm are necessary for observation of water at <100 ppm. Water also absorbs at 2.76-2.86μ (antisymmetric O-H stretch) with an absorptivity of 37 L mol^{-1} cm^{-1}. The actual absorption here can be lost in the "background" absorbance of this region.

Alternatively, water can be reacted with calcium carbide to yield acetylene which has a stronger absorption (ϵ = 89 L mol^{-1} cm^{-1}) at 3.05μ (69,70). Here, the acetylene is removed to the gas phase by heating and is observed directly.

Limitations in the availability of equipment dictate the observation of the antisymmetric stretch at 2.76-2.86μ as a method of water detection. The exact position of the peak is dependent upon the concentration of water that is present. A broad band is present when there is substantial hydrogen bonding present. As the concentration of water increases a sharper absorption (due to the presence of some free, non - H-bonded water) occurs at the lower wavelength.

In order to estimate the sensitivity of this direct method, the background absorption for the solvent at this wavelength was determined. First, a small quantity of "super-dry" 2MeTHF was prepared by refluxing the "purified" solvent over calcium hydride. The solvent was then distilled over the sodium-benzophenone ketyl directly into an infrared cell.

The 2MeTHF is presumed to be "anhydrous" upon the persistence of the in-situ generated, highly moisture-sensitive, colored radical. A quantitative measure of this visual indicator (71) showed that up to 20 ppm of water could be present with the blue of the Na-benzophenone ketyl.

The infrared absorption spectrum of this "anhydrous" 2MeTHF was taken (instrument previously described) in a 0.01 cm KBr cell from 2.5 to 3.3μ (Figure 7). A small absorption (A = 0.025) at 2.85μ was observed. Expanding the ordinate by 10× increased the "reading" (not the signal-to-noise ratio) to 0.251. Two more preparations of this kind were made and the absorbance persisted.

If in the worst case it is assumed that 20 ppm of water was present (the threshold limit of the blue ketyl) then the absorbance due to the presence of 20 ppm of water with a 0.01 cm cell and ϵ = 37 L mol^{-1} cm^{-1} would account for only 0.000075 of the 0.025 that was observed. In other words the "background" absorbance must be at least 0.025 - 0.000075 (= 0.024925). This number is of no significance since the

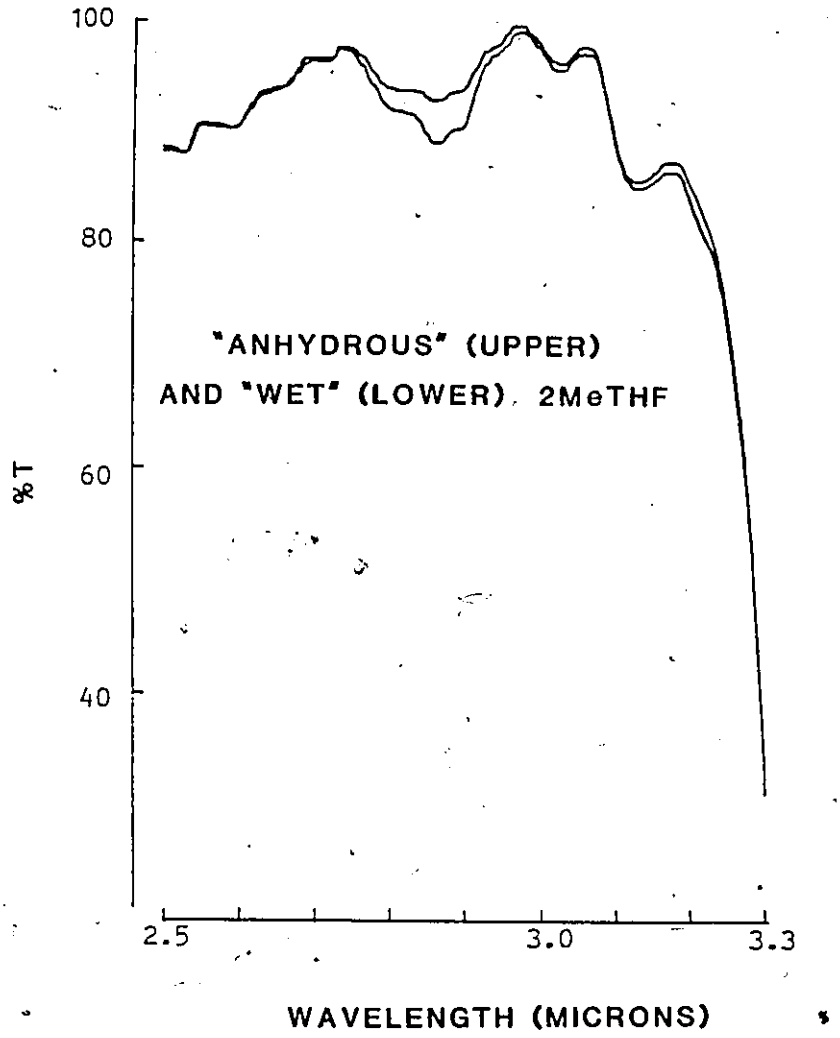

FIGURE 7

INFRARED SPECTRUM OF 2-METHYL-TETRAHYDROFURAN
2.5 TO 3.3 MICRONS SHOWING ANTISYMMETRIC O-H STRETCH

instrument is only sensitive to ± 0.001 absorbance units. The readability was "increased" by expanding the ordinate by a factor of 10. An absorbance change of 0.001 units would correspond to about 270 ppm of water (27 ppm on the expanded ordinate). Background absorbances of this order of magnitude have been commonly reported (69).

For comparison, 75 µL of distilled water was added to 100 mL of the "super-dry" solvent. This corresponds to a water content of about 4200 ppm or 0.42 mol%. The absorption at 2.85µ increased to 0.040. When the ordinate was expanded the absorbance read 0.398.

Samples of the solvent that were distilled by any of the three previous methods (all over blue Ketyl) all showed readable absorbances 0.025 (0.249 to 0.253 on the expanded ordinate).

The anhydrous solvent ~~is~~ desiccative and reactive. The usable lifetime of the solvent was about 1 week. After this time larger absorptions were observed for the O-H stretch. The possibility of peroxide formation contributing to this O-H absorption cannot be ruled out after the solution has been opened and used.

Typical assays of 2MeTHF appear in Table 3. Samples in excess of 500 ppm of 2MeF were rejected and the solvent reprocessed. A criterion for rejection based upon water content was not established other than that the blue Ketyl must be present on distillation.

TABLE 3

TYPICAL ASSAYS OF 2MeTHF

Preparation Method	2MeF/ppm	Water/ppm
None	4000-8000	5000-20000
Solvent Still	400-600	≤20
Bubble-Cap Column	180-240	≤20
Spinning-Band Column	180-240	≤20
Solvent Still (subsequent dist.)	350-500	≤20
Bubble-Cap Column (subseq. dist.)	180-240	≤20
Spinning-Band Column (subseq.)	180-240	≤20

2.3.2 THE ANALYSIS OF LITHIUM TRIFLUOROMETHANESULFONATE

After recrystallization and drying, no particular analysis was performed on the salt. The metal ions that were present before recrystallization were presumed to be present in <25 ppm quantities (total metals <100 ppm).

The major concern for the triflate was the quantity of water that the salt would introduce to the solvent upon forming the electrolyte. This analysis was performed subsequent to the formation of the electrolyte solution.

3. ELECTROLYTE PREPARATION

For the system under study, attention is focused on the mass-transport/charge-transfer processes occurring on both sides of the electrode surface for particular ions. In general, the ions of interest in the solution phase are in relatively low concentrations and it can be assumed that they are *not* significantly involved in the charge conduction process between the electrodes. This situation is usually resolved by adding a large concentration of supporting electrolyte to the solution in order to provide satisfactory electrolytic conductance between the electrodes (a particularly severe problem in non-aqueous solutions). When this supporting electrolyte is present, the effect of the solution conductance upon the interfacial phenomena can usually be ignored.

The electrodic reaction that is being examined - the discharge of lithium ions into a host lattice - requires that the processes occurring in the electrolyte be well understood and relatively simple. The reduction of metal ions in organic solvents is affected strongly by the nature of the supporting electrolyte. At strongly negative potentials small solvated cations e.g., K^+, are attracted to the electrode surface such that these ions can compete effectively in the double-layer with the relatively large solvated Li^+-ion. The distance of closest approach of cations to the

electrode increases with increasing size of the supporting electrolyte cation. As this distance becomes larger the potential at the inner Helmholtz plane becomes more negative. This accelerates the desolvation and electron-transfer at the inner Helmholtz plane resulting in greater reversibility for the reduction of alkali metal cations (in the presence of supporting electrolyte). However, the introduction of cations other than lithium into the electrolyte solution would necessarily make new species available to compete with lithium (and its complexes) in the intercalation reaction. This is an important assumption in the formulation of an electrolyte solution for these experiments.

The addition of more than one lithium salt or the presence of co-solvents would also complicate the situation: If one assumes that the kinetics and energetics of ion-pair formation and solvent coordination of the cation are important in the overall kinetic reaction, then the presence of additional anionic or solvent species will affect the overall predictability of the processes occurring on the solution side of the interphase. The importance of these assumptions will be more apparent later. Let it suffice at this point to recognize the importance for this system of minimizing the degrees of freedom in the electrolyte. For these prescribed reasons, only the one solute ($LiCF_3SO_3$) and one solvent (2MeTHF) will be used in the formulations described herein.

Solution Preparation - All solution preparative procedures were performed in an inert atmosphere of argon. Dry $LiCF_3SO_3$ and dry 2MeTHF were introduced to a glovebox (Vacuum Atmospheres Corp.) and the glovebox was purged and filled with Ar. The portions of both solute and solvent that were used for each solution were measured gravimetrically inside the glovebox and transferred to the solution preparation flask (Figure 8) which had been previously tared. After gentle stirring to dissolve the solute, a slow flow of Ar was initiated through a glass frit. This flow was continued for a minimum of six hours. When the flow of Ar was ceased the assembly was reweighed to determine any loss of solvent. The solution concentration was then calculated. A sample of the prepared solution (75 mL) was removed for analysis. Typically the electrolyte solutions were prepared in 1 L batches.

3.1 SOLUBILITY OF $LiCF_3SO_3$ IN 2MeTHF

The limit of solubility for $LiCF_3SO_3$ in 2MeTHF was not determined. However, solutions in excess of 2 M were routinely prepared during this project. This disputes the claim of Desjardins et al. (55) where the triflate was found to be of limited use in 2MeTHF because of low solubility (≈0.4 M). Early in the project when propylene carbonate was being utilized for preliminary measurements, the solubility of the triflate in PC was found to be about 1.1 M. Other

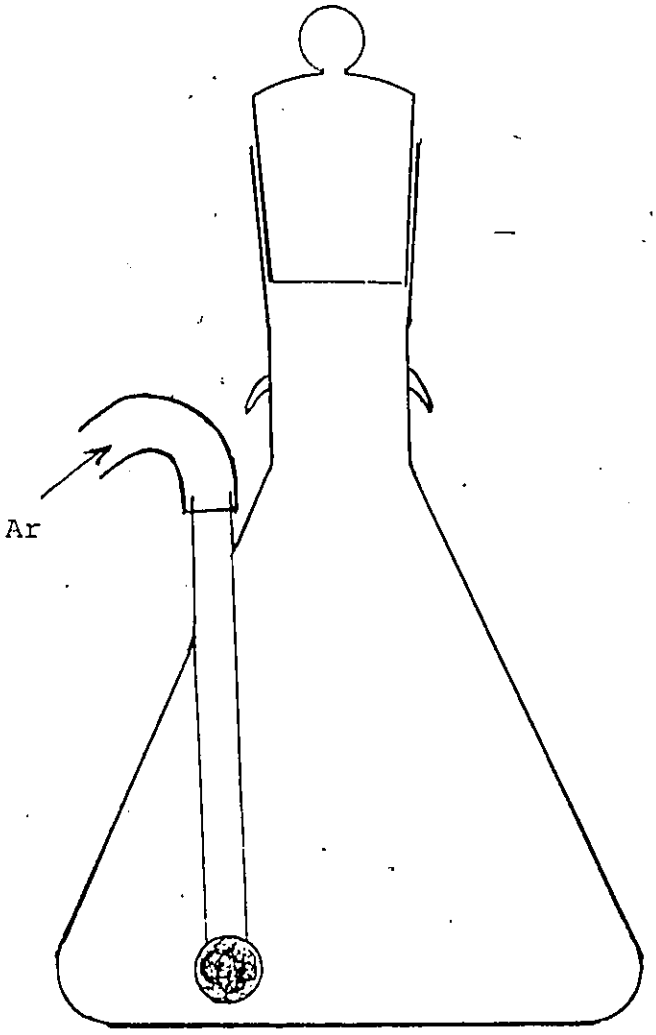

FIGURE 8

SOLUTION PREPARATION FLASK

Specially constructed flask for the preparation of electrolyte solutions. When argon is bubbling through the solution the top of the flask is replaced by a condenser.

solubilities that have been determined in this lab or reported elsewhere are included in Table 4.

3.2 TESTS FOR ORGANIC IMPURITIES

Analysis of the electrolyte solution for organic impurities is a redundancy of the analysis of the neat 2MeTHF. Characterization by Gas Chromatography and GC-Mass Spectroscopy were routinely performed on each electrolyte solution using procedures that were previously described. Assays of solutions that were prepared as described continued to show methylfuran concentrations of between 180 and 240 ppm (with slightly higher concentrations for solutions prepared with 2MeTHF from the solvent still).

TABLE 4

SOLUBILITY OF $LiCF_3SO_3$ IN VARIOUS SOLVENTS AT 298 K

Solvent	$[LiCF_3SO_3]$/mol L^{-1}	Reference
Water	10	39
THF	3.5	39
DME	>2	preliminary work
PC	1.1	preliminary work
PC	1.25	72
2MeTHF	0.4	55
2MeTHF	>2	this work

3.3 ANALYSIS FOR WATER CONTENT

It was assumed that any aliquots of 2MeTHF that were used for the preparation of an electrolyte solution were dry (i.e. they contained less than 20 ppm of water - the threshold value for the presence/absence of the blue Ketyl). The introduction of water to the electrolyte solution was caused by the solute, $LiCF_3SO_3$, even though the solute was processed and assumed to be "dry".

Two methods of analysis were performed for water content, the choice of which depended on the concentration range for the solute. The first method, which is somewhat empirical, was performed on the relatively low concentration solutions that were used for the conductivity measurements. These solutions had a concentration range of ca. 10^{-4} to 10^{-2} mol L^{-1} or about 200 to 2000 ppm of the lithium triflate. Even if (in a worst case scenario) the solute were as wet as 5% by weight of water, the introduction of the solute to the solvent would add 10 ppm of water to the 10^{-4} M solution and 100 ppm of water to the 10^{-2} M solution. These concentrations of water are too low to be practically measured via the infrared method that was previously described. Instead, a small aliquot of the electrolyte solution (50 mL) was placed in a 200 mL round-bottomed flask that had previously been charged with 0.1 g of benzophenone. The mixture was refluxed and after a short time the dark blue of the benzophenone

ketyl was observed. This was an indication that the water content of the electrolyte solution was less than 20 ppm. Since it was routinely possible to obtain the blue ketyl for solutions prepared for conductance measurements, any solutions that were not able to produce the blue ketyl were re-prepared.

Analysis for water in concentrated solutions was more quantitative. If, for a 2.0 M solution of the triflate in 2MeTHF, the solute was 1% by weight of water then the water content in the electrolyte solution would be about 3900 ppm. Concentrations of this magnitude allow for infrared detection of water with a sensitivity of about 27 ppm (expanded ordinate). The anhydrous solvent was used as a blank. A slight broadening of the O-H stretch was observed (free and coordinated water). Typically, each analyzed batch of electrolyte contained between 130 and 400 ± 30 ppm of water (an indication that the solute contained between 0.03 and 0.1% water by weight). For each lot of electrolyte that was used in electrochemical experiments, the water and MeF contents were recorded.

4. EXPERIMENTAL

Two techniques were utilized to investigate the electrolyte solution: electrolytic conductance and NMR shift measurements. The electrolytic conductance can be measured with relative ease and with high precision (error < 0.2%). Conductance measurements can be combined with other types of measurements (e.g., transference numbers) to yield information on the individual ions in solution. The limiting values of the molar conductance are functions only of ion-solvent interactions whereas their variations with concentration depend essentially on ion-ion interactions. Information on the structure of electrolyte solutions and on ionic equilibria can be derived from these properties. NMR is convenient and can be used to study solution properties in non-aqueous solvents. For example, information can be obtained on the nature and degree of ionic solvation, ionic association, selective solvation (in the case where more than one solute and/or solvent is used), solvation numbers and solvent exchange rates. A thorough review of NMR studies of ions in pure and mixed solvents has been given by Hinton and Amis (73) and more specifically for alkali metal ions by Lindman and Forsen (74).

Four types of information are desired from these solution-phase measurements: (a) an empirical determination of the types of ion-pairs that exist (i.e., solvent-separated pairs,

contact pairs, or multiple-ion clusters); (b) a measure of the relative quantity of these ion-aggregates (or conversely a measure of the concentration of ions that are free to conduct electrolytically); (c) a measure of the solvation number of the solvated cation (Li^+); and (d) a measure of the relative size of the solvated cation. Kinetic measurements of the rates of ion-pair formation and solvation processes were *not* examined though certain aspects of these rates can be inferred from the thermodynamic data and will be discussed later.

4.1 CONDUCTIVITY

Measurements of the electrolytic conductance of ions in solution can provide several types of useful information. A basic quantity of interest is the equivalent conductance of the electrolyte at infinite dilution, Λ_o. This parameter, when combined with transference number data, yields single ion conductances, λ_o^+ and λ_o^- and ionic mobilities μ^+ and μ^- for cations and ions respectively. The mobilities of ions are basic in estimating the degree of ionic solvation and ionic size. Information on ionic-association can be extracted from the variation of electrolytic conductance (or ion-mobilities) with concentration. When combined with an appropriate theoretical analysis, the concentration dependence gives the fraction of ions that are free to conduct

current. From these data, the association constant (or constants) for ion association of the various types of aggregates can be calculated.

4.1.1 CONDUCTIVITY CELL DESIGN

Measurement of the electrolytic conductance involves a measurement of the resistance (d.c.) or impedance (a.c.) of the electrolyte between the electrodes. Cell design is dictated in part by the method of measurement. For d.c. methods a four-electrode cell is usually employed - two to carry the current and two to measure the iR drop. A two-electrode cell is usually employed for a.c. impedance measurements, but this does not imply that the a.c. as simpler than the d.c. measurement to perform experimentally. When conductivity is determined with an a.c. bridge, the measured impedance is generally dependent upon frequency and this frequency dependence generally consists of several effects in addition to those associated with the movement of ions through the solution. These effects have been conveniently discussed by Braunstein and Robbins (75).

Some of the frequency dependent effects can be minimized by proper cell design but others are inherent to the processes occurring during the measurement. To understand their significance one must examine the equivalent circuit of the conductance cell (Figure 9). In order to measure R_S, the

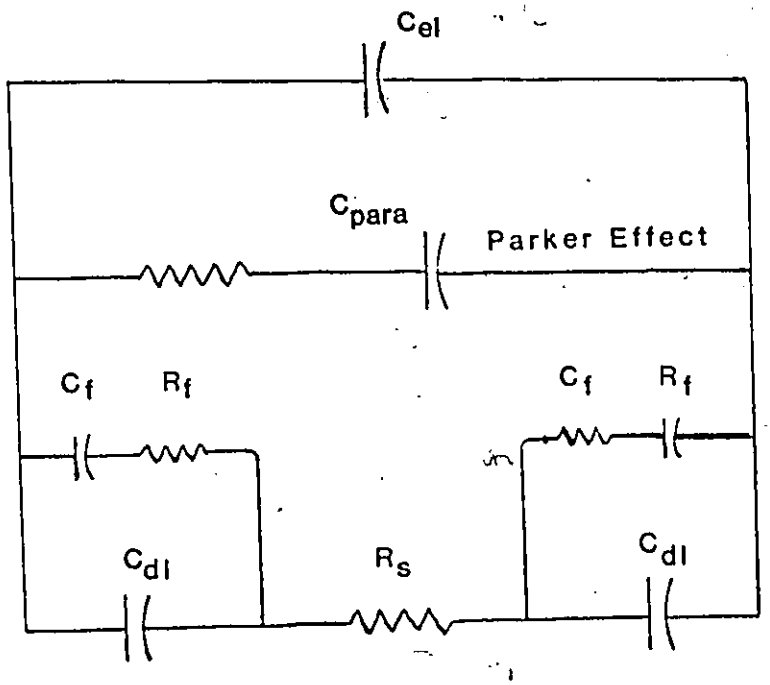

FIGURE 9

EQUIVALENT CIRCUIT OF ELECTROLYTIC CONDUCTANCE MEASUREMENT

resistance of the solution, some knowledge is required of the other electrical contributions introduced by the electrodes.

An obvious effect is that of the capacity C_{el} produced by the electrodes themselves behaving as a condenser with the electrolyte solution as a dielectric. This effect introduces an admittance of $\pi f C_{el}/2$ (where f is the a.c. frequency) with a magnitude of about $2 \times 10^4\ \Omega$ at 1000 Hz. Since C_{el} acts in parallel to R_s its effect will be very small unless $R_s > 10^4\ \Omega$ (75). The important contribution originates in the double-layer at each electrode/solution interface. The double-layer capacitance (C_{dl}) acts in series with R_s. For smooth electrodes the admittance ($\pi f C_{dl}/2$) of the double-layer is of the order of 10Ω at a 1 cm^2 electrode at 1000 Hz (75). The effect of the double-layer can be minimized by platinizing the electrodes (this increases the surface area and therefore C_{dl}). Faradaic processes can arise when the system under study has a high exchange-current density. The chance of electrolysis occurring can be minimized by using applied potentials with an amplitude of less than 100 mV. Most significant of the other effects are the parasitic capacitances (C_{para}) which, for example, occur between insulated leads passing through the solution, between connecting leads to the cell, or from stray currents resulting from a less than optimum design geometry for the cell. These effects are sometimes referred to as the Parker Effect.

The resistance of a cell is given by

$$R = \ell/\kappa A = K/\kappa \qquad [1]$$

where K is the cell constant relating to the geometry of the cell. The cell design should be such that R does not fall far below 1000 Ω (to minimize the relative errors due to polarization and cell leads) or much above 30 kΩ. When it is necessary to measure very high resistances, e.g., when determining the solvent correction, it is often necessary to shunt the cell with a known resistor of 10^4 or 10^5 ohm. The value of the cell resistance can then be calculated from

$$1/R_{obs} = 1/R_{cell} + 1/R_{shunt} \qquad [2]$$

For work with non-aqueous solutions of high specific conductivity κ, an appropriately small cell constant is achieved in a cell with electrodes very close together as in the cell depicted in Figure 10. If the cell is poorly designed, the cell constant will be found to vary with the specific conductivity of the solution. This is a result of the Parker effect with the consequence that the observed resistance is less than the true resistance. The effect is virtually eliminated by placing the electrical leads and electrolyte reservoir well away from each other (76,77).

One additional (and small) effect that was also considered in the design of the cell was investigated by Prue (78). The

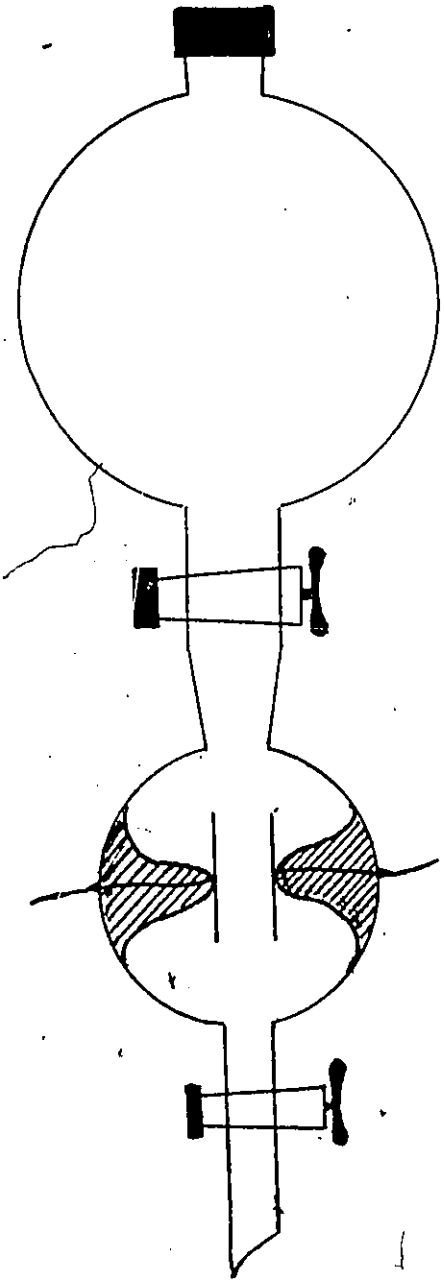

FIGURE 10

CONDUCTANCE CELL

conductivities of dilute solutions are often observed to drift upward by as much as 10^{-7} Ω^{-1} cm^{-1} per hour. The phenomenon appears to be caused by concentration of electrolyte at the polar glass surface as a result of ion-exchange processes. This effect is prevented by keeping the edges of the electrodes in a large bulk of the solution; lines of current flux would be produced behind the electrodes giving rise to a strong frequency dependence (large Parker effect).

The cell (Figure 10) was constructed with a large volume that was convenient for carrying out serial dilutions in situ via the addition of increments of solvent. The cell is divided into a preparation chamber (calibrated volume) and electrode compartment in order to avoid some of the previously mentioned stray capacitance effects.

The electrodes were prepared for platinization by brief immersion in aqua regia followed by concentrated nitric acid and water. Prior to platinization the surfaces were reduced by cathodic electrolysis in dilute sulfuric acid for 10 minutes (79). Platinization was performed in a mixture of 0.3% potassium chloroplatinate and 0.2% lead acetate in 0.025 M HCl, at a current density of 2 mA cm^{-2} with polarity reversal every 5 seconds until approximately 8 C cm^{-2} had been passed. The platinized electrodes were washed with water for 24 hours and for 4 hours with 2MeTHF. The electrodes were then stored in 2MeTHF.

Thick platinization (> 3 C cm^{-2}) can result in the electrodes adsorbing significant quantities of electrolyte and are thus unsuitable for work in measuring the *solvent conductance*. On the other hand, smooth electrodes introduce frequency dependent effects. Preparing the electrodes for solvent conductance measurement was as described above *except* that a light (0.4 C cm^{-2}) platinization was applied to the electrodes and the washing time was doubled.

4.1.2 CONDUCTIVITY MEASUREMENTS

Electrical measurements were performed by connecting the cell to a Solartron 1186 Electrochemical Interface (potentiostat). One of the electrodes was connected to the counter electrode input and the other electrode was connected to the working electrode input. One reference electrode input was connected to each electrode. The potentiostat was connected to either a Solartron Model 1172 or 1250 Frequency Response Analyzer (FRA) for signal generation, voltage and current measurement. A block diagram of the arrangement is presented in Figure 11.

The FRA was programmed to present a 1000 Hz signal with an amplitude of 50 mV to the potentiostat. The outputs of the potentiostat were connected to the x- and y- inputs of the FRA. The outputs of the analyzer yields the real (x) and imaginary (y) parts of the complex plane impedance. The

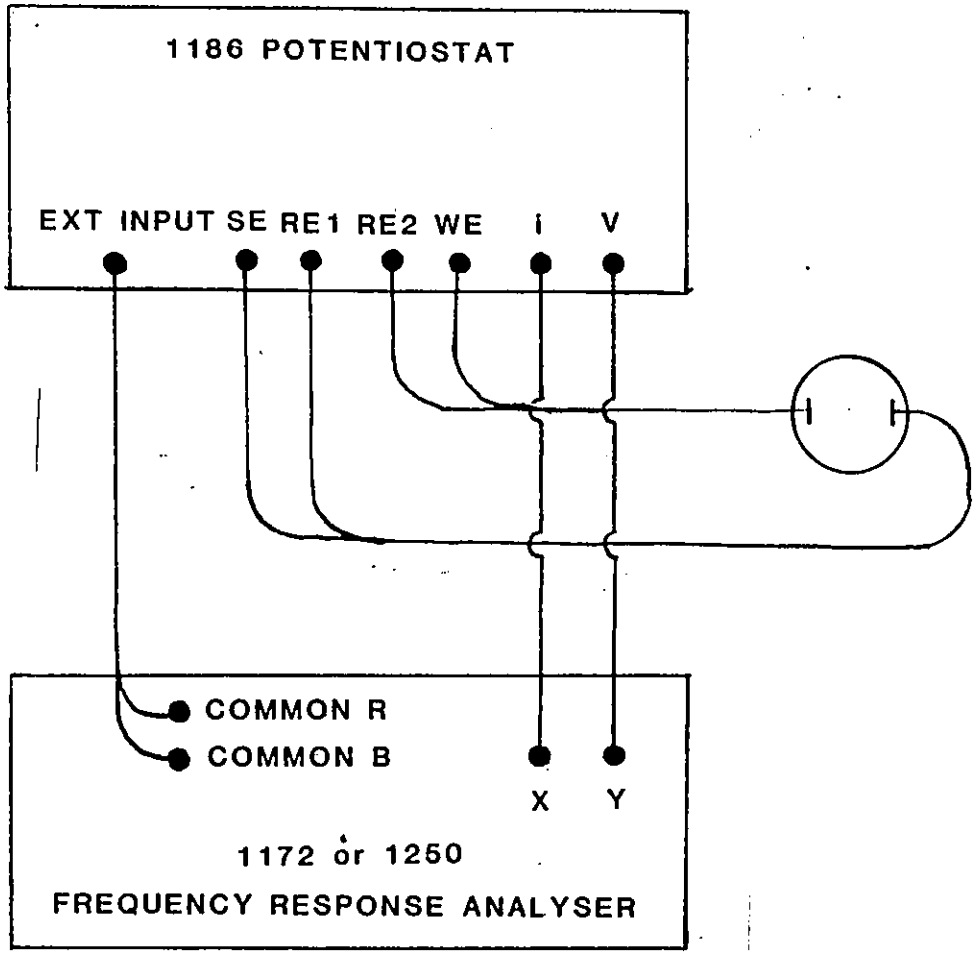

FIGURE 11

BLOCK DIAGRAM OF CONDUCTANCE MEASUREMENT SYSTEM

impedance of the electrochemical cell (equivalent circuit of Figure 9) is a complex number which can be represented in Cartesian coordinates as

$$Z(f) = ReZ + i\,ImZ \qquad [3]$$

where ReZ and ImZ are the real and imaginary parts of the impedance, respectively. In a properly designed cell the small contributions of C_{el} and C_{para} can be ignored and the two electrodes, now in a simple series arrangement with R_s, can be treated as one. When the double-layer capacitance is large (a condition that is largely fulfilled when the electrodes are heavily coated with platinum black) then the measured impedance is virtually equal to the solution resistance. In such cells the resistance of the solution is found to be virtually independent of the a.c. frequency.

Temperature control - Limiting ionic conductances rise with increasing temperature. This rise is largely parallel to the fall in viscosity of the solvent. The limiting molar conductances of most salts increase by 1 to 3% per °C. Therefore, precise and accurate control of the temperature is paramount for precise conductivity measurements. In order to achieve a precision of ±0.01% in measurement, the temperature must be controlled to within ±0.005 °C. This was achieved by placing the cell in a sand bath. Temperature adjustment and control of the sand bath was from a second (external) water (or oil) bath and a temperature controller (Haake, model F4).

Fluid from the water/oil bath was circulated in Tygon tubing to and through the sand bath. Because of the slow exchange of heat by the sand, the temperature that was desired took a long time to attain (6 to 24 hours) but remained stable to within measurement resolution (0.001 °C) for the lifetime of an experiment (30 to 60 minutes).

Cell Calibration - The conductance measurements that were made in this work are relative. The conversion of the measured cell resistance, R_S, or conductance, L, to absolute values of the conductivity, requires a proportionality factor. This factor is the cell constant K which is formally given by ℓ/A (equation 1). Because the effective distance between the electrodes, ℓ, will include the contribution made by the lines of current flux passing behind the electrodes, the determination of K with e.g., a ruler is impossible. The cell must be calibrated with a standard solution of known specific conductivity.

Standards were provided by Jones and Bradshaw (80). These standards have been followed for half a century and are still followed by some. With the adoption of the SI system of units (the units of temperature and resistance have slightly different definitions than at the time of Jones and Bradshaw), new calibration standards were recommended by IUPAC in 1976 (81,82). Conductance cells can be calibrated with a potassium chloride solution of known concentration together with an equation representing the molar conductance

over the appropriate concentration range. The equations below are given in terms of the molar conductance, Λ, which equals κ/C, and are able to reproduce the conductivities of the reference solutions to within 0.015%.

For measurements at 298.15 K, the equation that is appropriate for the concentration of KCl that was used (10^{-3} mol dm^{-3}) is the Justice equation (83), valid in the concentration range between $c = 10^{-4}$ and 0.04 mol dm^{-3}.

$$\Lambda(mS\ m^2\ mol^{-1}) = 14.984 - 9.484\ c^{1/2} + 5.861\ c \log c + 22.89\ c - 26.42\ c^{3/2} \quad [4]$$

The symbol S is used for siemens which is equal to the reciprocal of the absolute ohm.

For measurements at temperatures other than 298.15 K a temperature correction should be applied to the cell constant K. The precise cell geometry depends upon the thermal expansion of platinum and glass (81). For two large electrodes that are relatively close together this correction may be approximated (84) by

$$\frac{1}{K}\left[\frac{dK}{dT}\right] \approx \alpha_{glass} - 2\alpha_{Pt} = -15 \times 10^{-6}\ K^{-1} \quad [5]$$

where α represents the thermal expansion coefficient of each material.

Potassium chloride (Alfa-Ventron, Ultrapure™) was recrystallized from HCl and dried at 110 °C under vacuum for six

days. The salt was recrystallized once more from pyrolytically prepared water and dried at 500 °C for 24 hours. The salt was weighed on a micro-balance whose weighing compartment had been flooded with dry nitrogen. The sample weighed 0.1485 ± 0.0001 g. A volumetric flask (previously calibrated to contain 10.000 L ± 2.6 mL at 25 °C) was thermostated to 25.00 ± 0.01 °C and filled with freshly boiled pyrolyitic water. The solution produced with these components had a concentration of $1.9919 \times 10^{-4} \pm 0.0019 \times 10^{-4}$ mol dm^{-3}.

At this concentration, the specific conductivity as given by equation 4 is

2.958035×10^{-5} ($\pm$ 0.002823×10^{-5}) S cm^{-1}

The conductance cell was rinsed several times with the KCl solution and then filled and the assembly (including the attached leads) was allowed to reach thermal equilibrium. Upon attaining a temperature of 24.985 ± 0.003 °C, the resistance measurements could begin.

First, as a test of the cell design, the measurements of the real and imaginary components of impedance were measured at 0.1 kHz, 1.0 kHz, 10.0 kHz, and 100 kHz. The observation of a frequency dependence would be indicative of capacitance coupling and poor cell design. The results of these measurements are tabulated in Table 5. The small imaginary component of the measured impedance does not show a systematic frequency dependence; therefore, within the experimental

TABLE 5

IMPEDANCE OF CONDUCTANCE CELL CONTAINING STANDARD SOLUTION OVER FOUR DECADES OF A.C. FREQUENCY

f/kHz	*ReZ*/Ω	*ImZ*/Ω
0.1	909.548	1.490
1.0	909.550	1.903
10.0	910.454	1.960
100.0	909.892	1.953

Solution: 1.9919×10^{-4} mol dm^{-3}

Specific Conductivity: 2.958035×10^{-5} S cm^{-1}

Temperature: 24.985 ± 0.003 °C

V_{output}: 50 mV

limitations (concentration and temperature measurement) the precision of the resistance measurements at frequencies ≥ 1.0 KHz is 0.05%. Since subsequent measurements were to be taken at 1.0 kHz, the resistance value at that frequency was used in the determination of the cell constant.

From equation 1,

$$K = R\kappa = (909.550 \pm 0.45\ \Omega)(2.9580 \times 10^{-5} \pm 0.0028 \times 10^{-5}\ S/cm)$$

$$= 2.69048 \times 10^{-2} \pm 0.0039 \times 10^{-2}\ cm^{-1}$$

This is a first approximation of the cell constant. When the conductivity of the solution was measured no account was made for the conductivity of the water. The resistance of the water is measured and, using the first approximation of

the cell constant, a new cell constant is calculated from the corrected resistivity. Successive iterations were made until a self-consistent value was obtained for the cell constant. With a resistance of 15120 Ω for the cell containing water, the conductivity of the water was found to be 0.936×10^{-6} S cm^{-1}* with a self-consistent value for the cell constant of

$K = 2.86265 \times 10^{-2} \ (\pm \ 0.00415 \times 10^{-2}) \ cm^{-1}$.

Temperature correction - A temperature correction was applied to the cell constant as given by equation 5. This provides a value of the cell constant that is normalized to 25.000 °C. This normalized value is

$K = 2.86179 \times 10^{-2} \ cm^{-1} \ (25.000 \ °C)$.

Temperature corrections were applied as necessary to each subsequent measurement.

Specific conductivity of 2MeTHF - Dipolar-aprotic solvents typically have very large values of pK_s (>20) compared with water. As a result, a properly prepared solvent will have a very small specific conductivity (ca. 10^{-7} to 10^{-8} S cm^{-1}). Conductivity of this small magnitude in conjunction with the

---

*The value of $\kappa_{solvent}$ is not exactly the same as the measured value. This is because the introduction of solute will increase the ionic strength. The mobilities of the solvent "ions" decrease and the activity coefficients and degrees of dissociation of the water are affected.

cell constant used will produce a measured resistance of 286 kΩ to 2.8 MΩ. Under these conditions it is common practice to shunt the cell with a known high resistor, R_{shunt}, and to calculate R_{cell} from equation 2.

Shunt resistances for these measurements were provided by a Leeds and Northrup 4754 decade box (up to 100 kΩ) and by an IET Labs RS200 resistance box (up to 10.0 MΩ). Both had previously been calibrated. Measurements of the cell resistance were made versus shunt resistances of 10 kΩ, 15 kΩ, and 20 kΩ. The average value of R_{cell} from the three measurements was used to determine the specific conductivity. The value for κ was determined for each batch of solvent that was used in the conductivity studies with a mean value of

$$\kappa_{2MeTHF} = 9.01 \times 10^{-8} \text{ S/cm } (\pm 2.18 \times 10^{-8} \text{ S/cm}) \text{ at } 25.000 \pm ^{\circ}C$$

Conductivity measurements in $LiCF_3SO_3$/2MeTHF solutions - There are essentially three ways of proceeding with measurements of the molar conductance. For individual runs each solution is made up separately by weight from the solvent and solute. This is time consuming and wasteful of material (a concern here is with the time and expense of solvent preparation). For concentration runs a given quantity of solvent is placed in the cell and the solvent conductivity is measured first. Additions are then made of a concentrated stock solution or of the pure solute. Dilution runs were performed in this work. A specific amount of the concentrated solution

is placed in the cell and its conductivity is measured. After each measurement the solution is diluted with increments of solvent. The solvent additions were made gravimetrically. Two dilution runs were performed (on two different stock solutions) in order to provide more data for analysis. Several of the less concentrated solutions were prepared individually in order to minimize the uncertainty in their concentrations. The results of these measurements and the method of preparation of each solution are given in section 5.1

In making the dilutions and measurements two effects were to be considered and prevented. One was the drift of conductivity with time which was investigated by Prue (78). This effect is minimized by proper cell design, but will still tend to occur if the solution has been allowed to stand in the cell for a time before measurement (an unavoidable occurrence due to the finite time that it takes to thermostat a solution). Fortunately this effect can be wholly or partially reversed on shaking or stirring the solution. The second effect is the so-called Soret effect which was investigated by Stokes (85). When the cell containing solution at one temperature is immersed in a bath at another temperature, a temperature gradient which is introduced to the solution will produce a concentration gradient which may not dissipate for hours or days. The resistance of the cell will achieve an almost constant value after a few hours, but

this will not be the correct value. This effect can introduce an error of about 0.1% and is proportional to the initial temperature difference and upon the nature of the solute and solvent. The Soret effect can be minimized by stirring and by thermostating the solvent (for dilutions) before additions can be made to the cell. A period of 24 hours is usually allowed between dilution and measurement in order to be reasonably certain that the Soret effect has become dissipated.

A precision of 1 part in 10^3 or 10^4 was easily attained for the conductance measurements. As with the standard KCl solution, the frequency dependence was checked. A small variation (<0.5%) was observed and this effect was removed by measurement at 5KHz, 10KHz, 20KHz, 50KHz, and 100KHz and extrapolation to infinite frequency. The measured impedance quickly and asymptotically approaches a constant value.

4.2 NUCLEAR MAGNETIC RESONANCE

Measurements of NMR chemical shifts as a function of concentration can be used to study ion-association (73,74,86-89). Ionic-association can modify any or all of the usually measured NMR parameters - relaxation, chemical shifts and spin-spin couplings. Although chemical shift measurements are less sensitive than relaxation measurements, they are more convenient experimentally or computationally.

It is usually assumed that the measured shift is composed of a concentration weighted average of the shifts for the free ion and ion pair. Appropriate rearrangement of the pertinent relationships will yield linear equations (71,86) from which equilibrium constants can be derived.

The nuclear magnetic resonance of ^{7}Li offers a very sensitive probe for such studies. Cahen et al., (88) and Macell (89) have used the ^{7}Li NMR technique to study lithium ion solvation and ion-association, respectively. The chemical shifts of the $^{7}Li^{+}$ ion are sensitive to the solvent, the salt concentration, and the anion present. The method has become very popular in spite of the fact the knowledge of ion-ion interactions that is gained is somewhat disappointing due to inadequate theories for quantitative predictions of chemical shifts.

4.2.1 NMR MEASUREMENTS

In order to provide information on Li^{+} ion-pairing in solution, complementary to data derived from the conductance determinations, ^{7}Li NMR measurements were made at 28.6227 MHz in the pulsed Fourier transform mode on a Varian XL-100 Nuclear Magnetic Resonance Spectrometer. The field was locked (± 1 Hz) on a proton resonance with an external probe. All of the ^{7}Li shift measurements were referenced to an external solution of 1.0 M LiCl in D_2O. The measurements

were made at 25 ± 1 °C in 10 mm o.d. NMR tubes. The chemical shifts were recorded to ± 0.01 ppm unless otherwise noted.

Solution preparation - solutions for the NMR measurements were prepared in 2MeTHF as described in section 3 of this chapter. The concentration was varied over approximately three decades.

5. EXPERIMENTAL RESULTS

5.1 ELECTROLYTIC CONDUCTANCE

Since almost all the equations that are used for analysis of conductance data as a function of concentration are ultimately based upon the Debye-Hückel theory (indeed all of the equations are based upon some form of a limiting law), the approximations of this theory will limit the valid concentration range. For many authors, the "acceptable" upper limit of concentrations has been that which produces $\kappa a \approx 0.1$, where the κ is the inverse of the well known Debye-Hückel ionic atmosphere radius or shielding length and "a" is the "distance of closest approach" of the ions in solution. If one assumes an arbitrary value of 0.5 nm for a, then this concentration, for 2MeTHF, would be 3.4×10^{-4} mol/Kg (2.96×10^{-4} mol/L) at 298 K. In solvents of very low dielectric constant (6.26 for 2MeTHF at 298 K) the formation of triple-ions (and higher aggregates) must also be considered and this

places a further limitation on the concentration range. Fuoss and Accascina (90) have proposed an upper concentration (below which triple-ion formation can be neglected) limit for 1:1 electrolytes at 298 K in solvents of low dielectric constant. This limit, which considers ion-pair behavior only, is given by

$$c_{limit} = 3.2 \times 10^{-7}\varepsilon^3 \qquad [6]$$

where ε is the dielectric constant. Since triple-ions are conducting species, the full theoretical analysis of the data that are obtained at concentrations very much greater than c_{limit} is rather complex. This concentration in the case of 2MeTHF is 7.85×10^{-5} mol/L. This criterion presents a practical problem since measurements of conductance at the lower end of the concentration range are less precise.

Two somewhat arbitrary concentration limits for conductivity measurements have been presented (2.96×10^{-4} mol/L and 7.85×10^{-5} mol/L for 2MeTHF), above which the formation of triple-ions and higher aggregates must be considered. The fact that these "limits" differ by more than an order of magnitude is a moot point because of experimental limitations outlined below.

Limitations on the preparation of solutions for these measurements are obvious - very small quantities of desiccative solute must be weighed and very large quantities of anhydrous solvent must be prepared (and weighed). A further

and great practical problem exists in lithium salt solutions in low dielectric constant solvents where very large association constants and triple-ion formation arise: for solutions at concentrations less than 10^{-3} mol/L, the solvent correction is very large. That is, the measured conductivity for the solution is on the same order of magnitude as the conductivity of the pure solvent. Thus, measurements could only be made on solutions that were more than an order of magnitude higher in concentration than the prescribed concentration "limits". The consequences of this limitation will be discussed in the next section.

A full analysis of the conductance-concentration data requires additional information. A knowledge of the temperature, dielectric constant and viscosity are necessary for use in any of the theoretical equations. The viscosity and dielectric constant data were interpolated from the data in reference 1.

The results of the conductance measurements are presented in Table 6.

TABLE 6

MEASURED VALUES OF ELECTROLYTIC CCONDUCTANCE FOR $LiCF_3SO_3$/2MeTHF SOLUTIONS AT 298 K

Run	Concentration $\times 10^{-3}$ mol/L		Conductivity $\times 10^{-3}$ S cm^2/eq	
i. s.	1.0449	± 0.0013	0.3883	± 0.0211
i. s.	1.1317	± 0.0012	0.3678	± 0.0194
i. s.	1.4741	± 0.0010	0.3323	± 0.0149
1	1.5842	± 0.0065	0.3210	± 0.0139
1	1.9962	± 0.0052	0.2980	± 0.0110
2	2.3712	± 0.0058	0.2674	± 0.0092
1	2.6192	± 0.0041	0.2590	± 0.0084
2	2.9484	± 0.0048	0.2467	± 0.0075
1	3.7345	± 0.0031	0.2266	± 0.0059
i. s.	3.7850	± 0.0003	0.2195	± 0.0058
2	4.7141	± 0.0026	0.2068	± 0.0047
2	5.6773	± 0.0017	0.1939	± 0.0039
1	5.9717	± 0.0024	0.1946	± 0.0037
2	6.5317	± 0.0011	0.1831	± 0.0034
1	8.4922	± 0.0018	0.1741	± 0.0026
2	9.4551	± 0.0006	0.1677	± 0.0021
1	11.399	± 0.001	0.1598	± 0.0019
2	12.028	± 0.001	0.1592	± 0.0018
1	14.435	± 0.001	0.1557	± 0.0015
1	18.837	± 0.001	0.1493	± 0.0011
1	24.325	± 0.001	0.1476	± 0.0009
1	32.328	± 0.001	0.1469	± 0.0007
1	42.035	± 0.001	0.1506	± 0.0005
1	66.252	± 0.001	0.1618	± 0.0003

Run refers to the dilution run in the conductivity cell;
i. s. refers to individually prepared solutions.

5.1.2 ANALYSIS OF ELECTROLYTIC CONDUCTANCE DATA

A complete theory of electrolytic conductance data would allow the calculation of ion mobilities at infinite dilution and the mobilities at finite concentrations as the increase in the number of ions introduces interionic effects. At present, no sufficiently adequate theory exists. Because of this, the choice of a conductance equation for analysis of data is as important as cell design, solution preparation, etc., for obtaining meaningful results.

The early conductance equations were largely empirical and were directly derived from the Debye-Hückel theory for dilute electrolyte solutions. An equation developed by Onsager (91,92) for unassociated electrolytes is of limited use. The well known equation

$$\Lambda = \Lambda_\circ - Sc^{1/2} \qquad [7]$$

allows the extrapolation of conductance data to find $\Lambda_\circ$, but one is normally interested in analyzing data over a finite concentration range (where interionic effects are appreciable).

Extensions have been made to the Debye-Hückel model which take into account ionic size. For unassociated electrolytes, a frequently used form of these equations is, for example, that due to Fuoss, Onsager, and Skinner (93),

$$\Lambda = \Lambda_o - Sc^{1/2} + Ec \log c + (J - F\Lambda_o)c + J_2c^{3/2} \qquad [8]$$

which can be put into a more general form

$$\Lambda = \Lambda_o - Sc^{1/2} + Ec \ln c + J_1c - J_2c^{3/2} \qquad [9]$$

The terms S, E, J_1, and J_2 contain contributions from the electrophoretic effect and the relaxation effect. The J_1 and J_2 terms also contain a correction for viscosity changes.

In non-aqueous solutions, where the dielectric constant is usually quite low (<40), appreciable ionic association can occur which will contribute non-conducting species to the solution. For a reaction,

$$M^+ + A^- = MA \quad \text{(MA is non-conducting)} \qquad [10]$$

the association constant can be expressed as

$$K_p = \frac{[MA]}{[M^+][A^-]} = \frac{(1-\alpha)f_o}{\alpha^2 c f_\pm^2} \qquad [11]$$

where α is the fraction of free ions or degree of dissociation of MA, f_o is the activity coefficient of the ion-pair (usually taken as unity), and $f_\pm$ is the mean ionic activity coefficent of the dissociated ions. When ion-association is considered, equation 9 becomes

$$\Lambda = \Lambda_o - S(\alpha c)^{1/2} + E\alpha c \ln(\alpha c) + J_1\alpha c - J_2(\alpha c)^{3/2} - K_p\alpha c f_\pm^2 \qquad [12]$$

Other equations, e.g., the Pitts equation (94), make use of the same model for the electrolyte solution; however, the use of different boundary conditions to evaluate constants leads to differences in the results obtained by the Pitts equation versus those obtained by the Fuoss equations. Two other equations are of note: the Fuoss-Hsia equation (95) and the Justice equation (96). In the Fuoss-Hsia equation, the previous treatment of Fuoss and Onsager was modified by recalculating the relaxation field and retaining certain terms which had been neglected. For associated electrolytes, Justice modified equation 8 and the activity coefficient equation to include the Bjerrum distance, q, instead of the distance parameter, a. The choice of the Bjerrum distance ($q = z^2e^2/8\pi\varepsilon\varepsilon_o kT$) is a result of choosing Bjerrum's definition* of an ion pair rather than the definition of Fuoss.

Three parameters are obtained from analysis of conductance-concentration data via these "full" conductance equations. These are the limiting equivalent conductance, Λ_o, the so-called distance parameter, a, and the association constant for ion-pair formation, K_p. Where data are available that have been obtained in the prescribed concentration

---

*It is to be noted that Bjerrum's definition of q leads to an unrealistic ion-pair contact distance in low ε solvents, very much larger than that corresponding even to contact of solvated cation with solvated anion.

range, all of the equations will give essentially the same values for Λ_o. In most cases the equations will yield values of K_p that are very similar; this is particularly true for large values of K_p (large degree of ion-association). Proper interpretation of the distance parameter is not as obvious. It can only be concluded that the "distance parameter" is an effective collision distance in solution - a measure of the force field in solution and the average success of an ion in displacing solvent molecules from the immediate vicinity of another ion.

In solvents with very low dielectric constants ($\varepsilon<10$) higher states of aggregation are probable (triple-ions, etc.). Under these circumstances, the models for ion-association and the conductance equations that are based upon pair formation (e.g., equation 12) are invalidated.

The concept of triple-ion formation was first introduced by Fuoss and Kraus (97) to explain the occurrence of a minimum in the concentration-dependence of the electrolytic conductivity of electrolytes in solvents of low dielectric constant. This interpretation of the conductance data was most frequently used to determine the equilibrium constants for

$$MA + A^- = (AMA)^- \qquad [13a]$$

and

$$MA + M^+ = (MAM)^+ \qquad [13b]$$

with the assumption being made that

$$\frac{[AMA^-]}{[MA][A^-]} \cong \frac{[MAM^+]}{[MA][M^+]} = K_t \qquad [14]$$

The formation of quadruplets and higher states of aggregation is probable, but they have not been given extensive theoretical consideration. The effect of triple-ion formation is to remove some of the non-conducting species, MA, from solution and replace them with triple-ions which contribute to the conductance. The equation derived by Fuoss and Kraus for 1:1 electrolytes is

$$\Lambda c = \Lambda_o/K_p^{1/2} + \Lambda_o^t K_t c/K_p^{1/2} \qquad [15]$$

When interionic effects are taken into account, equation 15 becomes,

$$\Lambda g(c) c^{1/2} = \Lambda_o/K_p^{1/2} + (\Lambda_o^t/K_t K_p^{1/2})(1-(\Lambda/\Lambda_o))c \qquad [16]$$

with,

$$g(c) = f_\pm/((1-z)(1-(\Lambda/\Lambda_o))^{1/2}) \qquad [17]$$

and

$$z = S(\Lambda c)^{1/2}/\Lambda_o^{3/2} \qquad [18]$$

where S is the Onsager coefficient.

A plot of $\Lambda g(c)c^{1/2}$ versus $c(1-(\Lambda/\Lambda_o))$ should be a straight line with $\Lambda_o/K_p^{1/2}$ as the intercept and $\Lambda_o^t/K_tK_p^{1/2}$ the slope. In order to obtain values for K_p and K_t, a value for Λ_o must be assigned. A value for Λ_o can be estimated by Walden's rule ($\eta\Lambda_o$ = constant). For Λ_o^t, the limiting conductance of the triple-ion, the assumption is made that $\Lambda_o^t = \Lambda_o/3$ on the reasonable grounds that the species that make up the triple-ion collectively contribute only one charge, ±ze, to the solution.

Evaluation of the conductance parameters - Walden's rule is used along with the data in Table 7 to compute an estimated value for Λ_o. The calculated value of Λ_o for $LiCF_3SO_3$ in 2MeTHF is estimated as 135.09 S cm^2/equiv., which subsequently yields a value of 45.03 S cm^2/equiv. for Λ_o^t. Next, a value for the Onsager coefficient is estimated. This can be done using the calculated value for Λ_o through the equation

$$\Lambda = \Lambda_o - S(\alpha c)^{1/2} \quad \text{where} \quad \alpha = \Lambda/\Lambda_{o(calc)} \qquad [19]$$

The validity (or lack thereof) of obtaining the Onsager coefficient in this manner will be discussed later. Using equation 19, a value for S of 232 S $cm^{1/2}$/$equiv^{3/2}$ was obtained.

With this value for the Onsager coefficient, the denominator in equation 17 will be close to unity and the value for g(c) will be will be governed largely by the value of the activity coefficient. Thus, the form of the expression that

TABLE 7

DATA FOR ESTIMATION OF Λ_o FOR $LiCF_3SO_3$

Λ_o	$NaCF_3SO_3$	in DMSO	=	36.82 S cm^2/equiv	reference	98
$\eta\lambda_o^+$	Na^+	in DMSO	=	0.287 P S cm^2/equiv		99
$\eta\lambda_o^-$	$CF_3SO_3^-$	in DMSO	=	0.449 P S cm^2/equiv		99
λ_o^+	Li^+	in THF	=	36.6 S cm^2/equiv		100
η	DMSO		=	0.0199 P		7
η	2MeTHF		=	0.00457 P		1
η	THF		=	0.0046 P		1

is used for the activity coefficient becomes important as it may have a bearing on the result. Initially, the expression that was used was the Debye-Hückel limiting form with a correction for the finite size of the ions:

$$\log f_{\pm} = -Az_1z_2(\alpha c)^{1/2}/(1 + aB(\alpha c)^{1/2}) \qquad [20]$$

where

$$A = 1.8246 \times 10^6/(\varepsilon T)^{3/2} \quad L^{1/2}/mol^{1/2} \qquad [20a]$$

and

$$B = 5.029 \times 10^9/(\varepsilon T) \quad L^{1/2}/mol^{1/2}\ cm \qquad [20b]$$

Consideration was made for the use of the Davies form of the activity coefficient equation which includes an additional term linear in c, but at these small ionic strengths the addition of the extra term made no difference in the

result. Equation 20 does contain a distance parameter and two very different values were used for a. The Bjerrum distance (4.47 nm) was first used as a distance in the denominator. Then, for comparison, the Debye-Hückel relation was used with a distance that more closely resembles the "contact distance" for the ions. This value was arbitrarily set at 0.5 nm, a distance that is commonly reported as a contact distance or "best fit" distance for lithium salts in non-aqueous solutions.

The conductance-concentration data have been presented in the "traditional" manner - molar conductance versus square-root of concentration in Figure 12. However, with the data that were obtained, it is difficult to visualize the limiting behavior since the limiting molar conductance is almost three orders of magnitude beyond the range of this graph. The data have instead been presented in a log(molar conductance) versus log(concentration) format (Figure 13) which more clearly shows the relation approaching a limiting slope at low concentrations. The larger uncertainties at the lower concentrations reflect the larger magnitude of the solvent correction at low solute concentrations.

Numerical evaluation of the conductance-concentration data

The computations (through equations 16-18) were performed by means of the program ***FIT***. ***FIT*** executes a non-linear least-squares calculation based upon the general statistical method of Wentworth and Deming (101,102). The program assigns a

statistical weight to each data point which is related to the uncertainty in the measured value of that point. In this way the calculated parameters reflect the uncertainties of the experimental measurements in a more realistic way. Details of the program and a listing of *FIT* appear in the appendix.

Separate calculations were made utilizing the data from dilution runs 1 and 2. In both cases the calculations included data points that were generated from experiments on the individually prepared solutions. In addition, the data were processed by means of equation 15 (neglecting interionic effects) to facilitate the discussion of the interionic effects terms. The results are presented in Table 8 and graphically in Figures 12 and 13.

5.2 NMR RESULTS AND ANALYSIS

Experimental studies of the chemical shifts of ions in aqueous and non-aqueous solutions of inorganic salts have been mainly concerned with establishing the relative effects of different ions. Other aspects of the research have been concerned with the shape of the chemical shift versus concentration curve. In principle, significant quantitative information can be deduced about an ion-pair structure from the magnitude of the chemical shifts or from its dependence on the anion (for example, the distinction between solvent-separated and contact ion-pairs).

TABLE 8

EQUILIBRIUM CONSTANTS FOR ION-PAIRS AND TRIPLE-IONS AS DETERMINED BY THE FUOSS-KRAUS EQUATION FOR $LiCF_3SO_3$ IN 2MeTHF

	K_p M^{-1}	K_t M^{-1}
Using a = q = 4.465 nm		
Run 1	1.428×10^8	177.8
Run 2	1.246×10^8	133.9
All Data	1.423×10^8	177.1
Weighted Average	1.314×10^8	160.6
Using a = 0.5 nm		
Run 1	1.352×10^8	149.6
Run 2	1.255×10^8	124.7
All Data	1.352×10^8	149.3
Weighted Average	1.314×10^8	139.8
Using no interionic force term, i.e., g(c) = 1		
Run 1	1.248×10^8	110.8
Run 2	1.272×10^8	113.6
All Data	1.252×10^8	111.1
Weighted Average	1.257×10^8	111.9

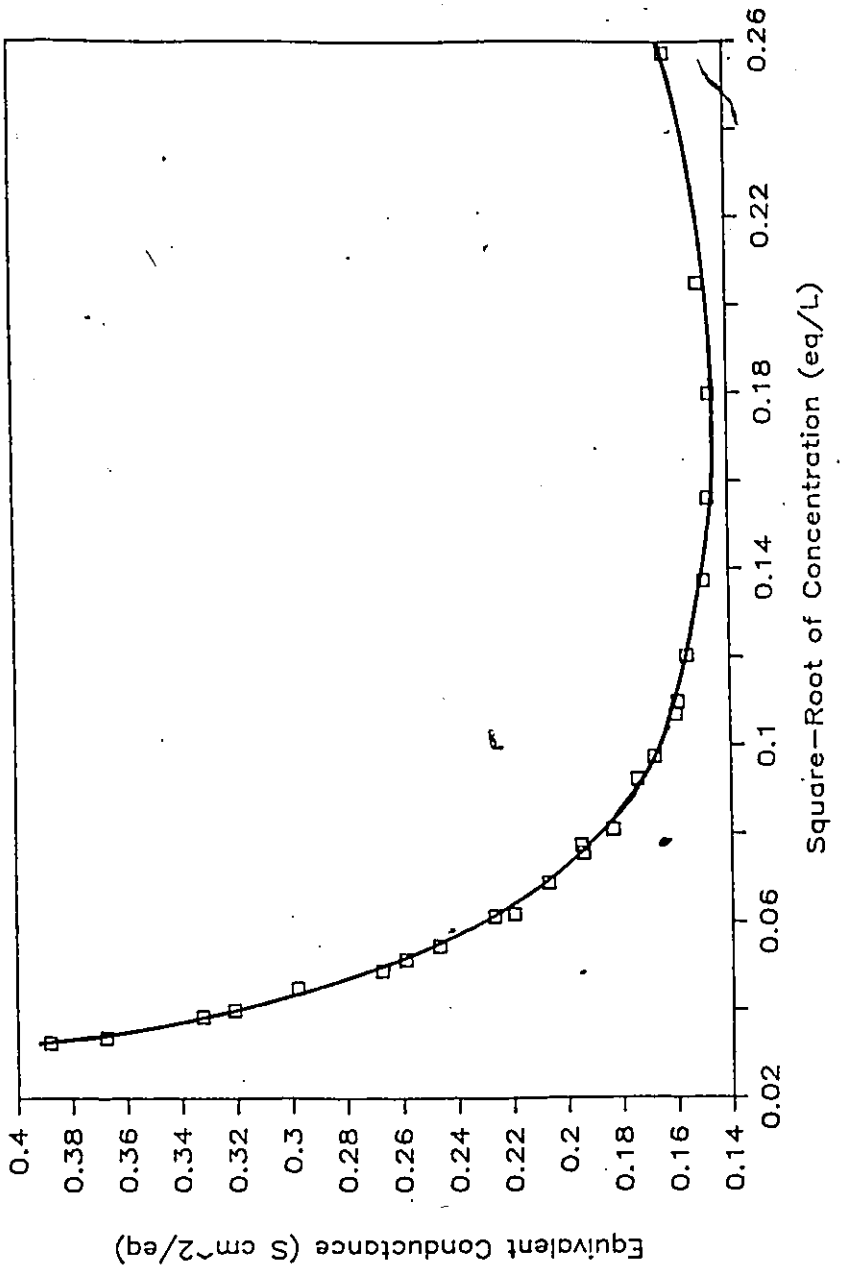

FIGURE 12

EQUIVALENT CONDUCTANCE VS SQUARE-ROOT OF CONCENTRATION FOR $LiCF_3SO_3$ IN 2-METHYL-TETRAHYDROFURAN

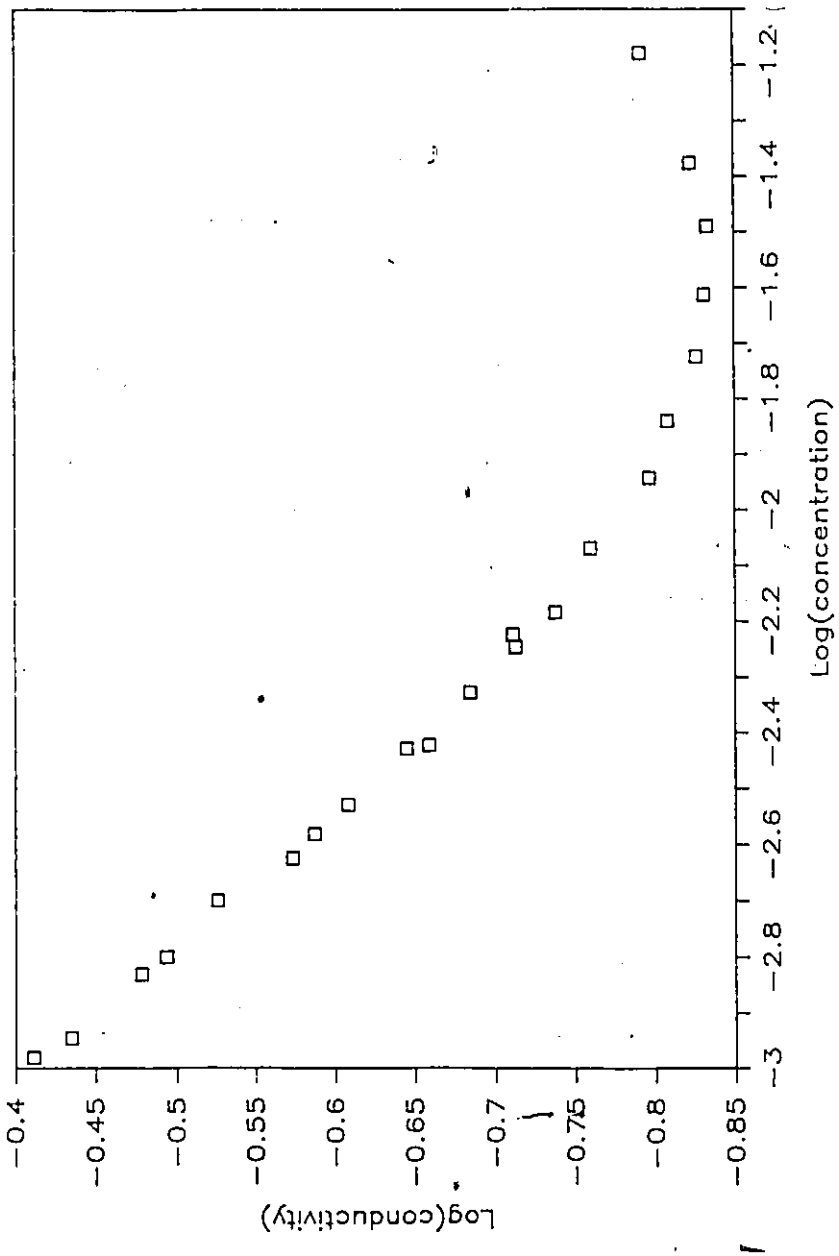

FIGURE 13

LOG(**EQUIVALENT CONDUCTANCE**) VS LOG(**CONCENTRATION**)
FOR $LiCF_3SO_3$ IN 2-METHYL-TETRAHYDROFURAN AT 298 K

The magnitude of the chemical shift change varies strongly among the alkali ions with the range of chemical shifts increasing on going from Li^+ to Cs^+. For an alkali metal cation in a given solvent it is seen that the chemical shifts for all of the salts of that ion approach the same limiting value at infinite dilution. It is reasonable to assume that this limiting value represents the chemical shift of the free alkali metal ion in that particular solvent.

Popov (87) measured ^{23}Na chemical shifts as a function of concentration in a number of solvents. A correlation was observed between the infinite dilution chemical shift and the solvating ability (as expressed by the Gutmann donor number, DN) for the solvents used. Nitromethane, the least solvating of the solvents that were examined, has the largest upfield (from water) chemical shift. Strongly solvating solvents, such as hexamethylphosphoramide, have the largest downfield shifts. It was also observed by Popov that there is *no correlation* between these chemical shifts and the polarity of the solvents, expressed either as the dielectric constant or the dipole moment. Popov plotted the infinite dilution ^{23}Na chemical shifts against the donor number for several solvents with the data yielding an approximately linear correlation. The two parameters *should* be of a different nature, since the donor numbers reflect a covalent interaction between a donor and an acceptor while the chemical shifts reflect electrostatic ion-dipole interaction. The correlation was attribu-

ted to a partial electrostatic character for the solvent-$SbCl_5$ bond (re the use of $SbCl_5$ in the determination of Gutmann donor numbers) and/or some degree of covalency in the solvent-cation interaction (87).

The concentration dependence of alkali metal chemical shifts has been attributed to the formation of contact ion-pairs (73,74,86-89). This raises the question of the definition of an ion-pair as recognized by NMR. If the measured chemical shift is a weighted average of the free-ion and ion-pair chemical shifts then, as the concentration of the salt increases and the concentration of ion-pairs increases, so too will the magnitude of the measured chemical shift. With electrolytic conductance, an ion pair is "formed" when the ions are close enough that they affect their mutual ability to conduct electricity. This may occur even when the ions are separated by one or more solvent molecules. In order for a species, e.g., an anion to affect the environment of the alkali metal ion's nucleus enough to effect the shielding of the cation nucleus and cause a shift in its resonance frequency, the counter species must approach very closely.

In the case of ions they must essentially be in contact. The chemical shift changes arise mainly from changes in paramagnetic shielding, an effect which varies as $1/r^3$. Thus, NMR would be expected to detect a tighter ion-pair than that detected by electrolytic conductance. The observation

of ion-pairing by NMR presupposes an appreciable difference between the chemical shifts produced by ion-ion and ion-solvent interactions. If the ion-solvent interactions are very strong then the analysis of the chemical shift data is much more complex.

The properties of the ^{7}Li nucleus are also favorable for nuclear studies. However, the magnitude of the chemical shifts is small, ranging from 2.90 ppm upfield (from water) in acetonitrile, to 2.54 ppm downfield in pyridine (87,88). In contrast to the case of ^{23}Na NMR, no correlation was found between ^{7}Li chemical shifts and the solvent donor numbers (87). For the ^{23}Na nucleus the paramagnetic screening constant is much larger than the diamagnetic screening constant while for lithium, the two terms are of approximately the same magnitude and tend to cancel each other. As a result, specific properties of solvent molecules, such as polarizabilities, become important for ^{7}Li chemical shifts. It has also been noted that in solvents of low or intermediate solvating ability, that the ^{7}Li chemical shifts are strongly influenced by the presence of small amounts of water (88). Since it is almost impossible to make organic solvents completely anhydrous, meaningful chemical shifts for the $^{7}Li^{+}$-ion can only be obtained if the concentration of water is much smaller than the concentration of the salt.

As mentioned previously, the observation of a concentration dependence of ^{7}Li chemical shifts is an indication of

the presence of contact ion-pairs. The studies have also indicated that the chemical shift is strongly influenced by the anion of the lithium salt (73,74,86-89).

Using the proton resonances of the methylene protons in $(nBu)_4N^+$, Buckson and Smith (86) followed ion association in the system

$$(nBU)_4N^+ + I^- = (nBu)_4N^+ \cdot I^-$$

with a relationship between the observed shift, Δ_{obs}, and the concentration c,

$$\frac{\Delta_{obs} - \Delta_i}{(\Delta_p - \Delta_{obs})} = \frac{K_p'}{(\Delta_p - \Delta_i)} c \qquad [21]$$

where K_p' is the ion-pair formation constant as determined by NMR, Δ_i is the chemical shift of the free-ions (i.e., the chemical shift of $^7Li^+$ at infinite dilution) and Δ_p is the chemical shift of the ion-pairs.*

---

*Recall that the observed chemical shift is a weighted average of the chemical shift for the free-ions and the ion-pairs

$$\Delta_{obs} = \alpha\Delta_i + (1-\alpha)\Delta_p$$

It should be noted that the degrees of dissociation that are derived from the NMR measurements are about two orders of magnitude greater than those derived from conductance measurements. For example, at a concentration of 50×10^{-3} mol/L the degrees of dissociation are α(NMR) $\approx$ 0.150 and α(conductivity) $\approx$ 0.001. This would be expected since NMR detects ions in close contact whereas conductance methods will detect a more loosely held pair.

In many cases ion-association is so prevalent even at the lowest accessible concentrations that the chemical shift is changing rapidly with concentration. This makes the determination of the chemical shift of the free ion (Δ_i) difficult. As with the value for Λ_o for conductance, the value of Δ_i can be estimated. It has been shown by conductance measurements that triiodide salts behave as strong electrolytes in non-aqueous solutions (103). It was also found that the chemical shifts of LiI_3 were essentially independent of concentration in all of the salts that were examined (88) and that the chemical shifts in 0.02 M LiI_3 are reasonably close to the limiting chemical shifts, Δ_i, for the Li^+ ion in the same solvents. ***NOTE***: in cases where the extrapolations of the chemical shifts to infinite dilution <u>are</u> possible, the value obtained for LiI_3 agrees with the extrapolated value (88). A value for Δ_i was obtained in this manner using a 0.02 M LiI_3/2MeTHF solution and measured as described in section 4.2.1.

At the higher concentrations it is expected that associated ions will predominate. Thus, it was assumed that the value of the chemical shift of the ion-pairs, Δ_p, could be given by the chemical shift that was approached at high concentrations.

The data from the ^7Li NMR chemical shift measurements are presented in Table 9. The measured values of the chemical shift have not been corrected for the bulk susceptibility of

TABLE 9

^{7}Li CHEMICAL SHIFTS FOR $LiCF_3SO_3$ IN 2MeTHF AS A FUNCTION OF CONCENTRATION

Concentration mol/L	Chemical Shift ppm
0.1782×10^{-3}	-0.54
0.9242	-0.58
3.94	-0.62
10.4	-0.65
19.7	-0.67
50.5	-0.70
51.5	-0.72
98.5	-0.75
107.5	-0.76
197.0	-0.82
220.8	-0.85
355.0	-0.89
492.5	-0.94
618.3	-0.92
884.0	-0.97
1201.1	-0.97

^{7}Li Chemical Shift of 0.02 M LiI_3 in 2MeTHF is +0.82 ppm

All chemical shifts are referenced to 1.0 M LiCl in D_2O. Temperature = 25°C

the solvent. This should not affect the results because of the relative nature of the measurements. The NMR data are presented graphically as Δ_{obs} versus $c^{1/2}$ (for clarity) in Figure 14. The data are also presented in Figure 15 as a $\log[(\Delta_{obs}-\Delta_i)/(\Delta_p-\Delta_i)]$ versus log(c) plot. The quantity $(\Delta_{obs}-\Delta_i)/(\Delta_p-\Delta_i)$ provides a chemical shift that is represented as a fraction of the difference between the chemical shift of the free-ions, Δ_i, and of the ion-pairs, Δ_p. This fractional chemical shift is referred to as the *normalized* chemical shift. It is interesting to note that the abrupt change in the slope of Figure 15 occurs at about the same concentration as the minimum in the log(Λ) vs log(c) curve. This minimum in the conductance was attributed to triple-ion formation.

The data were fitted to equation 21 using the program ***FIT***. For the concentration range 3.94×10^{-3} M to 107.5×10^{-3} M the data gave a straight line whose slope yielded a value of 399 M^{-1} for K_p' (Figure 16). Both below and above this concentration range the slope increases rapidly. The use of the lowest two concentrations (where the limiting slope is approached) yields a value of $K_p' = 4440\ M^{-1}$.

Triple-ion formation - Alternatively, the NMR shift data can be interpreted in terms of the formation of triple-ions. Such interpretations must rely on precise measurements (more precise than have been presented here) and upon assumptions - different than those made for the conductivity data analysis - regarding the nature of the triple ions that are formed and their associated equilibria.

The equilibria associated with these aggregates are as follows:

$$M^+ + A^- = MA \quad ; \quad K_p = \frac{[MA]}{[M^+][A^-]} \qquad [10]; [11]$$

$$MA + A^- = MA_2^- \quad ; \quad K_{t1} = \frac{[MA_2^-]}{[MA][A^-]} \qquad [13a]; [14a]$$

$$MA + M^+ = M_2A^+ \quad ; \quad K_{t2} = \frac{[M_2A^+]}{[MA][M^+]} \qquad [13b]; [14b]$$

For a solution with a salt concentration c, the material balance is given by:

$$\text{for M:} \quad c = [M^+] + [MA] + 2[M_2A^+] + [MA_2^-] \qquad [T\text{-}1]$$

$$\text{for A:} \quad c = [A^-] + [MA] + 2[MA_2^-] + [M_2A^+] \qquad [T\text{-}2]$$

with charge balance given by

$$[M^+] + [M_2A^+] = [A^-] + [MA_2^-] \qquad [T\text{-}3]$$

The subtraction of equation T-2 from T-1 yields equation T-3 thus leaving five equations in the five unknowns, $[M^+]$, $[A^-]$, $[MA]$, $[M_2A^+]$, $[MA_2^-]$.

In the absence of more precise data it can be assumed that the two ion-triplets M_2A and MA_2 are "equivalent" (the assumption is not phenomenologically correct, but it does allow for a simplified analysis congruous to the interpretation of the conductivity data). With this assumption, $K_{t1} = K_{t2} = K_t$ and the problem is reduced to three equations (10, 13a, T-1) in the three unknowns $[M^+]$, $[MA]$, and $[M_2A^+]$.

Let the fraction of M existing as M^+ be represented by

$$\alpha = \frac{[M^+]}{c}$$

and the fraction of M in ion-triplets by

$$\beta = \frac{2[M_2A^+] + [MA_2^-]}{c} = \frac{3[M_2A^+]}{c}$$

Thus, from equation T-1, the fraction of M existing in ion-pairs is given by

$$\frac{[MA]}{c} = 1 - \alpha - \beta$$

The NMR data are represented as follows:

Δ_1 = chemical shift of M as M^+

Δ_p = chemical shift of M in MA ion-pairs

Δ_{t1} = chemical shift of M in M_2A^+ triple-ions

Δ_{t2} = chemical shift of M in MA_2^- triple-ions

Δ_o = the observed chemical shift

The observed chemical shift is comprised of contributions from the chemical shifts of each of the existing species that

contain the M atom. Thus the observed chemical shift can be represented as

$$\Delta_o = \alpha\Delta_1 + (1-\alpha-\beta)\Delta_p + \frac{2[M_2A^+]}{c}\Delta_{t1} + \frac{[MA_2^-]}{c}\Delta_{t2}$$

$$= \alpha\Delta_1 + (1-\alpha-\beta)\Delta_p + \frac{[M_2A^+]}{c}(2\Delta_{t1} + \Delta_{t2})$$

With the assumption of the "equivalency" of the triple-ions a chemical shift due to the triple-ions (Δ_t) can be defined

$$3\Delta_t \equiv 2\Delta_{t1} + \Delta_{t2}$$

Thus,

$$\Delta_o = \alpha\Delta_1 + (1-\alpha-\beta)\Delta_p + \beta\Delta_t$$

$$= \alpha(\Delta_1-\Delta_p) + \beta(\Delta_t-\Delta_p) + \Delta_p$$

Utilizing the values of K_p and K_t that were derived from the conductivity measurements it is possible to calculate α and β. Equation T-4 can be solved by least-squares to find Δ_p, $\Delta_t-\Delta_p$, and Δ_p.

The approximate results yield $\Delta_p \approx -0.6$ ppm and $\Delta_t \approx 9$ ppm $\longrightarrow$ i.e., a very large downfield shift for the triple-ions. The conductivity and NMR data are compatible if $\Delta_t \approx 10$ is considered as a valid value for the chemical shift of the triple-ions. The results of these calculations, which were proposed by Prof. John Lorimer at the University of Western Ontario will be presented in a subsequent paper.

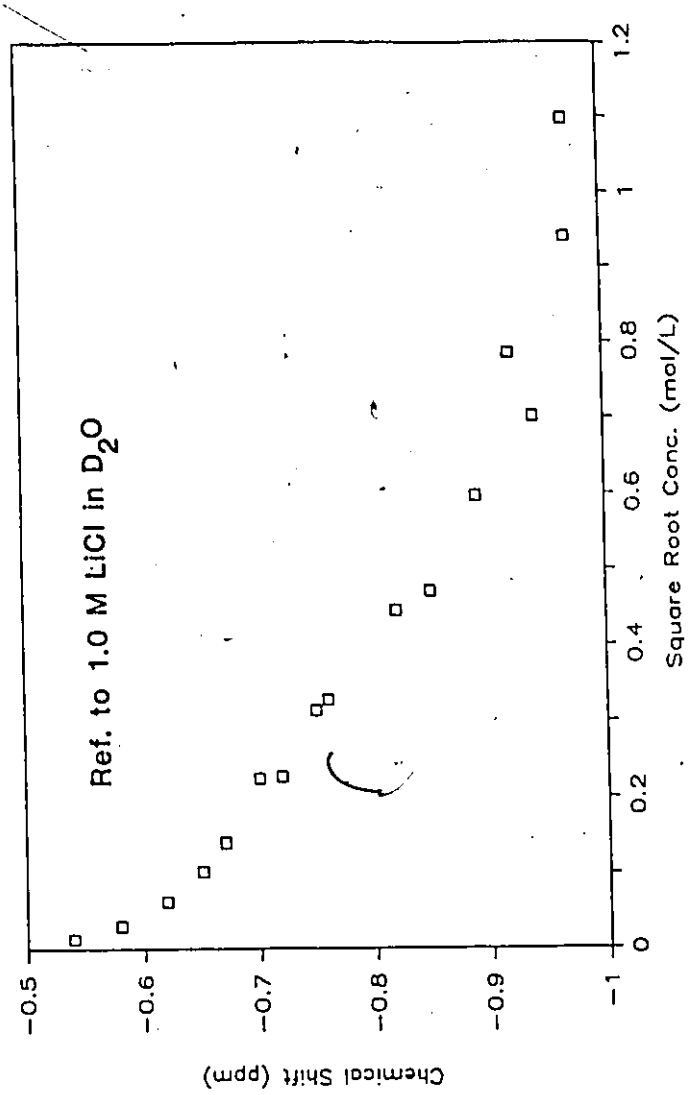

FIGURE 14

^{7}Li NMR CHEMICAL SHIFTS VS CONCENTRATION FOR $LiCF_3SO_3$ IN 2MeTHF AT 298 K

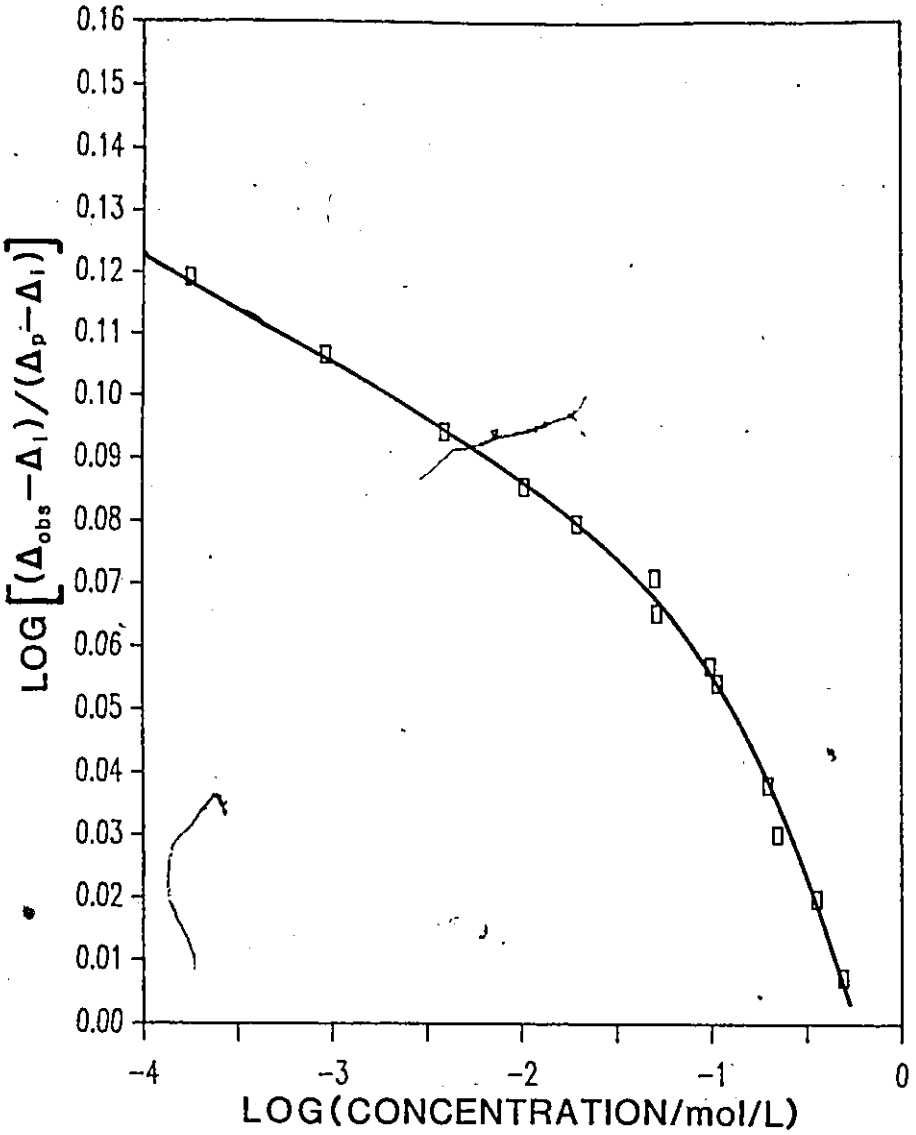

FIGURE 15

LOG(NORMALIZED CHEMICAL SHIFT) VS LOG(CONCENTRATION) FOR $LiCF_3SO_3$ IN 2MeTHF AT 298K

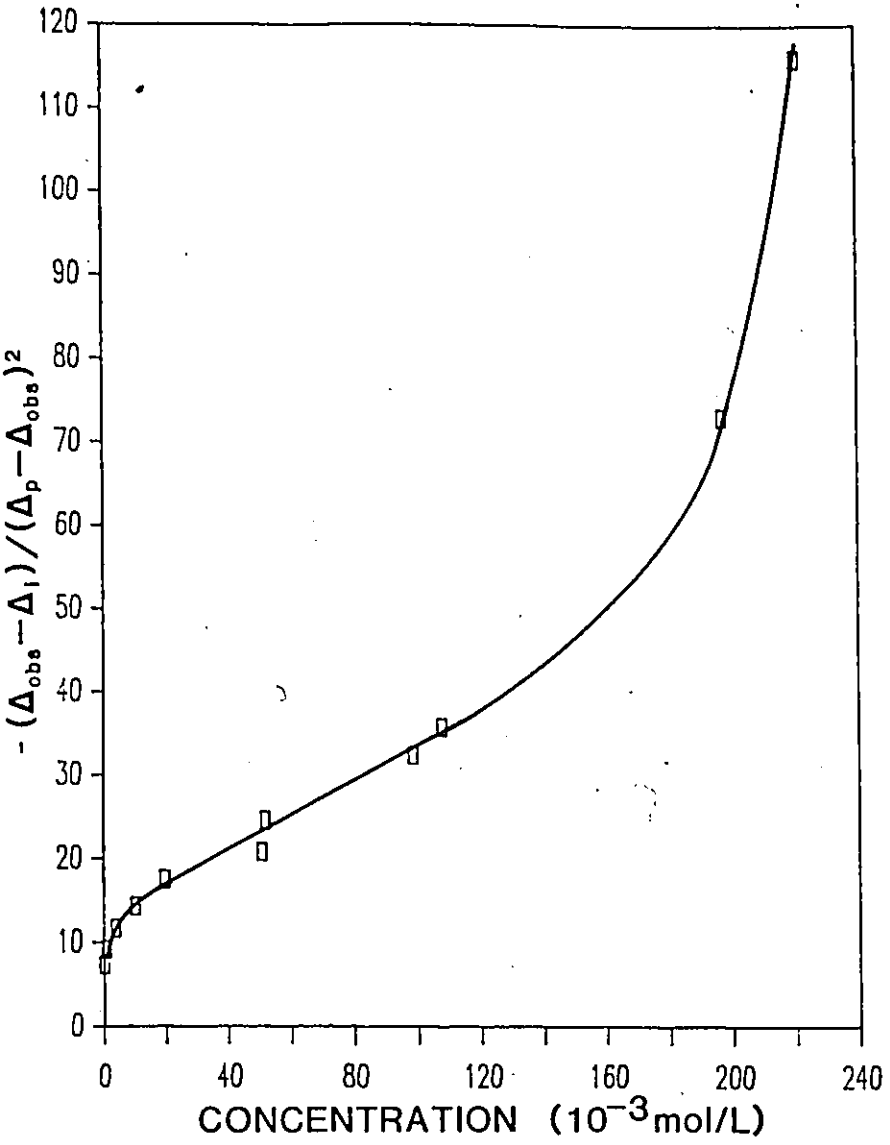

FIGURE 16

RESULT OF FITTING CHEMICAL SHIFT - CONCENTRATION DATA TO EQUATION 21 USING THE PROGRAM *FIT*
$LiCF_3SO_3$ IN 2MeTHF

6 DISCUSSION

As one would expect in a solvent with a very low dielectric constant, the electrostatic interactions are quite large. The conductance passes through a minimum with concentration, an indication that triple-ions have been formed (97). The data can be fitted well to the Fuoss-Kraus equation which takes into account this phenomenon. The magnitude of K_p would indicate that there are very few ions in solution, i.e. almost all of the lithium triflate exists in solution as ion-pairs with a small fraction existing as triple-ions. The values for K_p and K_t compare favorably with the results for other lithium salts in 2MeTHF (104). Delsignore et al. (104) made the assumption that Λ_o^t was equal to $2\Lambda_o/3$. That assumption results in a value for K_t that is one-half of the value that is obtained with the assumption that $\Lambda_o^t = \Lambda_o/3$. No change in the magnitude or in the meaning of the result occurs.

The magnitude of K_p with respect to $K_t - 10^6$ – should make it reasonable to fit some of the lower concentration data to an equation that is based upon ion-pairing (e.g., the Fuoss-Hsia equation). In order to do this, an estimate of Λ_o such as that obtained here from the Walden products and the value of K_p obtained from the Fuoss-Kraus equation would be necessary as initial estimates in such an analysis. It would seem that <u>any</u> estimate for the distance parameter would be

appropriate: there is a relatively small distance in the values of K_p and K_t from using the Bjerrum model of ion-association to that of Fuoss when ion-pairs are dominant ($K_p > 10^3$). A fit to an equation such as the Fuoss-Hsia one (95) was not performed, however, due to the larger uncertainties for the data obtained at lower concentrations.

There is some doubt as to the validity of the value of the Onsager coefficient as determined by equation 19 and utilized in equation 18. If the Onsager coefficient is to represent the limiting slope of the conductance-concentration behavior (or at least the most concentration-dependent parameter in the theoretical slope), then the value of 232 S $cm^{1/2}/equiv^{3/2}$ is unrealistically too small. With Λ_o approximated as 135.09 mS $cm^2/equiv$, the limiting slope is more than an order of magnitude greater than this. The result of using a higher value for the Onsager coefficient, e.g., 4400 S $cm^{1/2}/equiv^{3/2}$, would result in $Z > 1$ (from equation 18) which leads to negative values for K_p and K_t. These two extremes (the low and high values for the Onsager coefficient) result in an undercompensation and an overcompensation of the interionic forces.

Difficulty may arise in having obtained an estimate of Λ_o from the Walden product (the only method readily available). The rule is only approximate and is best used for ions of larger radii. There is little doubt that a refined expression is necessary for the interionic effects in such a

treatment of the electrolytic conductance. Such an expression should include a viscosity correction for these more concentrated solutions. Although the activity of the ion-pairs is taken as unity, the effect of the ion-pairs on the bulk and local dielectric constant should be accounted for. It would be expected that the dielectric increment for the ion-pairs would be high (and an average of "pairs" formed at different distances). With these high dielectric increment species constituting the predominant form of the lithium triflate in solution they would be likely to preferentially solvate the "free" lithium ions thus creating the triple-ions. At higher concentrations the likelihood of this occurrence increases and the conductance passes through its expected minimum.

The ion-pair formation constant, K_D', determined from the slope of the NMR measurements (Figure 16) is about six orders of magnitude less than that obtained by conductance. Assuming that these values accurately reflect the data, then this is a curious result considering that both results are based upon the formation of "contact" ion-pairs. If this is the case, then the contact pairs that are detected by NMR are much "tighter" than those detected by conductance. Based upon the conceptual ideas of ion-pairs in each method, this is not unexpected.

More low-concentration chemical shift data would perhaps clarify the question of the observed limiting slope for

Figure 16. This type of limiting behavior was not observed for $(nBu)_4NI$ in nitrobenzene (87). Association in 2MeTHF is much more prevalent than in nitrobenzene (ε = 34.8) perhaps accounting for the limiting behavior at low concentration in 2MeTHF. Ion-pairs are already dominant at very low concentrations and this, combined with the strong deshielding of the $^7Li^+$ by the $CF_3SO_3^-$, produces very pronounced chemical shifts. It is in this region where comparatively fewer ion-pairs exist that the data can reveal the value of K_p'. At higher concentrations the chemical shift data reflect a saturation of these species in solution and the change in the chemical shift with concentration becomes small and reaches a limiting value (Δ_p). With the small range of chemical shifts for ^7Li, these solutions are best studied at low concentrations.

It should be mentioned that in any analysis of the NMR data that might be based upon the formation of triple-ions, the assumption that the two types of triple-ions, $(MAM)^+$ and $(AMA)^-$, are essentially equivalent (an assumption made in the analysis of the conductance data in terms of triple-ions) will not be valid. While the two triple-ions contribute similar amounts of charge to the solution, the constitution of the ions would be expected to have different effects upon the ^7Li nucleus.

THE TITANIUM CHALCOGENIDES AND LITHIUM ION INTERCALATION

1. REASONS FOR THE CHOICE OF $TiCh_2$ MATERIALS

$TiCh_2$ layer-lattice materials provide very suitable hosts for electrochemical intercalation of Li^+.

Much of the early research and development that was performed on secondary lithium batteries comprised the rapid scanning of various materials as potential hosts to be used as cathodes in Li^+-intercalation type cells. However, much of the work was "quick and dirty" to see if a particular compound would yield a suitable free energy of the intercalation process to merit further consideration.

A number of workers, most notably Stanley Whittingham, have proposed the following requirements for intercalation-type solid-state cathode materials (41,105), especially with Li^+ as the guest ion:

1. A <u>large free energy</u> of reaction for the formation of the Li^+ intercalate. This affords a high cell voltage through the basic equation $\Delta G = - nFE$. (See footnote on p. 120.
2. A <u>large compositional range</u>, i.e., x in Li_xMCh_2. That is, the ability to incorporate a large quantity of guest species within the host. This leads to large cell capacities (normally given in ampere hours).

3. A **high diffusivity of the guest species** within the host. This allows a larger current and hence, a larger power density which would be required for some applications. (The power density is normally given in W/Kg.)

4. **Minimal structural change** as a function of composition. Large structural changes during the intercalation reaction may lead to disproportionation (the formation of more than one solid-solution compound and perhaps the creation of more than one phase in the solid) and ultimately to an irreversibility of the reaction.

5. The host compound should have **good electronic conductivity**; this would minimize the resistive heat generation and eliminate the need for conductive additives in the electrode.

6. The host should **not be soluble in the electrolyte**. The electrode should certainly not have a tendency to disappear into solution. Having an insoluble host minimizes self-discharge within the cell.

The rapid scanning by industry of many compounds was a search to find a compound that would fit these requirements to a good approximation.

A suitable host will also have a large enough opening to allow the incorporation of an alkali metal, e.g., lithium, and provide a pathway for diffusion of the guest to take place. Several structures have large enough openings and

meet most of Whittingham's criteria for a good host. One example is the Perovskite-type structure. Compounds of this structure characteristically contain large cavities that are often occupied by large cations such as calcium or barium. This cavity is vacant in a number of compounds e.g., rhenium trioxide and vanadium pentoxide. These compounds contain an extended network of cavities generated by the sharing of equivalent square faces of the individual cavities. Assuming that the guest species can diffuse between cavities only by passing through square faces, the potential dimensionality for lithium diffusion through the structure is reduced by the blockage of these faces. Because of this high dependence on direction for diffusion in these compounds, they are very susceptible to crystal defects which would lead to blockage of long-order diffusion thus limiting the amount of guest that can be incorporated into the host.

The problem of limited-long-order diffusion is circumvented by using a **van der Waals bonded structure** as a host. The basic structural unit is essentially layers of two-dimensional crystals with relatively weak van der Waals bonding between the layers. The list of such layered compounds is headed by graphite, well known to incorporate a wide variety of guest species into its van der Waals gap. A large number of compounds are known to form layered structures, so much so that several symposia and a major review (106) have been dedicated to this class of compounds.

One technologically interesting group of layered compounds are the transition metal (M) chalcogenides (M = Ti, V, Cr, Zr, Nb, Mo, Hf, Ta, W, Re, and Pt). The primary stoichiometry of these layered compounds is MCh_2 although other stoichiometries are known. The unit building block of the dichalcogenides consists of two hexagonally close-packed chalcogen layers between which reside the transition metal atoms. The metal atoms are found either in sites of trigonal prismatic symmetry or in sites of octahedral symmetry. The extended structural unit is essentially layers of these two-dimensional crystals with relatively weak van der Waals bonding between the layers.

The layered transition metal chalcogenides have been of particular interest to the battery industry because of their ability to incorporate lithium reversibly. Among the most interesting of these is titanium disulfide, largely due to its low molecular weight and correspondingly high theoretical energy density. TiS_2 has been tested extensively in lithium battery systems with various electrolytes with the components of the electrolyte chosen mainly for improved performance of the lithium electrode.

Some general conclusions can be drawn about the stabilities of the lithium intercalates from a consideration of the thermodynamics of formation of the host compounds. Table 10 lists the ΔG°_f values for several of the transition metal sulfides. The data, which came from several sources, are not

TABLE 10

ENERGIES OF FORMATION AND REACTION OF SOME SULFIDES (kJ/mol)

Compound	$-\Delta G^\circ_f$	$-\Delta G^\circ_{disp}$
HfS_2	573	75
ZrS_2	562	78
US_2	427	112
TiS_2	396	120
NbS_2	346	132
TaS_2	345	132
MoS_2	268	152
WS_2	236	160
ReS_2	170	176
SnS_2	142	183

From Ref. 41

Displacement Reaction:

$$4Li + MS_2 \longrightarrow 2Li_2S + M$$

$$\Delta G^\circ = \Delta G^\circ_{disp} = (\Delta G^\circ_f)_{Li_2S} - (\Delta G^\circ_f)_{MS_2}$$

Intercalation Reaction:

$$Li + MS_2 \longrightarrow LiMS_2$$

$$\Delta G^\circ = \Delta G^\circ_{int} = (\Delta G^\circ_f)_{LiMS_2} - (\Delta G^\circ_f)_{MS_2}$$

as complete for the selenides and tellurides. The Gibbs energy of the displacement reaction, $4Li + MS_2 \longrightarrow 2Li_2S + M$ is also given. The magnitude of the $\Delta G°_{disp}$ must be less than the Gibbs energy change for the intercalation process*, $\Delta G°_{int}$ (≈200 kJ/mol), if a stable intercalate is to be formed. Compounds with a higher $\Delta G°_f$ make the formation of the intercalate more favorable than the displacement reaction. In comparison with published data, it is found that those compounds with a $\Delta G°_f$ higher than that of MoS_2 form stable intercalates with lithium. It is apparent that the stable intercalates in the transition metal sulfides come from those transition metals on the left-side of the Periodic Table. Although hafnium sulfide and zirconium sulfide form stable intercalates, they are generally not considered for use in power sources because of their low theoretical energy density (229 Wh/kg for $LiHfS_2$, 353 Wh/kg for $LiZrS_2$, as compared to $LiTiS_2$ which is 481 Wh/kg). Not surprisingly, no intercalates of US_2 have been reported.

In the case of TiS_2 a single, homogeneous phase (solid solution) has been found for the entire range of x values $0 \leq x \leq 1$ in Li_xTiS_2. A composition at $x = 1$ corresponds to all of the octahedral sites in the van der Waals gap being

---

*$\Delta G°_{int}$ must be defined for unit Li^+ activity in the external solution. $\Delta G°_{int}$ varies with x in Li_xMCh_2 (cf. adsorption on a two-dimensional surface where $\Delta G°_{ads}$ varies with the fractional coverage θ.

occupies by a lithium atom. At the other extreme of stability, for molybdenum sulfide, the intercalate Li_xMoS_2 will be stable up to a concentration x = 0.13. Beyond this point a two-phase compound results because the displacement reaction is favored and lithium sulfide is formed. The intercalation reaction is then no longer reversible. Before the intercalation starts, the free energy of the reaction corresponds to the change

$$xLi + MoS_2 \longrightarrow Li_xMoS_2 \qquad [22]$$

with an associated $(\Delta G°_{int})_x$ for the intercalation (this would correspond to the open-circuit voltage of the fully charged cell. As more intercalation takes place, lithium is entering a lattice that is already partially filled with lithium,

$$dxLi + Li_xMoS_2 \longrightarrow Li_{x+dx}MoS_2 \qquad [23]$$

Clearly, the free energy of this process will be different. The experimentally measured value of $\Delta G°_{int}$ is decreasing i.e., $\left|(\Delta G°_{int})_x\right| > \left|(\Delta G°_{int})_{x+dx}\right|$. It can be concluded that intercalation will take place so long as $\Delta G°_{int} < \Delta G°_{disp}$. For MoS_2 the inequality does not hold above x = 0.13.

There are several ways that the lithium, the guest species studied in the present work, can be made available for insertion into the host. Rudorff (107,108) formed the first alkali metal intercalation compounds in 1959 by reacting MS_2 with a solution of metallic lithium in liquid ammonia at a temperature below -33 °C. The ammonia is co-intercalated and must be removed by vacuum treatment or by heating. The thermodynamic activity of the alkali metal in these ammonia solutions is very close to that of the pure alkali metal so that the reduction of the chalcogenide may proceed beyond the intercalation stage to lower chalcogenides or to the transition metal itself. The co-intercalation of the ammonia assists in the insertion of the lithium atoms by opening up the layers, minimizing the polarization of the lattice by the metal atom, and thereby enhancing the diffusion of the lithium. In several instances, for example, in the intercalation of europium, this is the only method that works (109). This metal dissolution method is not reversible.

A very simple method for the formation of the lithium derivative involves the use of n-butyl-lithium. To lithiate the compounds the host structure is simply immersed in an approximately 1.5 M solution of n-butyl-lithium in hexane. In this reaction, no polar solvents are used so that co-intercalation does not occur. An advantage of this method is that the electrochemical activity of the lithium is about 1V less than that of the lithium metal so that the reaction is

not as likely to cause complete reduction of the transition metal (110).

Electrochemical methods were introduced by Whittingham in 1974 (111). He used the dichalcogenide as the cathode in an electrochemical cell. The empty host lattice represents the fully charged state of the cathode. The anode is frequently the pure metal. The composition of the intercalate can be controlled by monitoring in time, the total charge passed. Unlike the previous (chemical) methods, this reaction can be reversed by applying a potential of reversed polarity.

Titanium disulfide: this is the best known of the transition metal chalcogenide hosts. The compound has been widely studied as a solid-state cathode for lithium batteries and the great interest in this material is largely due to its properties. The intercalation of lithium takes place with a relatively large ΔG°_{int} (-200 KJ/mol) with an initial voltage of 2.44 V. The change in free energy with composition is relatively small (even at $x = 0.6$ the voltage is still 2.1 V; ΔG°_{int} = -203 KJ/mol). As $x \rightarrow 1$, however, diffusion problems (of the Li within the host) decrease the voltage rapidly. The discharge curve for a Li/TiS_2 cell is smooth, leading to the conclusion that there is a single solid phase for Li_xTiS_2 over the entire composition range $0 \leq x \leq 1$. A sudden drop in the curve would indicate that energy is being expended to generate a new phase. This is not observed for TiS_2 for $x \leq 1$. This is in contrast to the insertion of the larger sodium

species where a sharp phase transition occurs at x = 0.44 (112) (Figure 17).

Other properties of TiS_2 which have made it an attractive compound for power source studies include the small c-lattice expansion of only about 10% in going from x = 0 to x = 1. A full 80% of this expansion takes place by the time x = 0.4. From a practical standpoint a 10% expansion of the lattice should not cause substantial mechanical problems in a cell. The diffusion rate of the lithium within the van der Waals gap is very high. Diffusion can involve either jumps between trigonal prismatic sites or between tetragonal and octahedral sites. The differences in the sizes of the sites and the activation energies for the jumps diminishes as the chalcogen layers are separated (with the onset of intercalation) and all of the sites increase in size. The mobility of an ion is also affected by the ionicity of the lattice. In the highly ionic CrS_2 the variation in potential that is seen by the lithium ion is much greater than in the more covalent TiS_2. The result is that the mobility is expected to be higher in TiS_2 than in CrS_2.

As the lattice becomes filled ($x \rightarrow 1$) the mobility of the ion will decrease because the number of available sites for lithium to jump to is decreasing. Silbernagel and Whittingham (113), utilized ^7Li-NMR spin-lattice measurements and recorded a diffusion coefficient of 10^{-9} cm^2/s for x = 1 (Li

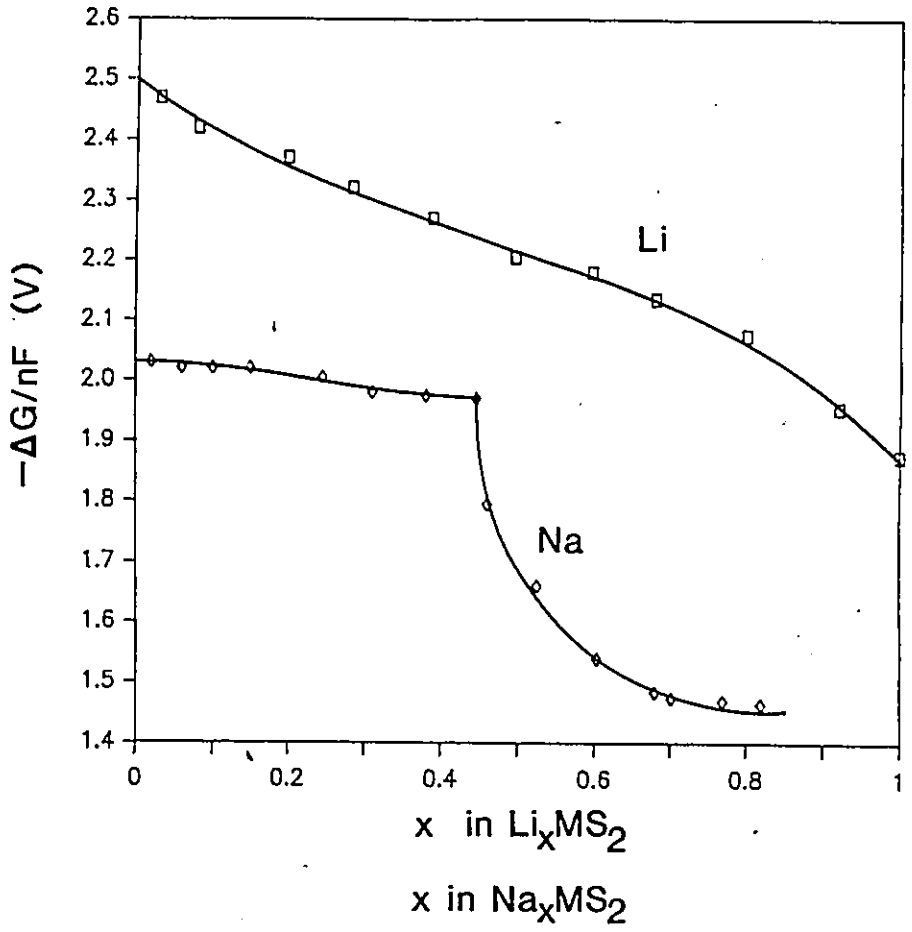

FIGURE 17

FREE ENERGY VERSUS COMPOSITION
FOR SODIUM AND LITHIUM INTERCALATION INTO TiS_2
(AFTER REF. 112)

in TiS_2) with a variation of only about a factor of two in the diffusion coefficient for the range $0 \leq x \leq 1$ (114).

As a conductor, TiS_2 behaves as a semi-metal thus minimizing the need to add conductive diluents to any cathode structure.

TiS_2 is stable in any of the organic solvents that have been commonly used in lithium battery research. However, the TiS_2 is not stable to oxidation by either oxygen or water (115). Thus, the handling of TiS_2 should take place in a dry, oxygen-free atmosphere.

The c-lattice parameter of TiS_2 is a well defined function of the composition. In the absence of a phase change the lattice parameter (and other physical properties) varies in a smooth, but not necessarily linear manner, with composition as given by Vegard's rule (116). This can be taken advantage of since it is practically possible to measure the lattice parameter to within 0.01%. The stoichiometry of the metal chalcogenide is of critical importance. If the "y" in M_yCh_2 is greater than 1.00, then the extra metal atoms will reside between the chalcogen layers - covalently bonded to them and thus "pinning" the layers shut and preventing intercalation. The variation of the c-lattice parameter of the host with composition is discussed in section 3 of this chapter. It is also possible to measure the value of x in Li_xMCh_2 from a measurement of the lattice parameter, but this is done more effectively by coulometry.

TiS_2 has a variety of interesting and attractive properties that make it a convenient host for a kinetics investigation. However, in any kinetic study, it is desirable to compare the result to a reference measurement of a similar kind. Measurements could be made on "different" host compounds, TiS_2, $Li_{0.1}TiS_2$, $Li_{0.2}TiS_2$, etc., but these are variations of the same structure. This would be somewhat analogous to a reaction at a bare electrode, the same electrode with 0.1 of a monolayer, 0.2 of a monolayer, etc. While these are indeed significant differences in the electrode, a more fundamental change was sought. Argument could be made for the study at the interfaces of the other Group IVB sulfides, ZrS_2 and HfS_2; here the kinetics of intercalation could be studied as a function of the ionicity of the host. Another study might have involved other compounds whose lattice opens up by the same amount on intercalation as titanium disulfide's does (HfS_2, $TiSe_2$, $NbSe_2$, etc.) or with compounds with a van der Waals gap similar to that of TiS_2.

What has been chosen for the present work is a study of a second chalcogenide - the selenide - of titanium. (A study of the telluride was desired, but a cracked tube during the synthesis of TiS_2 raised objections of some to the processing of the more toxic tellurium.) The ionicities of TiS_2 and $TiSe_2$ are approximately the same; $TiTe_2$ is somewhat more covalent. The compounds present a different van der Waals

gap to the guest species and differences in the initial size of the octahedral sites that are present. (As pointed out previously, as intercalation begins, the lattice opens up and the significance of these site differences is diminished.) The author has calculated the size of the van der Waals gap and the size of the octahedral sites for TiS_2, $TiSe_2$, and $TiTe_2$ and they appear graphically in Figure 18. The error limits given with each point reflect the uncertainty in the lattice parameters as they were propagated through the calculation. It was felt that the similarity of the ionicities together with the larger gap presented by the selenide would provide some significant kinetic differences.

2. PREPARATION OF $TiCh_2$ COMPOUNDS

2.1 PREVIOUSLY REPORTED TECHNIQUES

Crystalline and amorphous $TiCh_2$ compounds have been synthesized by a variety of methods. Although the basic recipies for the preparation are available in the literature, many of the details are of a proprietary nature. The use of laboratory-grown TiS_2 is a necessity since the purchased TiS_2 including the "battery-grade" TiS_2 from CERAC was either non-stoichiometric or contained impurities whose nature depends upon the method of preparation. The previously reported techniques include:

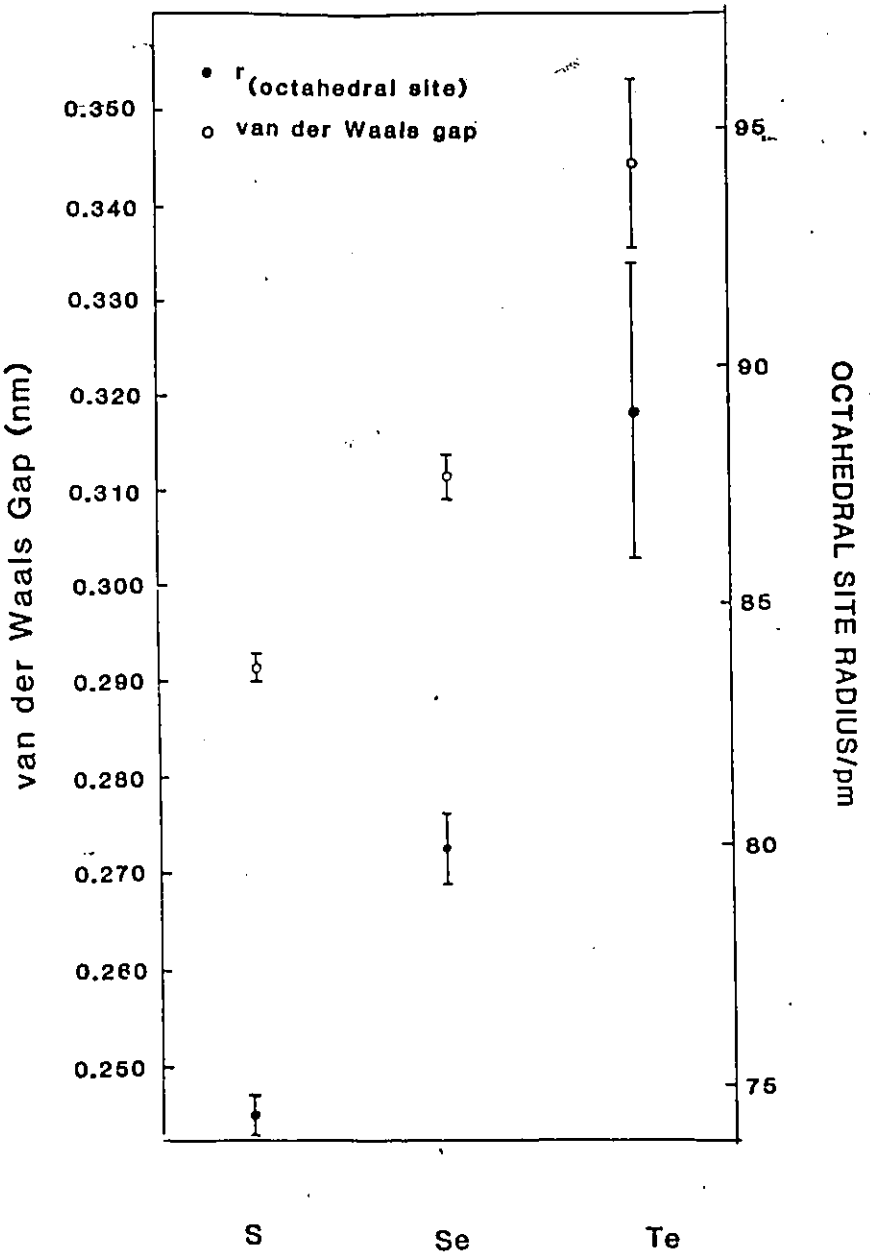

FIGURE 18

VAN DER WAALS GAP AND OCTAHEDRAL SITE RADIUS
FOR THE TITANIUM CHALCOGENIDES

$$Ti + 2Ch \xrightarrow{>400\ ^\circ C} TiCh_2 \qquad \text{References 117, 118}$$

$$TiCl_4 + 2H_2Ch \xrightarrow{>400\ ^\circ C} TiCh_2 + 4HCl \quad \text{(gas phase rxn.)} \quad 119$$

$$\left\{ \begin{array}{l} TiCl_4 + 2Li_2Ch \xrightarrow[THF]{25\ ^\circ C} TiCh_2 \cdot THF + 4LiCl \\ TiCh_2 \cdot THF + \text{pyridine} \longrightarrow TiCh_2 \cdot \text{pyridine} + THF \\ TiCh_2 \cdot \text{pyridine} \xrightarrow{\text{vacuum}} TiCh_2 + \text{pyridine} \end{array} \right\} \quad 120$$

The synthesis of stoichiometric $TiCh_2$ powder is required for the preparation of a proper intercalation electrode. As previously mentioned, if the composition of the $TiCh_2$ is not stoichiometric, then the result will be a reduction of the diffusion rate in the host lattice (where the excess Ti, when present, "pins" the layers shut). Stoichiometries with an excess of chalcogen (e.g., TiS_3) produce a host where the diffusion of the lithium is of a higher dimensionality (cf. Perovskite-type structures) (121,122). The preparation of a powder is considered necessary since the intercalation reaction takes place on the edges of the crystal layers and <u>not</u> on the basal plane of the $TiCh_2$.

The high-temperature preparation of $TiCh_2$ from $TiCl_4$ and H_2Ch can result in non-stoichiometry of the product unless

very careful control is maintained of the equilibrium of the reaction. Preparations from the tetrachloride usually result in chlorine impurities in the product (this was also observed in the "battery-grade" TiS_2 from CERAC). The use of H_2Se was also considered an unnecessary hazard; thus the high-temperature preparation from $TiCl_4$ was not considered for $TiSe_2$.

The low-temperature preparation of the dichalcogenide from $TiCl_4$ in THF as a solvent produces an amorphous product with THF in between the chalcogen layers. The THF is removed by soaking the product ($TiCh_2$·THF) in excess pyridine with pyridine replacing the THF in the $TiCh_2$ structure. The pyridine must be subsequently removed under vacuum. The amorphous product must then be annealed at high-temperature (>500 °C) by vapor transport to produce the crystalline or powdered product.

Crystalline, stoichiometric $TiCh_2$ is effectively produced via the high-temperature synthesis from the elements (117,118). The high-temperature reaction (>500 °C) is performed with powdered sulfur and either titanium wire or sponge. Titanium powder - which is used in some fireworks - is emphatically not recommended. The use of iodine for transport during the synthesis and growth is not recommended because of the difficulty in removing I_2 from the product. Instead, the use of sulfur (or selenium) for transport is recommended (117,118). Temperatures that have been reported

for the preparation range between 550 °C and 1000 °C with reported times of 24 to 240 hours.

2.2 PREPARATION OF $TiCh_2$ - THE PRESENT WORK

Titanium chalcogenides were prepared by high-temperature synthesis from the elements. In addition, amorphous TiS_2 was prepared from Li_2S in THF with subsequent annealing at high-temperature. A sample of the "battery-grade" TiS_2 from CERAC was also annealed to see if it was possible to improve its stoichiometry.

High-temperature preparation of TiS_2 from the elements - Titanium disulfide was first prepared from the elements in a high-temperature synthesis with sulfur transport. Titanium wire (0.75 mm diameter, 0.999, Alfa-Ventron) was cut into 1 cm pieces and placed in a 12 mm i.d. × 200 mm Vycor tube. Sulfur powder (Puratronic™, Alfa-Ventron) was added to the tube with a stoichiometric weight determined by the amount of titanium employed. In addition, an excess of sulfur was added for vapor transport. The amount of excess sulfur used was 5 mg per cm^3 of tube volume. A vacuum was then pulled on the tube for several minutes and the tube was sealed with a hydrogen flame. After the tube had cooled, the ingredients were distributed by shaking and rolling into the center two-thirds of the tube. The tube was carefully placed in a tube furnace (Lindberg) with the end of the tube that was flame

sealed placed nearest to the opening (colder area) of the furnace. The heat (controlled by a Variac) was then turned on. The furnace temperature was monitored by three thermocouples that were placed against the Vycor tube in the furnace.

Details of titanium disulfide synthesis from the elements to produce a stoichiometric, electrochemically active product are for the most part proprietary. For this reason it was necessary to perform the synthesis under various conditions of reaction temperature, time, and batch size in order to establish optimum conditions. This was one of the most time consuming aspects of the project because the reaction times ranged from four to twenty four days.

As a measure of the quality of each batch, samples were analyzed by x-ray diffraction and/or atomic absorption (section 3) to determine the stoichiometry.

The synthesis that was determined to be most effective involved a reaction and growth time of three weeks with a batch size of 6 grams in a tube with a volume of 20 to 22 cm^3. The temperature profile that was used (and followed quite closely for subsequent preparations) is depicted in Figure 19. The reaction mixture was brought up to the reaction temperature (500 °C) very slowly (a four day period was used) to maintain equilibrium in the mixture and to guard against imperfections in the Vycor tube (In the early stages of the reaction the tube could crack under the pressure of

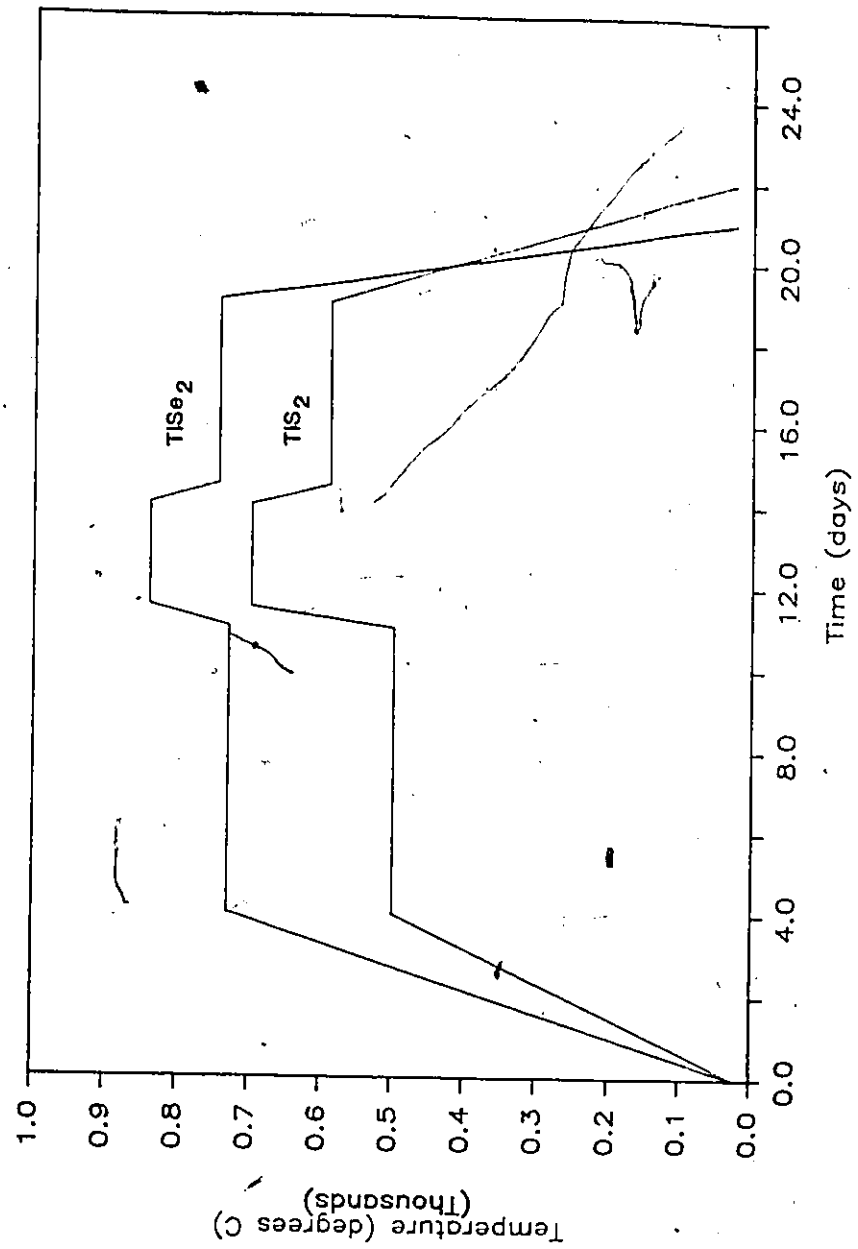

FIGURE 19

TEMPERATURE-TIME PROFILES
FOR THE GROWTH OF ELECTROCHEMICALLY ACTIVE $TiCh_2$

the boiling sulfur. One such event occurred during the program prompting the removal of tellurium from the program.). The reaction temperature was maintained for 7 days and then increased to 700 °C for 3 days to complete the reaction and to promote transport. The reaction temperature was decreased to 600 °C for 5 days as transport and growth were completed. The tube was then cooled over a period of three days (about 8 °C/h) to room temperature.

The tube was removed from the furnace and held horizontally at all times. This is because the "hot" end of the tube (the region which sat in the middle of the furnace) contained the TiS_2 and the "cold" end contained stoichiometries corresponding to higher amounts of sulfur (TiS_3, etc.). The tube was cracked open under an inert atmosphere and the products were carefully removed and stored under argon.

The titanium sulfide that was so produced was in the form of small, gold colored, hexagonal crystallites with an average size of about 0.5 mm in diameter. During the series of preparations it was observed that without the period of reaction at 600 °C or if the reaction mixture was cooled to slowly (<5 °C/h), then the crystals that were formed were larger flakes (> 2 mm) and as a result they were very low in electrochemically active surface area.

At the "cool" end of the tube were the titanium sulfides of higher stoichiometries (TiS_y, $y>2$). The material was

bright violet in color and highly crystalline. Analysis by x-ray diffraction showed that the violet product was largely TiS_3.

High-temperature preparation of $TiSe_2$ from the elements - Titanium selenide was prepared in a similar high-temperature synthesis. Selenium beads (1 mm diameter, 0.999, Alfa-Ventron) were used in the same fashion as sulfur. Due to the higher boiling point of selenium (685 °C vs 444 °C for sulfur) a higher reaction temperature, 740 °C, was used so that vapor pressures of selenium similar to that attained by sulfur would be reached during the reaction. During the second phase of the reaction, the temperature was raised only to 850 °C because of the danger of approaching the softening point of the Vycor glass (900 °C) too closely. The temperature-time profile for the preparation of $TiSe_2$ is also depicted in Figure 19. The cool-down phase of the reaction-growth regime was accelerated (≈15 °C/h) in order to keep the size of the crystallites small.

The titanium selenide crystals were red-violet and metallic in appearance. The selenides of higher stoichiometries were black in appearance and highly crystalline.

Preparation of TiS_2 in THF at room-temperature - Titanium disulfide was prepared from $TiCl_4$ and Li_2S in THF. The procedure is outlined in the appendix. The product had a higher bulk density than the TiS_2 produced from the elements. The x-ray diffraction lines that were obtained from this

sample (after a period of crystal growth by transport) were not as sharp; in fact there were some extra lines in the powder pattern. This would indicate that the removal of pyridine under vacuum was incomplete. However, extended treatment of the product by evacuation did not result in an improvement in the quality of the product.

Recrystallization and growth of CERAC TiS_2 - A sample of "chloride-free battery-grade" TiS_2 was sealed in a Vycor tube with a small excess of sulfur. The CERAC TiS_2 was made up of fine crystallites typically 0.1 mm in diameter. The recrystallization in the Vycor tube at 600 °C for one week produced a product of mixed stoichiometry as determined by x-ray and spectroscopic methods.

3 VERIFICATION OF THE STOICHIOMETRY OF $TiCh_2$

The best method for determining the structure of a molecular crystal is by x-ray diffraction. Since the range of structures that would be present in the products as prepared is limited, a detailed structure determination with a single crystal is not necessary. The x-ray diffraction of a "powdered" sample can be used to identify simple structures and give the size of the molecular unit. The experimental principles and mathematical relationships for the "powder" method of x-ray diffraction have been described elsewhere (e.g., in 123-126). Several indices have been published in

which the d-lattice spacings and relative intensities of the lines in powder photographs of a large number of materials are listed (127,128).

For the powder method, a sample of the crystalline is ground to a fine powder and packed into a Lindemann glass capillary on the order of 0.5 mm in diameter. An amount of finely ground silicon equal to about one-third of the total sample volume is added to the sample as an internal standard. The sample was mounted in the center of a Debye-Scherrer camera and the film was exposed using Cu-Kα radiation.

Titanium dichalcogenides are known to crystallize in the CdI_2 structure (hexagonal) (106,127). From the Bragg equation, the line spacings for the hexagonal system will be given by the relation

$$\sin^2\theta/(\lambda^2/4) = 1/d_{hkl} = Q = (4/3a^2)(h^2 + hk + k^2) + l^2/c^2 \qquad [24]$$

The films were measured on a travelling microscope and the lines were indexed according to the allowable integer values for a hexagonal system (as dictated by equation 24). The values of Q that are determined from the measured film are matched to the Miller indices by prescribed methods (123,125, 126). Data in the form of Q, h, K, and l for each line were analyzed by the rigorous least-squares method that was previously described. This yields approximate values for the

a- and c-lattice parameters. With these approximations, the high-angle data (more accurate because of the nature of the linear measurement of the film) are re-evaluated. This yields a second approximation of the lattice parameters.

For most powder specimens, the main angle-dependent error is that due to the absorption of the x-ray beam in the specimen, which causes a shift in the position of the peak of the powder line. It has been shown (125) that in these circumstances the error in the calculated lattice parameter is approximately proportional to $\frac{1}{2}(\cos^2\theta/\theta + \cos^2\theta/\sin\theta)$, the Nelson-Riley function. Extrapolating the high-angle values of the lattice parameter versus the Nelson-Riley function to 90° yields the correct value for the lattice parameter.

Values of the lattice parameters of the titanium chalcogenides are well known (41,106,127). In addition, for titanium sulfide, the lattice parameter is well known as a function of stoichiometry for values of $y = 1.0 \pm 0.1$ in Ti_yS_2 (41,106,127). This, along with accurate and precise determinations of the lattice parameters, aids in the verification of the stoichiometry of titanium disulfide. Stoichiometric TiS_2 has lattice parameters of $a = 0.3406 \pm 0.0002$ nm and $c = 0.5696 \pm 0.0003$ nm. It has been shown that at stoichiometries with $y>1$, that the c-lattice parameter increases noticeably. At $y = 1.1$, the c-lattice parameter opens up to 0.5715 nm. From the large number of values of the c-lattice parameter that have been reported, it

was concluded that when the measured lattice parameter is higher than 0.5700 nm the titanium sulfide stoichiometry was metal-rich. For lattice parameters at or below 0.5700 nm, the titanium sulfide is either stoichiometric or metal-poor (128-130). Information on the c-lattice parameter of $TiSe_2$ as a function of composition was not as readily available.

Wet analytical techniques were performed to provide complementary results to those derived from x-ray determination of TiS_2 stoichiometry and for a determination of titanium selenide stoichiometry.

A small sample (0.5 g) of the titanium chalcogenide was dissolved in warm dilute HCl. Potassium chloride was added to a 0.1% w/v concentration. The total volume of the preparation was 250 mL. The sample was then analyzed by ICP on a Perkin Elmer 3030 Atomic Absorption spectrophotometer. A wavelength of 399.9 nm was used with a nitrous oxide-acetylene flame. Under these conditions, the sensitivity of the measurement is 3.8 mg/L. With the sample size and concentration that were used this allows for a determination of y in Ti_yCh_2 to within ± 0.005.

Several batches of titanium sulfide were analyzed by x-ray diffraction only. Others, and all samples of titanium selenide, were analyzed by both x-ray diffraction and by ICP. The results of both types of analysis for the titanium chalcogenide samples are listed in Table 11.

TABLE 11
STOICHIOMETRIC ANALYSIS OF TITANIUM CHALCOGENIDE PRODUCTS

Sample*	Lattice Parameters		Stoichiometry as y in Ti_yCh_2	
	a/nm	c/nm	x-ray	AA-ICP**
TiS_2 1	0.3417	0.5687	<1.00	
1b	0.3407	0.5691	1.00	
1c	0.3389	0.5704	>1.00	
1d	0.3391	0.5700	1.00	
2	0.3408	0.5797	1.00	
2b	0.3413	0.5713	>1.00	
3	0.3406	0.5689	<1.00	
3b	0.3401	0.5685	<1.00	0.993
3c	0.3399	0.5691	<1.00	
4	0.3407	0.5697	1.00	0.997
4b	0.3409	0.5703	>1.00	
5	0.3412	0.5687	<1.00	
5b	0.3407	0.5697	1.00	1.000
5c	0.3408	0.5693	1.00	
6	0.3417	0.5702	>1.00	
6b	0.3410	0.5710	>1.00	1.013
6c	0.3402	0.5716	>1.00	
7	0.3391	0.5700	1.00	
7b	0.3399	0.5696	1.00	0.994
7c	0.3402	0.5697	1.00	
$TiSe_2$ 1	0.3528	0.6004		
1b	0.3520	0.6010		1.008
1c	0.3529	0.6001		
2	0.3537	0.5986		
2b	0.3531	0.5995		0.995
2c	0.2531	0.6001		
3	0.3529	0.6004		1.007
3b	0.3523	0.6008		
4	0.3531	0.6002		1.000
4b	0.3537	0.6001		

* Sample numbers refer to preparations that were used in further experiments. Several batches were rejected outright due to either poor stoichiometry on analysis or, before analysis, due to a poor appearance on physical inspection.

Sample number subscripts (b,c, etc.) refer to samples taken progressively toward the "cold" end of the synthesis tube.

**Atomic absorption results are for the average of 3 determinations.

The sample size that was taken for the ICP was large enough to measure the overall product stoichiometry - an average of any localized stoichiometries. The sample size that was taken for the x-ray diffraction was quite small and may only represent localized composition and not the overall product stoichiometry.

The difficulties in obtaining electrochemically active $TiCh_2$ economically and in quantity have contributed to the decline in popularity of electrochemical devices based upon the intercalation process. Several batches of these materials were rejected for non-stoichiometry, a frustrating end to three weeks of adjusting and monitoring an oven.

Although great hopes were held for stoichiometric analysis by x-ray diffraction, the results that were obtained were qualitative at best. The analyses by ICP were reproducible if not always of the desired accuracy.

Samples were taken from several areas of the tube for x-ray analysis with samples being taken successively closer to the "cold" end of the tube to see if there was a systematic change in stoichiometry with position in the oven. No detectable systematic variations were observed.

THE ELECTROCHEMICAL SYSTEM

INTRODUCTION

In the past few years, the intercalation of lithium by layered and channeled hosts has been studies by several investigators. The particular interest in these compounds is for their use as cathodes in secondary lithium batteries. The intercalation reaction, also termed topochemical, occurs without appreciably modifying the structure of the host material. The chemistry of such compounds, and specifically the intercalation reaction has been the subject of two major reviews (41,132) and very many papers. As discussed previously, it was recognized early that titanium disulfide could incorporate lithium ions with a high energy and, at low current densities, a high degree of reversibility.

Much of the work that has been performed to date has been investigations of the cathode suitability of a large number of host materials. An enormous amount of data relating to the synthesis, structure, properties and electrochemical performance with lithium has been generated. Much of the physical data is viewed from the standpoint of solid-state physics and crystal chemistry. Most of the electrochemical data are somewhat empirical, with cell discharge curves versus a lithium anode constituting a majority of the reported results. Some of the reported data, however, have

been devoted to kinetic and mechanistic effects at intercalating interfaces (132-138). These studies have included an analysis of the reactivity of the basal planes (van der Waals surface) of the layered hosts (135). Among the techniques that have been employed are cyclic-voltammetry (133,138), galvanostatic polarization, chronoamperometry, chronopotentiometry (133,134), AC-impedance and electrochemical potential spectroscopy (138-140).

While the physical mechanisms of intercalation pertaining to the diffusivity of the guest within the host are well understood, the electrochemical mechanisms near the interface are not as well understood. In particular, the structure and rate-limiting processes occurring at the host/solution interface need to be addressed. Other workers have considered the host structure in terms of a "traditional" electrode with a reaction and electron-transfer occurring at the "surface" with double-layer and mass-transport considerations viewed as taking place on the solution side of the interface. The structure and reactivity in the double-layer is largely determined by the electric field gradient that is set up at the solid/liquid interface and this can be externally controlled to some extent by the experimenter. Irreversibilities both real and quasi that have been observed have been attributed to either slow charge-transfer or to slow diffusion of the guest within the host (133,134). In order to distinguish between the different possibilities for the

mechanisms and rate-determining step a more complete model is needed for the double-layer for these types of electrodes.

The "traditional" view of the electrode/electrolyte interface consists of mobile species (charged or uncharged) forming an electrical double-layer on the solution side and an "equivalent" image of the charges of the double-layer set up by the electrons in the conducting or semiconducting solid electrode (141). Here, the situation prior to the onset of intercalation is similar (Figure 20). The driving forces for the start of intercalation are, however, conceptually different than for the processes at the electrode in Figure 20a. The intercalating host is at the same time a semiconductor (capable of electronic conduction with mobile electrons available to form an "image" of the charges of the solution double-layer) **and** a dielectric medium (capable of "solvating" charged or otherwise polarizable species).

When the host structure is immersed in the electrolyte a double-layer is set up at the edge* of the host's lattice (Figure 20b). The presence of the dielectric lattice and the image charges by themselves are not enough to cause the guest species to lose its solvation sheath (in the case where the guest is an ion) and enter the lattice. When the potential

---

* The structure of the double-layer in this model is considered for the edges only and is ignored along the unreactive basal plane (van der Waals surface (0001). These surfaces have been investigated for a number of layered transition metal dichalcogenides and found to be quite inert (135).

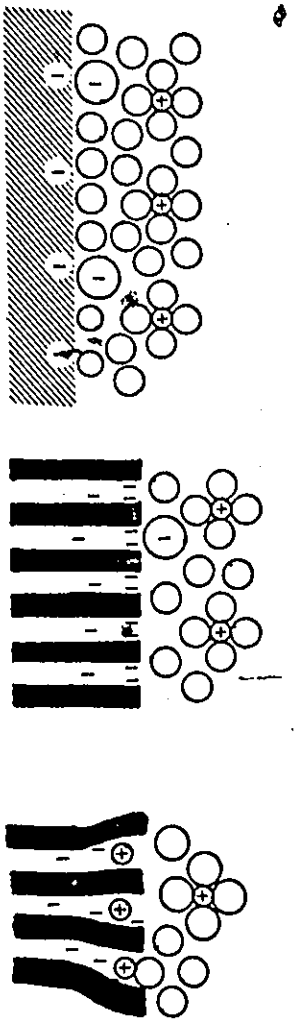

a

Double-layer model of Bockris, Devanathan and Müller for a regular metal electrode/solution interface.

b

Double-layer set-up at the edge of a layered host prior to intercalation. The only mobile charges in the host are electrons.

c

Coupled double-layers. After the onset of intercalation there are both positive and negative charge carriers within the host.

FIGURE 20

DOUBLE-LAYER MODELS
FOR PLANAR AND INTERCALATING ELECTRODES

of the host is changed externally, the activation energies for these processes can be sufficiently diminished that the guest may readily enter the lattice. Once intercalation has begun, the guest species (in the present case lithium ions) reside within the electrode as mobile charges and must therefore contribute to the overall structure of the interphase. At this point, (Figure 20c) a second double-layer is formed. For the electrode side of the interphase of Figures 20a and 20b, the double-layer consists of an image charge of electrons moving about the rigid lattice of the electrode. Conceptually, the solution-side double-layer (SDL) is unchanged.

The solid-solution or electrode double-layer (EDL) is limited both dimensionally and in the types of species that can make up the EDL. In addition to the complexity of having two distinct double-layers, the electrode is changing as a (mono)layer of the guest is formed inside the host. This is somewhat analogous to monolayer formation of e.g., an oxide on a metal electrode. The increased concentration of guest species within the host will have a profound effect on the structure of the electrical double-layer.

In some significant ways, it is seen that the electrochemical intercalation of Li^+-ions into $TiCh_2$ is analogous to ion-transfer from solution into a membrane or across the interface of two immiscible liquids except that in these cases no electron-transfer accompanies the ion-transfer.

Ignoring most of the published evidence, many authors have characterized the intercalation reaction, e.g., of lithium into titanium disulfide, as either

$$Li + TiS_2 \longrightarrow LiTiS_2 \qquad [25]$$

with half-reactions represented by

$$Li \longrightarrow Li^+ + e^-$$

and

$$Ti(IV) + e^- \longrightarrow Ti(III)$$

or

$$Li^+ + TiS_2 \longrightarrow LiTiS_2 \quad (e^- \text{ not accounted for}) \qquad [26]$$

with the half-reactions either not defined or ill-defined.

There is a tendency among most electrochemists to consider the intercalation reaction as an electrochemically driven/controlled redox process with charge-transfer occurring either as a reduction of the titanium disulfide or by lithium ions entering the lattice with an electron being donated to the conduction band of the host.

The latter mechanism seems more likely, as electrons are supplied to the conduction band of the host through the external circuit (from the oxidation at the anode) while

lithium ions are able to enter the lattice. The lithium ions reside in the van der Waals gap. This model in which the lithium atoms in the host exist substantially as ions is supported by measurements of the ^{7}Li-NMR Knight shift (142) and by measurements of the magnetic susceptibility of $LiTiS_2$ (and $LiTiSe_2$) (143).

With the lithium remaining ionic and the electrons in the band structure of the TiS_2 it would appear that mechanisms which consider the reduction of the host can be discounted. (As the lattice fills up with lithium and the nature of the host changes this may not always be true.)

The mechanism of conduction is not unrelated to the diffusivity of the guest species (lithium ions) within the host. Electron density within the layer structure of the host would intuitively be localized (but not confined to) the regions where the lithium ions reside in the lattice. As the intercalation reaction proceeds, the lithium ions will migrate towards the substrate (and the incoming source of electrons). Lithium ions will also tend to form ordered structures within the lattice assuming positions within the host that are relatively far (when possible) from other lithium ions (138), minimizing their free energy. If for any reason the diffusivity of the guest within the host were to be impeded, this would also affect the ionic component of conduction through the host.

This model of coupled double-layers re-opens the question of the nature of the "electrode" processes at an intercalating interface. Depending upon the conditions of cell operation, the current can be limited by mass-transport on either side of the interface. For a given system, (host, guest ion, solvent) there will be a set of conditions under which the mass-transport current limitations can be transferred from the solution to the host and that, once this transfer has taken place, the ability to reverse this situation is limited.

The mechanism involved in such processes can be envisioned as several steps and associated equilibria occurring in the liquid solution and several steps occurring in the host (solid-solution). In the following sequences, the trifluoromethanesulfonate anion is represented by A^- and the solvent molecules are represented by S.

$$(Li_2A)^+ = (Li^+A^-) + Li^+ \qquad K = 1/K_t \qquad [27]$$

$$(LiA_2)^- = (Li^+A^-) + A^- \qquad K = 1/K_t \qquad [28]$$

$$(Li^+A^-) = Li^+ + A^- \qquad K = 1/K_p \qquad [29]$$

$$(LiS_n)^+ = Li^+ + nS \qquad [30]$$

} at electrode interface or in solution

$$Li^+ + TiS_2 + e^-(external) = Li^+ \cdot TiS_2 \cdot e^-(internal) \qquad [31]$$

$$(LiS_n)^+ TiS_2 + e^-(external) = (LiS_n)^+ \cdot TiS_2 \cdot e^-(internal) \qquad [32]$$

} at electrode interface

$$Li^+(octahedral) \longrightarrow Li^+(tetrahedral) \longrightarrow Li^+(octahedral) \qquad [33]$$

$$(LiS_n)^+(oct) \longrightarrow (LiS_n)^+(tet) \longrightarrow (LiS_n)^+(oct) \qquad [34]$$

} in host

In a "normal" reaction sequence at low polarizations, some combination of processes 27-30 produce positively charged lithium-containing species and makes them available for intercalation. Either the production or the diffusion of these positively charged lithium-containing species to the interface would constitute the mass-transport limiting process on the solution side of the interface. The onset of intercalation occurs when electrons from the external circuit enter the band structure of the host lattice and make it sufficiently negative for the lithium ions to enter the lattice with some degree (usually complete) of desolvation and reside there as ions in equilibrium with the equivalent extra electrons in the host (equation 31). Under the continuing influx of electrons from the substrate (through the external circuit), the lithium ions migrate through the lattice via site-to-site jumps (equation 33). The mutual repulsion of the lithium ions aids in the energetics of this process. Other site-to-site jumps are possible (41), but are not important to the development of the model.

The diffusion of the lithium ions through the host via these site-to-site jumps is seemingly quite fast with the diffusion coefficient of Li^+ in TiS_2 being reported to be ca. 1.5×10^{-9} cm^2/s as measured by chronoamperometry, chronopotentiometry and NMR spin-lattice relaxation (the range of reported values, however, spans more than two orders of magnitude) (114,134,144-146).

Under conditions of high polarization, the mass-transport effects become more complex. Stirring the solution may serve to increase the rate of mass-transport in the solution but this is not possible for the solid-solution, thus making it difficult to distinguish between charge-transfer and mass-transport kinetically in the electrical double-layer. If the polarization is great enough, then it is possible that there would be insufficient time for the processes in equations 27, 29, and 30 to occur and that a reaction similar to equation 32 would take place.

With these larger lithium-containing cations, $(LiS_n)^+$, now in the lattice, it is probable that slower diffusion of these larger species within the host (equation 34) will be the rate-limiting process for continued intercalation. In principle, it should be possible to measure the rate of formation of Li^+ (as an average of equations 27 and 30) by determining the current <u>beyond</u> which the formation of Li^+ by these processes does not have time to occur. This approach is flawed, however, since the rate at which species can enter the lattice of the host depends upon the properties of the lattice, e.g., van der Waals gap, ionicity, etc., desolvation from solution. The results for the same processes using TiS_2 and $TiSe_2$ would be different.

Cyclic-voltammetry of $LiAsF_6$ solutions at a TiS_2 electrode exhibits several reduction peaks (133) indicating the presence of several steps for the process of intercalation.

When different solvents are employed there is an observed shift in the potentials at which electrode processes occur (as found in the present work and in ref. 133). This suggests an important role for the solvent during the process of intercalation.

A determination of the mechanism is further complicated by the particulate nature of the electrode and the irregularity of electrochemically active surface areas. A model for a particulate electrode in contact with a liquid electrolyte is shown in Figure 21 (134). The active particles of the electrode material are only those particles which are in contact with the liquid. Electron-transfer can occur quite easily between the "dry" particles (the $TiCh_2$ are reasonably

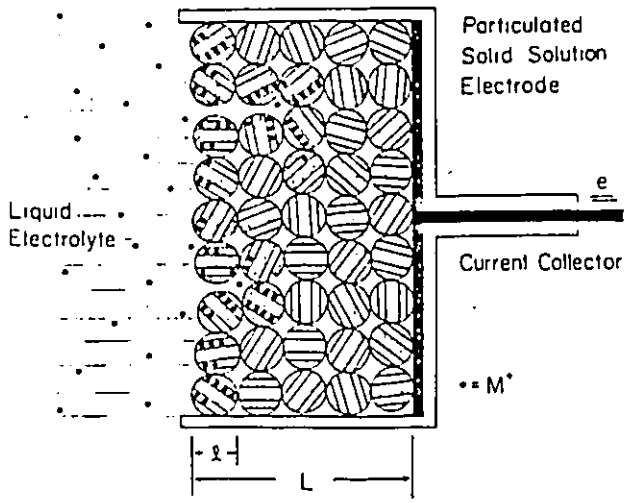

FIGURE 21

PARTICULATE SOLID SOLUTION ELECTRODE

(After Ref. 134)

good conductors). Conduction in the "wet" particles is largely by ionic mechanisms (e.g., equation 33); however, ionic transport across interparticle boundaries (i.e., from one $TiCh_2$ crystallite to another) is not likely. Thus, the electrode behaves as a thin layer interface where the path for solid-state diffusion (ionic-conduction) is not greater than the average particle diameter (134).

In order to study the interface of an intercalating electrode (specifically, double-layer phenomena) it is necessary to have a large single-crystal with one edge of the crystal presenting itself to the electrolyte solution in order to produce a well-defined surface area for intercalation. Even when one is able to use a single-crystal, the surface area does not remain constant. As x in Li_xTiCh_2 becomes greater than zero the lattice expands in a regular way. In principle, it is possible to estimate the changing surface area by monitoring the amount of charge that is passed (in either direction) coulombic efficiency must be taken into account). In a practical sense, large single-crystals are difficult to grow and are quite fragile. Single-crystals have a small surface area-to-mass ratio which is why most workers in seeking a battery electrode opt for the high surface area powders. Because of the difficulty of measuring the true surface areas of these interfaces, any "current densities" that are reported should be a function of the number of moles of host used and the average particle

size. Without large, well-defined single-crystals of the layered hosts, an investigation of the interface based upon the coupled double-layer model (or any model) is not practical.

With further knowledge of the interfacial "limitations" from mass-transport on either side of the interface it should be possible to create a mathematical model of the coupled double-layer utilizing the mass-transport data from both sides of the interface.

The contribution in the present work to this problem will be the investigation of the interfacial limitations of charge-transfer and mass-transport for $LiCF_3SO_3$/2MeTHF electrolytes in cells using particulate electrodes of TiS_2 and $TiSe_2$. Without single-crystals this must be part of a larger effort to investigate these unique interfaces.

While it is generally accepted that the rate-limiting process is the diffusion in the host structure, the multi-stage oxidations and reductions that have been observed in voltammetry reemphasize the complexity of the interface. There has been no unambiguous evaluation of the kinetics of cell performance. This is due in part to the largely proprietary way in which these electrodes are made and consequently the experimental conditions and data differ between authors, or are not fully known. These data depend upon material stoichiometry, particle size, preparation

procedure (including the use of binders such as Teflon) and upon the electrochemical method of evaluation.

The mathematical treatment of particulate electrodes by Atlung et al. (147) serves as a guide for the design of experimental electrodes. They consider the "solvent" properties of the host and have calculated a "dielectric constant" for the TiS_2 planes (148). Treatment is given to the concentration profiles of Li^+ in the electrolyte and in the solid-solution during charge and discharge of a cell. During a galvanostatic load, a steady-state, linear concentration-distance (from the interface) profile will rapidly develop in the electrolyte. In the host material, no steady state is possible during load. When the interfacial concentrations of Li^+ are non-zero, the result is the creation of a transport overvoltage for the operation of the host as an electrode. The assumption is made that the process of Li^+ entering the lattice (equation 31) occurs quickly and reversibly, with a negligible overvoltage.

The time that is taken for a cell to discharge completely at a given load is not determined by these overvoltages but by the limiting conditions occurring when $[Li^+]_{soln} \rightarrow 0$ or when x in Li_xTiCh_2 approaches a limiting value (theoretically 1). (***NOTE:*** Discharge can continue beyond x = 1, but not without some free-energy being expended to form new solid-solution phases. Reactions occurring beyond x = 1 are not generally reversible.)

These two limitations will affect the interface and the utilization of the host in different ways. If the current density drawn on the host is high then $[Li^+]_{soln}$ quickly approaches zero and acts to limit the current. It is also possible that reactions such as that represented by equation 32 (the intercalation of $(LiS_n)^+$) could occur, further limiting diffusion within the host. The conditions where $[Li^+]_{host}$ approaches a limiting value are depicted in Figure 22 (after ref. 147). For a specific load during discharge, the amount of host material corresponding to the hatched area is not utilized (147). The result is that the coulombic efficiency of the cathode is reduced by a fraction proportional to the utilized part of the host. This reduction can

FIGURE 22

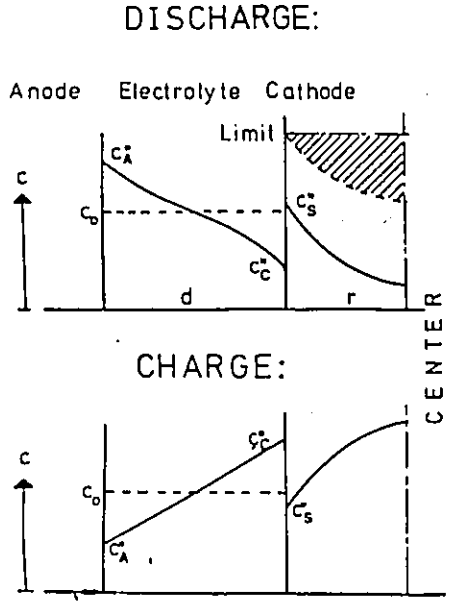

CATION CONCENTRATION PROFILES IN THE ELECTROLYTE AND IN THE SOLID SOLUTION CATHODE.

C_A^*, C_C^*, C_S^* are the interfacial concentrations.

C_o is the initial concentration in the electrolyte.

-·-·- is the profile at surface saturation.

Hatched area: unutilized part of electrode.

(From Ref. 147)

be considerable if the concentration gradient is steep (moderate current densities) or if the electrode is *thick*.

What is thick? Atlung et al. (147) develop their model based upon three types of "particles" for the electrode: infinite plane sheets of thickness 2r with both sides exposed to the electrolyte; infinitely long cylinders with radius r; and spheres of radius r. The diffusion equations were solved in terms of these "particles". They determined that for a planar particulate electrode of TiS_2 in an electrolyte of 1 M $LiClO_4$ in PC operated at the limiting current the product of r and the separation between the electrodes, d, should be less than 1.3×10^{-3} cm^2. Their value depends on the diffusion of Li^+ in the electrolyte solution and thus upon the solvent. For a system where the anode and cathode are separated by a 5 mil (0.013 cm) membrane, the cathode must be less than 1 mm thick. Smaller particle sizes, e.g., 10 μm to constitute this electrode will provide for a small grain boundary distance.

With a consideration for mass-transport on both sides of the interface, the general current-overpotential equation for the $Li^+/TiCh_2$ interface is given (134) by

$$I(t) = I_o[(C_o/C)\exp(-\alpha nF\eta/RT) - (C_s/C_b)\exp((1-\alpha)nF\eta/RT)] \qquad [35]$$

where I_o is the exchange-current, C and C_o are the bulk and interfacial concentrations of Li^+, respectively, C_s is the

concentration of Li^+ within the host at the solution interface (this is maintained constant by a constant applied potential), and C_b is the initial bulk concentration of Li^+ within the host (equal to zero for a fresh electrode). At short times, when $C_s >> C_b$, the current response will obey the Cottrell equation and

$$I(t)t^{1/2} = nFA(C_s-C_b)(D/\pi)^{1/2} \equiv nFAC_s(D/\pi)^{1/2} \quad [36]$$

Very quickly after the application of a potential, the lithium concentration in the host near the interface (C_s) reaches a maximum value, C_m, and a limiting current is attained

$$I_\ell(t)t^{1/2} = nFAC_m(D/\pi)^{1/2} \quad [37]$$

Equations 36 and 37 are combined to obtain an expression for C_s/C_b in terms of the experimentally measured currents,

$$(C_s/C_b) = (C_m/C_b)(C_s/C_m) = (C_m/C_b)w \quad [38]$$

where C_m/C_b is a constant and

$$w = C_s/C_m = I(t)t^{1/2}/I_\ell(t)t^{1/2} \quad [39]$$

Dividing equation 35 by $I_\ell(t)t^{1/2}$, substituting equations 38 and 39 into the result and suitably rearranging yields a dimensionless current-overpotential equation

$$1/w = a \cdot \exp(\alpha\theta) + b \cdot \exp(\theta) \qquad [40]$$

where

$$a = (C/C_o)(I_\ell(t)t^{1/2}/I_o t^{1/2} \qquad [41]$$

$$b = (C/C_o)(C_m/C_b) \quad \text{and} \qquad [42]$$

$$\theta = nF\eta/RT$$

With the continuing assumption that the current is limited by the rate of diffusion of Li^+ within the host, C_o will be independent of the overpotential and the quantities a and b may be regarded as constants to be evaluated by reduction of the current-potential data. With a and b known, the rate of charge-transfer may be compared with the rate of solid-state diffusion by

$$b/a = C_m/C_b = I_o t^{1/2}/I_\ell(t)t^{1/2} = K^\circ t^{1/2}(C/C_b)^{(1-\alpha)}/(D/\pi)^{1/2} \qquad [43]$$

with

$$I_o = nFAK^\circ C^{(1-\alpha)}C_b \qquad [44]$$

Since C_b is difficult to measure, equation 42 may be solved for C/C_b and substituted into equation 44 thus obtaining an expression for the heterogeneous rate constant k° in terms of the diffusion coefficient for solid-state diffusion

$$k^\circ(t/D)^{1/2} = (C_o/C_m)^{(1-\alpha)} b^\alpha/a\pi^{1/2} \qquad [45]$$

With the assumption that C_o ($[Li^+]_{interfacial}$) is equal to C ($[Li^+]_{bulk\ electrolyte}$), this equation will result in an estimation of a maximum value for $k^\circ(t/D)^{1/2}$ (134).

The data to be evaluated were acquired in the time domain for which the Cottrell equation is valid ($Dt < 0.25\ \ell^2$) where ℓ is the average grain size.

The value for D itself may be estimated from the time at which the deviations from the Cottrell behavior (linear log I versus log t) occur and a knowledge of the average grain size for the host material. It should be pointed out that these values that are obtained for D and k° are not independent of x in Li_xTiCh_2. Here, they will be determined for values of x that are zero or very close to zero.

This work will show that the rate limitations and reversibility of these systems can be permanently and detrimentally altered by the application of an intentional or accidental peak current (in excess of I_ℓ). This current can cause species such as $(LiS_n)^+$ to enter the lattice and remain there due to slow diffusion. These processes will be investigated

for 2 M $LiCF_3SO_3$ in 2MeTHF for both TiS_2 and $TiSe_2$. The role of the solvent will also be discussed in a comparison with data from other workers.

1 EXPERIMENTAL

1.1 CELL DESIGN

The three electrode cell is a modification of a design by Dr. Viola Birss, when at the University of Ottawa, that was used for very small quantities of particulate oxide electrode materials. The cell used here (Figure 23) consists of a gold cup and wire embedded in Epo-Mix™ Epoxy (Buehler) and sealed in a piece of 20 mm (o.d.) glass tubing (piece #3) which is further sealed in a piece of 20 mm (i.d.) tubing (piece #2). This cup, which is about ½ mm deep constitutes the current collector (e.g., Figure 21) for the particulate cathode material. The current collectors for the counter and reference electrodes were prepared by sealing platinum (instead of gold, for added strength) in Epo-Mix™ in a similar 20 mm o.d. tube. The platinum wires were allowed to extend a short distance from the surface of the epoxy so that they could penetrate the reference and counter electrode materials.

The Epo-Mix™ was examined for stability in 2MeTHF at ambient and elevated (70 °C) temperatures. The solvent was

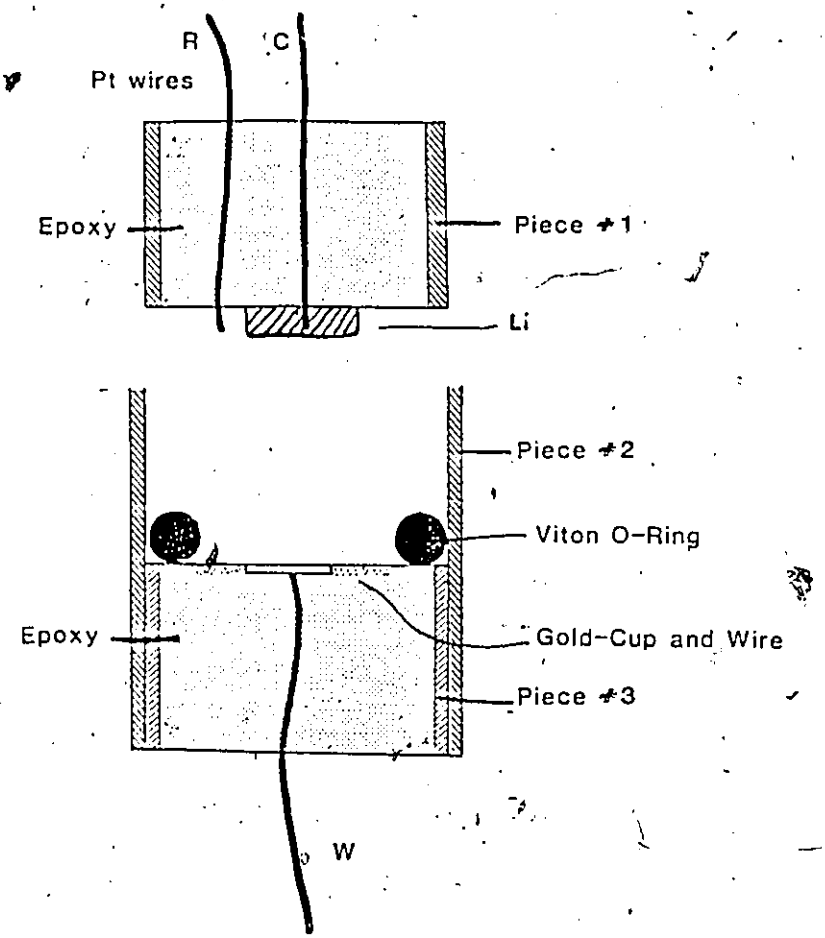

FIGURE 23

THREE-ELECTRODE ELECTROCHEMICAL CELL
FOR CHRONOAMPEROMETRY AND CYCLIC VOLTAMMETRY

analyzed by gas chromatography after one, two, and seven days for decomposition products or dissolved products. At ambient temperature it was found that the epoxy could remain in contact with the 2MeTHF for at least two days without detectable degradation. At 70 °C the epoxy showed signs of discoloration and degradation products were found in the solvent after just one day.

The gold "cup" is to contain a weighed sample of the host electrode material. This material is held in place by a separator membrane of 10 mil (0.25 mm) woven glass fiber paper (without binder or wetting agents)(Mead Corporation). The separator was held down by a Viton O-ring which also served as a spacer to allow room for the reference and counter electrodes. The whole assembly is held together using a spring clamp. Two holes were drilled in the epoxy counter/reference electrode piece so that electrolyte could be introduced into the cell with a syringe.

1.2 REFERENCE ELECTRODE

The electrochemical reaction

$$Li^+ + e^- = Li$$

has a relatively high exchange-current density in non-aqueous solutions (149). The electrode potential responds in a Nernstian fashion to changes in cation concentration (150)

and when lithium metal (wire, foil, or rod) is used, the electrode behaves to a good approximation as a non-polarizable electrode. These properties make it suitable for use as a reference electrode.

Lithium wire (0.125 in. diam., battery-grade - low sodium, Foote Mineral Co.) was used as a reference (and counter) electrode. A small piece was cut with a plastic blade and impaled on the platinum wire in the cell. Lithium is used as a counter electrode to supply lithium ions to the solution as lithium ions are discharged from the solution into the host lattice.

1.3 ELECTROCHEMICAL MEASUREMENTS

The chronoamperometry measurements were performed using a Princeton Applied Research (EG&G) model 273 Potentiostat/Galvanostat which was interfaced to either an Apple IIe or IBM PC computer for data acquisition/experiment control. The 273 has a built-in signal generator to execute simple waveforms ($E = f(t)$ in voltammetry with the 273 is actually a staircase ramp instead of a smooth ramp). More complicated waveforms and holding potentials can be achieved by using the computer to program the signal. The programmed signal in this case is actually a square wave of constant E held for the duration of the experiment (2000-6000 s). The apparatus was also used

for cyclic-voltammetry to investigate the anodic limit electrochemical stability of the solvent.

1.4 ANODIC LIMIT OF STABILITY OF 2MeTHF

In order to verify the stability (and purity) of the $LiCF_3SO_3$/2MeTHF electrolyte, a 2 M solution was injected into the cell which had been prepared with a lithium counter and reference electrode. The working electrode was gold (0.72 cm^2). A linear potential sweep starting at the rest potential (1.9 V vs Li/Li^+) and sweeping anodically at 100 mV/s was performed. The potential at which the anodic current-density reached 100 $\mu A/cm^2$ (an arbitrary value, after ref. 16) was recorded. The anodic limit determined in this manner was 4.18 V vs Li/Li^+. This is to be compared to 4.15 V for 1 M $LiAsF_6$ in 2MeTHF on a glassy carbon electrode (16). A very small rate of oxidation (< 2 $\mu A/cm^2$) was observed at 3.42 V and a corresponding reduction at 2.43 V. The potential at which the electrolyte solution oxidizes determines the maximum charging potential that can be used for removing Li^+ from $TiCh_2$.

1.5 CONDUCTANCE OF 2 M $LiCF_3SO_3$/2MeTHF

The conductivity of 2 M $LiCF_3SO_3$ in 2MeTHF was determined using the conductance cell that was described previously. The conductivity at 25 °C was determined to be 1.04×10^{-3} S/cm.

1.6 ESTIMATION OF GRAIN SIZE BY SEM

A series (3 - 4 photos) of scanning electron micrographs were taken of each sample of $TiCh_2$ in order to estimate the average particle size for the particulate electrodes. Even after grinding the sample in an agate mortar, there was a large variation in grain size and microstructure. The variation in grain size was over a factor of 2 to 6 for most samples. For the TiS_2 samples, the average grain size was typically 5 to 20 μm and for $TiSe_2$, 5 to 25 μm. The large range of the grain sizes and the difficulty in determining their average size means that the value for the diffusion coefficient that is extracted from the results is a mean value having a large uncertainty.

The micrographs were taken on an ISI-40 (International Scientific Instruments) scanning electron microscope. Examples of photographs taken for TiS_2 are shown in Figure 24.

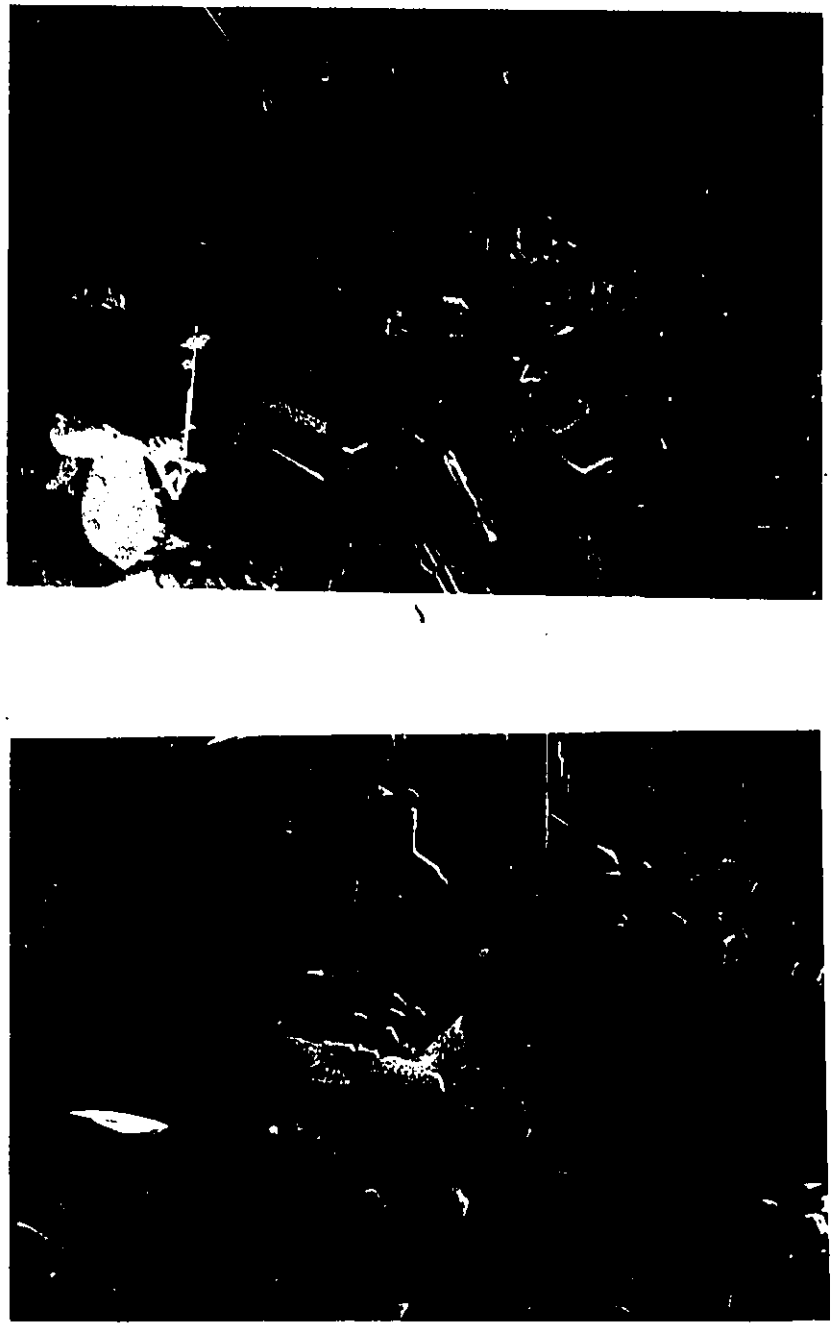

FIGURE 24

SCANNING ELECTRON MICROGRAPHS OF TiS_2

1.7 EXPERIMENTAL REGIME

Chronoamperometry was performed on TiS_2 and $TiSe_2$ electrodes at several overpotentials. The solid-state diffusion coefficient and heterogeneous rate constant were evaluated for each system. A fresh electrode was used each time because the application of an anodic current does not assure complete removal of Li^+ from the $TiCh_2$.

Next, a peak current, arbitrarily chosen to be about five times the limiting current for the electrode, was applied for 100 ms. At this current-density (using the apparent electrode area), even if the electrode were operating at 100% coulombic efficiency, only 10^{-7} C of lithium-containing ions are passed. The crystals at the surface of the electrode appeared to swell. X-ray crystallography of some of these crystals near the surface show that the c-lattice parameter of the host had increased beyond what would be expected for the incorporation of unsolvated lithium ions. For TiS_2 the c-lattice parameter was determined to be 1.64 ± 0.17 nm and for $TiSe_2$ the value was 1.73 ± 0.26 nm. The relatively large uncertainty in these results was due to the mixed composition of the analysis sample and the presence of some diffuse lines in the powder pattern. The increased lattice parameter can be attributed to the incorporation of $(LiS_n)^+$ (the determination of the value of n cannot be made without more complete structural information).

The small amount of intercalated species should not affect the theoretical treatment of the I-t data - the bulk solid concentration of Li^+, C_b, can still be approximated as being near zero.

After the application of the peak current, the electrode was allowed to rest for ca. 20 minutes until the potential recovered to an equilibrium (open-circuit) potential. After the rest potential was attained, the same series of potential steps was applied to the conditioned electrode. After each potential step, a new electrode must be prepared and conditioned with a peak current. This increases the uncertainty of the results so obtained.

2 EXPERIMENTAL RESULTS AND ANALYSIS

The results for the chronoamperometric measurements on TiS_2 and $TiSe_2$ are presented graphically in Figures 25 - 28. The applied overpotentials versus Li/Li^+ are indicated on the figures. Values for the various parameters of equations 36 to 45 were extracted from these graphs in the following way:

First, the time at which deviations from the Cottrell behavior occurred (t_C) was determined from the graph. Using this time and the average grain size, ℓ, as determined by SEM, a value is determined for the diffusion coefficient through the relation

$$Dt = 0.25\ell^2 \qquad [46]$$

Using this value of D, the I-t data in the region where Cottrell behavior is observed is used to calculate $A(C_s-C_b)$ at each overpotential. In the Cottrell region (linear log(I) versus log(t) behavior) this value for $A(C_s-C_b)$ is independent of time. A is the **effective** area of the $TiCh_2$ electrode and its value depends upon grain size and electrode preparation procedures (e.g., the use of Teflon binders) which would affect the available surface area. The value of $A(C_s-C_b)$ is evaluated through

$$A(C_s-C_b) = I(t)t^{1/2}\pi^{1/2}/nFD^{1/2} \qquad [47]$$

This value is first "normalized" to the apparent electrode surface area and electrolyte concentration, C. This normalized value, $A(C_s-C_b)/A_{app}C$, is then passed on to a rearranged form of equation 40,

$$i/w = I_\ell(t)t^{1/2}/I(t)t^{1/2} = \frac{A(C_m-C_b)/A_{app}C}{A(C_s-C_b)/A_{app}C} = a\cdot e^{\alpha\theta} + b\cdot e^{\theta} \qquad [48]$$

which is further rearranged to

$$\frac{1}{A(C_s-C_b)/A_{app}C} = \frac{a\cdot e^{\alpha\theta}}{A(C_m-C_b)/A_{app}C} + \frac{b\cdot e^{\theta}}{A(C_m-C_b)/A_{app}C} \qquad [49]$$

The data pairs ($A(C_s-C_b)/A_{app}C$ and the overpotential as $\theta = n\eta F/RT$) are fitted to equation 49 using the program ***FIT*** (see appendix). The parameters that are obtained from this fit are $A(C_m-C_b)/A_{app}C$, a, b, and α. The initial estimates for a, b and α were obtained from the data for $LiAsF_6$ in DME (a solvent of similar dielectric constant to that of 2MeTHF) (134). The estimate for the value of $A(C_m-C2b)/A_{app}C$ was obtained from a plot of $A(C_s-C_b)/A_{app}C$ versus η. At high η, the current approaches a limiting value and C_m is attained at the host interface. This corresponds to the limiting current and to $A(C_m-C_b)/A_{app}C$.

With these parameters having been obtained, the heterogeneous rate constant is evaluated through equations 43 and 45. The results of these calculations are presented in Table 12.

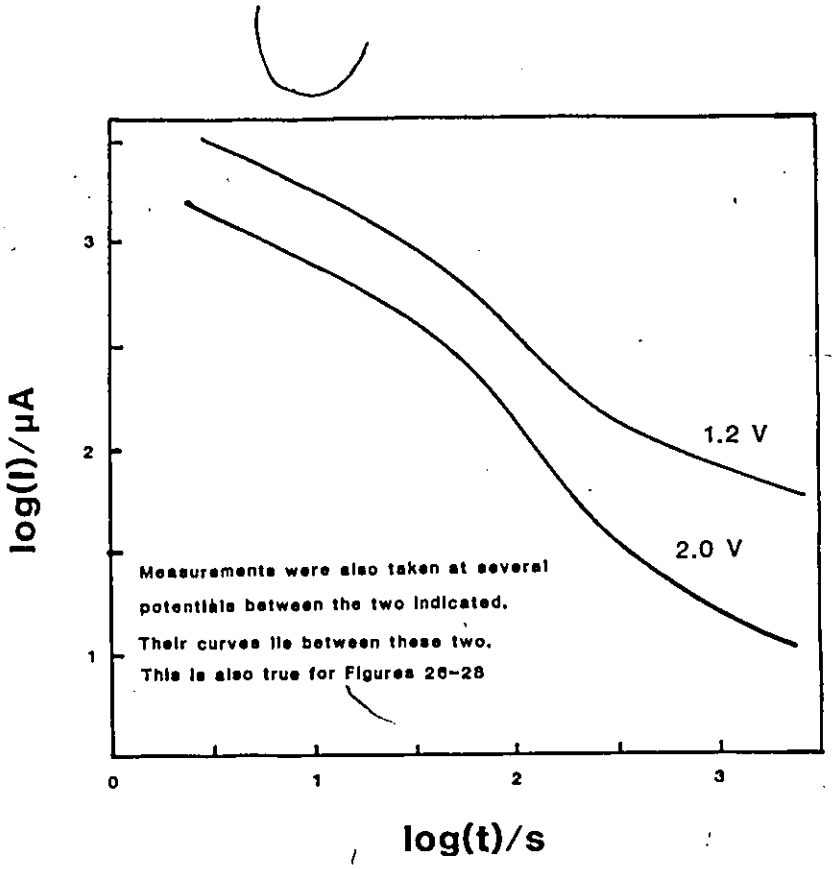

FIGURE 25

LOG(CURRENT) VS LOG(TIME) FOR CHRONOAMPEROMETRIC MEASUREMENT AT $TiSe_2$ (FRESH) IN $LiCF_3SO_3$/2MeTHF

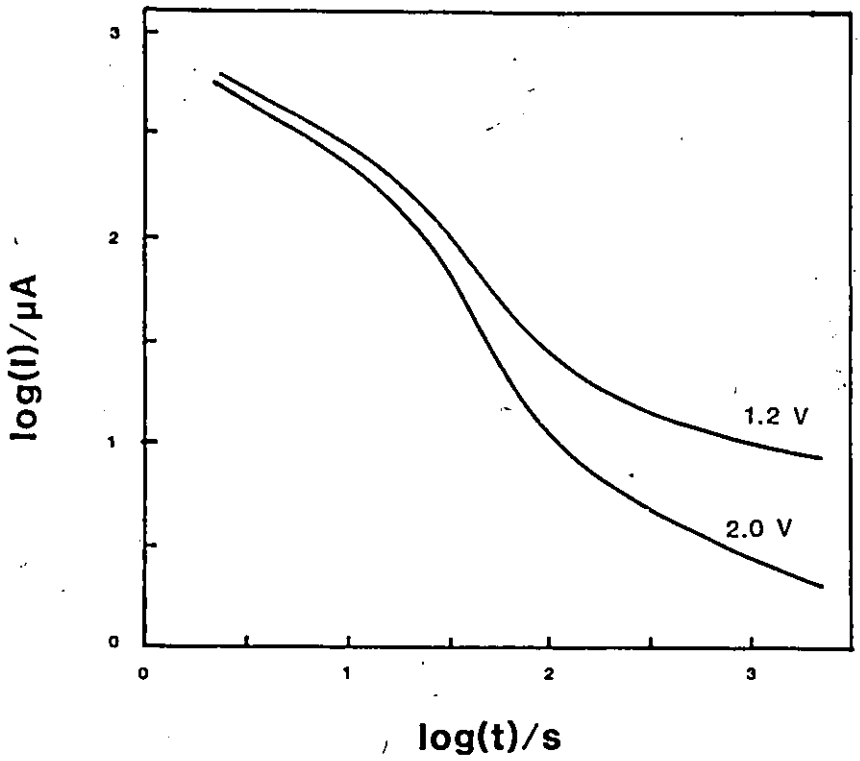

FIGURE 26

LOG(CURRENT) VS LOG(TIME) FOR CHRONOAMPEROMETRIC MEASUREMENT AT TiS_2 (FRESH) IN $LiCF_3SO_3$/2MeTHF

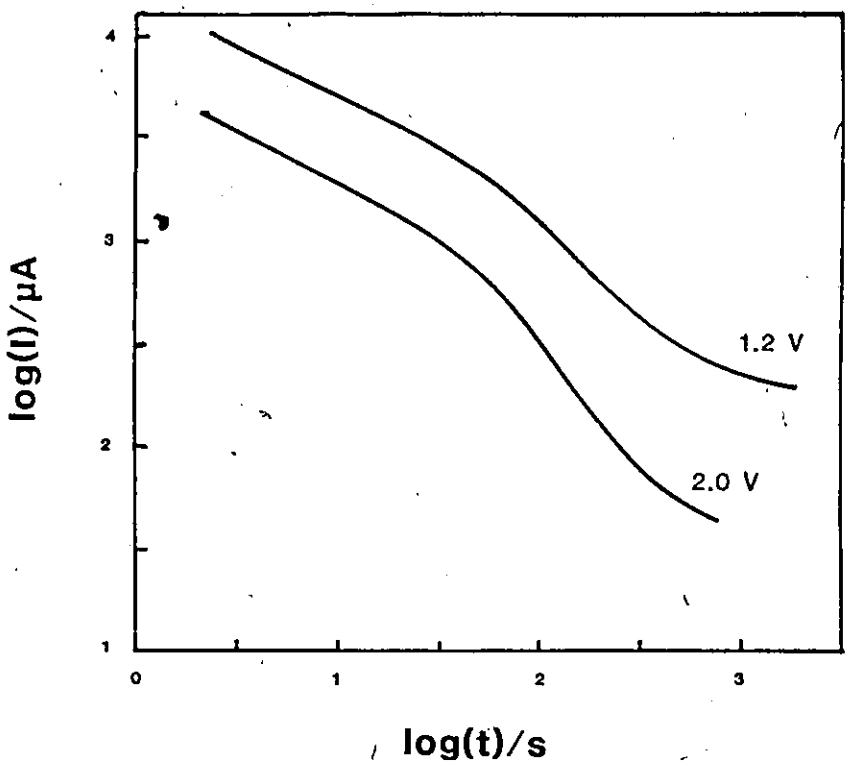

FIGURE 27

LOG(CURRENT) VS LOG(TIME) FOR CHRONOAMPEROMETRIC MEASUREMENT AT $TiSe_2$ (STRESSED) IN $LiCF_3SO_3$/2MeTHF

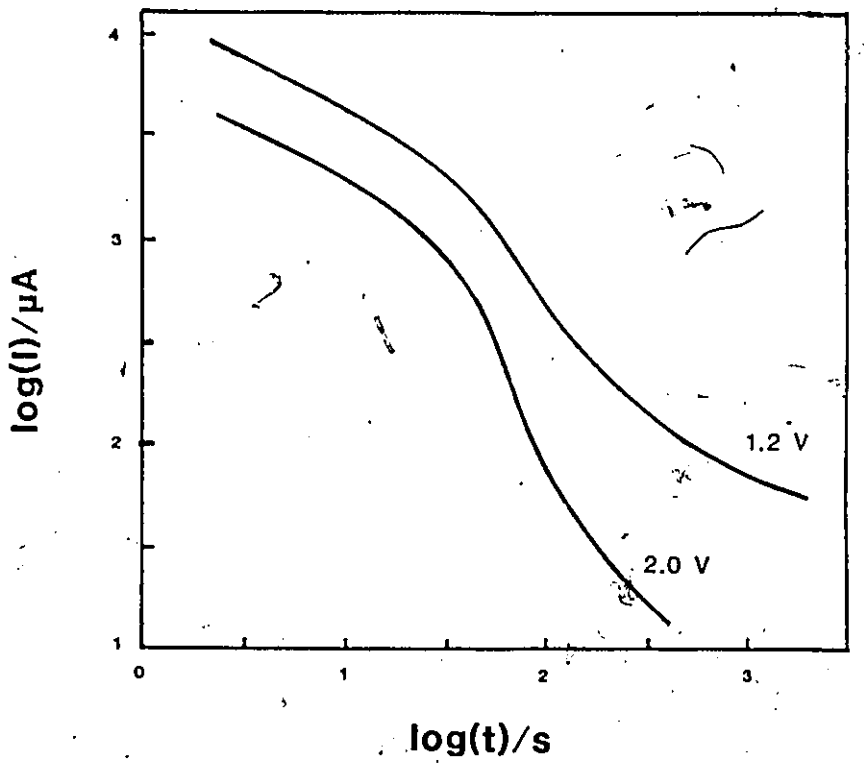

FIGURE 28

LOG(CURRENT) VS LOG(TIME) FOR CHRONOAMPEROMETRIC MEASUREMENT AT TiS_2 (STRESSED) IN $LiCF_3SO_3$/2MeTHF

TABLE 12

CHARGE-TRANSFER AND MASS-TRANSPORT PARAMETERS FOR $LiCF_3SO_3$/2MeTHF AT TiS_2 AND $TiSe_2$

	TiS_2	$TiSe_2$
t_C/s	13	39.5
$D/cm^2\ s^{-1}$	7.51×10^{-9}	4.08×10^{-9}
a	2.23	4.84
b	218.6	1939.
α	0.018	0.0155
$k°/cm\ s^{-1}$	7.51×10^{-7}	6.93×10^{-7}
$A(C_m-C_b)/A_{app}C$	2.83	1.57
$k°t_C^{1/2}/D^{1/2}$	0.0312	0.0636
	stressed TiS_2	stressed $TiSe_2$
t_C/s	21.5	50.8
$D/cm_2\ s^{-1}$	4.54×10^{-9}	2.77×10^{-9}
a	2.34	4.31
b	73.3	311
α	0.016	0.0131
$k°/cm\ s^{-1}$	4.65×10^{-7}	4.46×10^{-7}
$A(C_m-C_b)/A_{app}C$	2.71	1.42
$k°t_C^{1/2}/D^{1/2}$	0.032	0.0604

3 DISCUSSION

These studies of the discharge of the host material (as a cathode opposed by a lithium anode) were motivated by a desire to obtain an understanding of the relationship between charge-transfer and mass-transport at such an interface. In addition, the role of the solvent with respect to these processes is of interest. The difficulty in working with such interfaces should not be underestimated and this limits the types of experiments that can yield quantitative information. Without a complete study with single crystals, the double-layer models remain as conceptual guidelines for interpretation of results. As can be seen from the results (Figures 25-28 and Table 12), the larger van der Waals gap and octahedral site size for $TiSe_2$ does not mean that lithium ions will diffuse more quickly. In the absence of a major difference in the ionicities of TiS_2 and $TiSe_2$, the behavior can be attributed to differences in the Fermi levels of the two hosts and the larger activation energy for site-to-site jumps by Li^+ in $TiSe_2$ (the octahedral sites in $TiSe_2$ may be larger than those in TiS_2, but the gap between the sites is smaller). Thompson (140) has shown that the free energy for the formation of **ordered phases*** in Li_xTiCh_2 is greater for

---

*Ordered phases refers to the ordering of Li^+ within the $TiCh_2$. Thompson (140) clearly demonstrated the ordering of Li^+ in TiS_2 at x = 1/9, 1/4 and 6/7. The ordering at x = 6/7 is an ordering of the vacant octahedral sites.

$TiSe_2$ than for TiS_2. This may help to explain the slower diffusion of Li^+ in $TiSe_2$.

The diffusion coefficients that are reported here are larger than those reported for $LiAsF_6$ and $LiClO_4$ in DMF. The donor number for DMF is 30.9 (5) and that for THF is 20 and the donicity of 2MeTHF should be similar to the latter figure. The dielectric constant of DMF is also much larger (36,7) than of 2MeTHF.

Popov et al. (151,152) has shown that for alkali metal salts in solvents with a donicity comparable to that of DMF, the position of the vibrational absorption bands are independent of the nature and mass of the anion. Thus, the absorptions were attributed to ion-solvent interactions. Edgell et al. (153) reported their observation of the vibrational spectra of lithium, sodium and potassium salts of $Co(CO)_4^-$ and $Mn(CO)_5^-$ in THF. The absorptions in the case of the latter anion were 20 to 30 cm^{-1} higher with the results being explained as an ion-ion interaction (ion-pair formation) for the salts in THF. Solvation of the lithium ion is more likely in DMF due to the stronger solvating ability of the solvent and this probably allows solvated lithium ions (which would diffuse slower in the host) to enter the lattice. This is evidenced by the much larger degree of swelling observed for the intercalate in DMF than in 2MeTHF (this work, 134). While the application of a peak current did cause some larger species to enter the host (as evidenced by the x-ray analy-

sis), these larger species did not slow the measured diffusivity by more than 30-40%. It is possible that the slight expansion of the lattice opened the intergranular boundaries to the electrolyte, thus increasing the effective surface area.

It is also interesting to note that the product $K^{o}t_{C}^{1/2}/D^{1/2}$ remains approximately constant in going from the unstressed electrode to the electrode that was stressed by a peak current. This ratio compares the rate of charge-transfer to the rate of mass-transport (solid-state diffusion).

The rate of charge-transfer is somewhat larger than for the DMF-based system and this can be attributed to less involvement by the 2MeTHF in the intercalation process. However, the rate constants for intercalation in 2MeTHF-based solutions would yield low exchange-current densities. The values obtained for the transfer coefficient would imply that the process of removing species from the host is much easier than that for inserting them. Intuitively, just the opposite would be true – intercalation takes place with relatively low polarizations, the process of removing lithium ions from the host is never complete and the host material is often a much better "solvent" for lithium ions than is the organic solvent (a dielectric constant of 31 has been calculated for TiS_2 (148)). Because of the apparent irreversibility of the systems and the low exchange currents, the assumption that the actual process of intercalation (equation 31) is rapid

and reversible may not be entirely correct. If the assumption is correct, then the mechanism of charge-transfer occurs inside the lattice and is not necessarily a consequence of the process at the actual interface. As a part of the coupled double-layer model – it may be that charge-transfer is not complete until the lithium ions entering the lattice are several atomic diameters into the host where its electrical field no longer "sees" the electrolyte, i.e., it has passed beyond the host's (internally generated) compact double-layer. A solvent with a stronger donicity (e.g., DMF) would slow this process more than a non-involved solvent.

In spite of its low conductivity, the non-involvement of the 2MeTHF solvent (as well as its relatively small reactivity with lithium and $TiCh_2$) seems responsible for the longer cycle life of lithium intercalation cells based upon this solvent. The role of the solvent donicity in the intercalation process in intriguing when one normally considers as suitable for electrochemical power sources those solvents with the strongest solvating ability.

The important processes in solution that present lithium ions to the interface are

$$(Li_2A)^+ = (Li^+A^-) + Li^+ \qquad K = 1/K_t \qquad [27]$$

$$(Li^+A^-) = Li^+ + A^- \qquad K = 1/K_p \qquad [29]$$

$$(LiS_n)^+ = Li^+ + nS \qquad [30]$$

The rate constants on going from left-to-right will determine the rate at which Li^+ becomes available for intercalation. For a weakly solvating solvent such as 2MeTHF, lithium ions are produced rapidly with the application of an applied potential. However, since almost all of the lithium ions exist in solution as ion-pairs or higher aggregates, this process becomes relatively unimportant. The rate limiting process in solution will be the rate at which lithium ions are produced by the processes represented by equations 27 and 29. Upon the application of the peak current to "stress" the electrode, one or more of the left-to-right processes that are represented above will not have time to occur and a large species (e.g., $(Li_2A)^+$ or $(LiS_n)^+$) will likely enter the lattice.

Energy must be expended in initially opening up the layers of the host for incorporation of the guest species. The energetics, mechanism and reversibility of this process has not been accounted for in any of the models of the intercalation process. As mentioned above, it is often assumed that the actual process of insertion (which is accompanied by an opening of the layers) is both rapid and reversible.

Once the lithium ion has entered the lattice the electron density within the host's band structure is redistributed to balance the charge that is introduced by the ion. The increased number of electrons that are required to balance the charge are supplied by the external circuit. With the

continued flux of electrons from the external circuit, the lithium ions will migrate through the lattice in the direction of the source of these electrons. The movement of lithium ions through the host must continuously work to open the layers of the host as the "wave front" of intercalated species migrates toward the source of electrons (cf. ref. 41).

When the external circuit has been broken and the flux of electrons has ceased, the movement of lithium ions within the lattice may continue with the energy for the site-to-site jumps being provided by the mutual repulsion of the lithium ions. In this way, the localized concentrations of lithium ions in the host (near the interface) can be redistributed to a "bulk" concentration of the species within the host. This is analogous to the processes occurring in solution except that the charge carriers within the host are more discretely separated. The role of the host as a "solvent" in these processes, which was introduced by Atlung et al. (148), needs to be investigated further.

APPENDIX

A. RIGOROUS LEAST-SQUARES ADJUSTMENT

The original computer program was written in BASIC by Mark McNeil and Earl K. Ralph of Memorial University, St. Johns, Nfld. The present program, called *FIT*, was adapted from the original program for the IBM PC be Tom Clune and Ernest Grunwald and further modified by Larry Dominey and the present author at Brandeis University, Waltham, MA.

Introduction - The program *FIT* executes a nonlinear least-squares calculation based upon the general statistical method of Wentworth and Deming (101,102). The user specifies the number of variables, parameters and constants, the function that is to be fitted, and the partial derivatives of this function with respect to both variables and parameters. The latter are required in the rigorous calculation.

The present calculation is longer than that involved in the common method of least-squares; however, it offers significant advantages. In the common least-squares method one assumes that the data are completely accurate and tests whether the chosen function will reproduce them. Key quantities are the standard errors of fit and the correlation coefficients. "Best fit" values are obtained for the parameters and if due attention is paid to assigning statistical weights, the parameters are indeed quite good. On the other hand, the errors assigned to these parameters in the

common least-squares method make no allowance for experimental errors in the data and thus are unrealistically small. Since the parameters have physical significance (e.g., Λ, K_a) and are often used further, the absence of realistic error estimates is a problem.

Wentworth's method overcomes this problem. When the data are entered, a standard deviation σ is specified for each data point. The statistical weight of the point is taken to be $1/\sigma^2$. The effect of the error on the function, F, is then computed by multiplying the statistical weight of the given data points, $x(I)/\sigma^2$, by $[\partial F/\partial x(I)]^2$. From a statistical point of view the parameters obtained by this method are better than those obtained by the common method of least-squares, and the standard deviations assigned to the parameters now include the effects of the experimental errors in a realistic way.

Starting the program. The program disc contains IBM's "advanced BASIC" interpreter - BASICA, the program ***FIT***, and some files for the temporary storage of data during program operation. The operations are as follows:

1. Turn on the computer and optionally supply the date and time when the prompts appear. When the prompt A> appears type BASICA and press <CR> to load the basic interpreter. When the prompt "OK" appears, type LOAD "FIT" and press <CR> to load the program.

2. To run and initialize, press the user-defined key, F2 on the left of the keyboard. (F2 is equivalent to the command RUN<CR>). This will take you to the Help Screen and allow you to select an appropriate subroutine.

Notation - The following notation is used.

Variables are denoted by X(1), X(2), . . . X(i).

Parameters are denoted by C(1), C(2), . . . C(j).

Constants are denoted by B(1), B(2), . . . B(K).

For example, a straight line might be written as

```
X(2) = C(1) * X(1) + C(2)
```

The function to be fitted is always written in the form F = 0. Thus, for the preceeding straight line

```
F = C(1) * X(1) + C(2) - X(2)
```

The partial derivatives are denoted as follows

∂F/∂X(I) is denoted by F1(1,I)

∂F/∂C(J) is denoted by F1(2,J)

This notation, which may be unfamiliar, is dictated in part by BASIC syntax.

Running the program. The program is divided into convenient subroutines which are accessed by pressing user-defined keys. To see a list of these subroutines go to the Help Screen by pressing F9.

Subroutine F4 will take you to a screen which lists the functions which have already been programmed. These functions are stored in separate files. If you wish to use one, you must first "merge" it with the main program. Just follow the prompts, then press F2 to initialize the merged program.

If the desired function is not listed, press F3 to enter it. This is a bit intricate, so follow the prompts precisely. It will be helpful to prepare a list of the desired function and of its partial derivatives using BASIC notation. When you are all done you can check your typing by pressing F1. If you find a mistake, you need only retype that particular prompt. In response to prompts that need no correction, simply press F10.

Subroutine F6 enables you to enter your data. Just follow the prompts. After all data have been entered, the program will display them in a Table. Use the "delete data sets" and "add data sets" prompts to make corrections. The program is written so that you can only make corrections by deleting and adding an entire data set (that is, X(1), Y(1) pairs etc.).

Before leaving the data-entering routine, the program will save your data on a disk. You have two options. If you need only temporary storage, the data will be saved in the file "DATASETS". More likely you will want more permanent storage. You get this by naming your own file.

Having entered your data, you may proceed to the least-squares calculation either by choosing "menu item 5", or by

returning to the help screen and pressing F7. The calculation involves numerous multiplications and divisions as well as inversion of an N by N matrix. The program may take several minutes to run.

The least-squares calculation is by successive approximations. To get it started you must enter (when prompted) the initial estimates for the parameters. These estimates should be fairly accurate, especially when F is not a simple algebraic function, to assure convergence.

In answer to the prompt "How many cycles?" - two are recommended. The program will display the results of each iteration, and at the end will ask you if you want more. After you are satisfied that convergence has been achieved, you may print out the final results by pressing F8.

Format of printout. The printout lists the parameters and their standard deviations. It then prints a Table listing the Set Number, F, the X(I) values and their standard deviations. If the fit is good, the values of F will be nearly zero, and the sign of F will vary between + and - in a random fashion.

The Table then lists the covariances (discussed below) and finally the equation for F.

Interpretation of parameters obtained with *FIT*:

If the standard deviation of a parameter is much greater than the value of the parameter, then the parameter is statistically insignificant and may be equated to a constant value of

zero. Accordingly, any terms multiplied by the parameter in the original function may be dropped from F and the fitting repeated using the simpler function.

If the magnitudes of F are considerably greater than the experimental error, or if the signs of F are not in a random sequence, then F is probably not an acceptable fitting function.

FIT

The program ***FIT*** executes a non-linear least squares calculation with particular attention given to the uncertainties in the physically measured data. The program is described at the beginning of the appendix. This version is written in Microsoft BASIC (Ver 3.0) on an IBM-XT personal computer.

```
1    KEY OFF:CLS
5    OPEN "DATA" FOR OUTPUT AS #1:H=0:M=0:N=0:O=0:I=0:WRITE
     #1,H,N,O,I,M:CLOSE
10   OPEN "DATA" FOR INPUT AS #1:INPUT #1,H:CLOSE
15   ON H GOTO 425, 355, 350
20   OPTION BASE 1:CLS
21   DEFDBL A,B,C,F,L,R,T,X,W
22   DEFINT M,N,O,P,I,Q,K,J,H
25   KEY 2,"RUN"+CHR$(13)
30   KEY 3, "GOTO 565"+CHR$(13)
35   KEY 4, "GOTO 8000"+CHR$(13)
40   KEY 5, "CONT"+CHR$(13)
45   KEY 1, "GOTO 80"+CHR$(13)
55   KEY 6, "GOTO 1422"+CHR$(13)
60   KEY 7, "GOTO 955"+CHR$(13)
65   KEY 8, "GOTO 1350"+CHR$(13)
67   KEY 9, "GOTO 10000"+CHR$(13)
70   KEY 10, "GOTO 10"+CHR$(13)
75   GOTO 10000
80   CLS: LIST 90-311
90   F=C(1)*X(1)*(1-C(3)*X(1))+C(2)*X(2)*(1-C(3)*X(2))-X(3)
91   RETURN
110  F1(1,1) = C(1)-2*C(1)*C(3)*X(1)
111  RETURN
120  F1(1,2) = C(2)-2*C(2)*C(3)*X(2)
121  RETURN
130  F1(1,3) = -1
131  RETURN
210  F1(2,1) = X(1)-C(3)*X(1)^2
211  RETURN
220  F1(2,2) = X(2)-C(3)*X(2)^2
221  RETURN
230  F1(2,3) = -C(1)*X(1)^2-C(2)*X(2)^2
231  RETURN
309  'THE ABOVE LIST SHOWS THE FUNCTION AND ITS DERIVATIVES'
310  'CHOOSE ANOTHER UDK.  FOR ASSISTANCE, PRESS F9.'
330  M=3: N=3: O=0
331  RETURN
350  CLS:OPEN "DATA" FOR INPUT AS
     #1:INPUT#1,H,N,O,I,M:CLOSE:I=1:GOTO 365
355  OPEN "DATA" FOR INPUT AS #1:INPUT #1,H,N,O,I,M:CLOSE
360  I=I+1:CLS
365  IF I<=M THEN 382
370  GOTO 420
```

```
380  END
382  IF I=1 THEN PRINT "DERIVATIVES OF THE FUNCTION F WITH
     RESPECT TO THE VARIABLES.":PRINT
385  PRINT "STARTING AT LINE ";100+I*10;"AND INCREMENTING
     THE LINE NUMBER BY 1,":PRINT "WRITE A SUBROUTINE WHICH
     DEFINES   THE PARTIAL OF `F' WITH RESPECT TO
     X(";I;").":PRINT "CALL THIS PARTIAL F1(1,";I;").":PRINT
     "USE NO MORE THAN 10  LINES."
390  PRINT "THE LAST LINE OF THIS SUBROUTINE MUST BE
     `RETURN'."
395  PRINT "THEN PRESS F10 TO CONTINUE."
400  H=2
405  CLOSE:OPEN "DATA" FOR OUTPUT AS #1
410  WRITE #1,H,N,O,I,M
415  END
420  I=1:GOTO 435
425  OPEN "DATA" FOR INPUT AS #1:INPUT #1,H,N,O,I,M:CLOSE
430  I=I+1
435  CLS:IF I<=N THEN 452
440  OPEN "DATA" FOR OUTPUT AS #1:WRITE #1,H,N,O,I,M
445  PRINT "Now write the END line, using line number 309,
     as follows:"
448  PRINT  "309 END          <CR>,  then press F9 to
     continue"
450  END
452  IF I=1 THEN PRINT "DERIVATIVES OF THE FUNCTION F WITH
     RESPECT TO THE PARAMETERS.":PRINT
455  PRINT "STARTING AT LINE ";200+I*10;"AND INCREMENTING
     THE LINE NUMBER BY 1,":PRINT "WRITE A SUBROUTINE WHICH
     DEFINES THE PARTIAL OF `F' WITH RESPECT TO
     C(";I;").":PRINT "CALL THIS PARTIAL F1(2,";I;")."
457  PRINT "THE LAST LINE OF THIS SUBROUTINE MUST BE
     `RETURN'.":PRINT "USE NO MORE THAN 10 LINES."
460  PRINT "THEN PRESS F10 TO CONTINUE."
465  H=1
470  CLOSE:OPEN "DATA" FOR OUTPUT AS #1
475  WRITE #1,H,N,O,I,M
480  END
495  CLS:PRINT "STARTING AT LINE 90 AND INCREMENTING THE
     LINE NUMBER BY 1,":PRINT "ENTER A SUBROUTINE WHICH
     DEFINES THE FUNCTION `F'.":PRINT "USE NO MORE THAN 10
     LINES":PRINT "THE LAST LINE OF THIS SUBROUTINE MUST BE
     `RETURN'."
500  PRINT "FOR EACH LINE, AFTER TYPING THE LINE, PRESS
     <CR>"
505  PRINT :PRINT :PRINT "EXAMPLE: IF YOUR FUNCTION IS
     X(2)=C(2)+C(1)X(1);"
510  PRINT :PRINT "90 F=C(2)+C(1)*X(1)-X(2)          <CR>"
515  PRINT :PRINT "91 RETURN       <CR>"
520  PRINT :PRINT :PRINT "TO COMPLETE THE OPERATION, PRESS
     F10."
525  PRINT :PRINT
```

```
530  H=3
535  OPEN "DATA" FOR OUTPUT AS #1
540  WRITE #1,H,N,O,I,M
545  END
565  CLS:ON ERROR GOTO 1435
566  PRINT "THIS IS LEAST-SQUARES PROGRAM 'FIT'.  YOU MAY
     USE"
568  PRINT "UP TO 5 VARIABLES AND UP TO 10
     PARAMETERS.":PRINT
569  PRINT "THERE IS NO LIMIT ON THE NUMBER OF
     CONSTANTS.":PRINT
570  INPUT "HOW MANY VARIABLES";M
575  INPUT "HOW MANY PARAMETERS";N
580  INPUT "HOW MANY CONSTANTS";O
585  ON ERROR GOTO 1435
590  ERASE X
595  ON ERROR GOTO 1440
600  ERASE C
605  ON ERROR GOTO 1445
610  ERASE B
615  DIM X(M),C(N):IF O>0 THEN DIM B(O)
620  PRINT
625  PRINT "THE VARIABLES WILL BE CALLED:"
630  FOR I=1 TO M
635     PRINT "  X(";I;")";SPC(5);
640  NEXT
645  PRINT
650  PRINT "THE PARAMETERS WILL BE CALLED:"
655  FOR I=1 TO N
660     PRINT "  C(";I;")";SPC(5);
665  NEXT
667  PRINT
670  IF O=0 THEN 698
680  PRINT "THE CONSTANTS WILL BE CALLED:"
685  FOR I=1 TO O
690     PRINT "  B(";I;")";SPC(5);
695  NEXT
698  PRINT :PRINT
700  I=0
705  OPEN "DATA" FOR OUTPUT AS #1
710  WRITE #1,H,N,O,I,M
720  CLOSE #1: GOTO 495
730  CLS
735  INPUT "HOW MANY DATA SETS";P
740  CLS
745  ON ERROR GOTO 1450
750  ERASE W
755  ON ERROR GOTO 1455
760  ERASE X1
765  DIM W(P,M),X1(P,M)
780  FOR I=1 TO P
785     FOR J=1 TO M
```

```
790         PRINT "SET NUMBER ";I,"X(";J;")=";
795         INPUT X1(I,J)
800         PRINT TAB(30): INPUT "STANDARD DEVIATION=";W(I,J)
805         W(I,J)=1/W(I,J)^2
810      NEXT
815      CLS
820   NEXT
835   CLS: PRINT "SET" TAB(8) "X(ODD)" TAB(22) "ST.DEV."
      TAB(48) "X(EVEN)" TAB(62) "ST.DEV."
850   FOR I=1 TO P
852      PRINT: PRINT
855      FOR J=1 TO M
858         T=80*((J+1)/2-INT((J+1)/2)): IF J=1 THEN PRINT I;
860         PRINT
            TAB(8+T);CSNG(X1(I,J));TAB(22+T);(1/SQR(W(I,J)));
865      NEXT
870      IF I/5-INT(I/5)=0 AND I<P THEN GOTO 872 ELSE GOTO
         875
872      PRINT: PRINT: PRINT "PRESS F5 TO CONTINUE.": STOP
875   NEXT
880   PRINT: PRINT: PRINT "PRESS F5 TO CONTINUE.": STOP
885   IF CHOICE=6 THEN GOTO 955 ELSE GOTO 1425
890   CLS
895   INPUT "ENTER SUBSCRIPT NUMBER OF DATA SET TO BE
      DELETED";I
900   P=P-1
905   IF I=P+1 THEN 945
910   FOR J=I TO P
915      FOR K=1 TO M
920         X1(J,K)=X1(J+1,K)
925         W(J,K)=W(J+1,K)
930      NEXT
935   NEXT
945   GOTO 835
950   END
955   CLS:PRINT "LEAST SQUARES CALCULATION.":PRINT
956   PRINT "A METHOD OF SUCCESSIVE APPROXIMATIONS IS USED."
957   PRINT "FIRST, ENTER A SET OF STARTING PARAMETERS.
      THESE SHOULD"
958   PRINT "BE AS ACCURATE AS POSSIBLE WITHOUT LEAST
      SQUARES.":PRINT
960   FOR I=1 TO N
965      PRINT "STARTING VALUE OF C(";I;")=";
970      INPUT C(I)
975   NEXT
985   GOTO 1310
990   CLS
995   P=P+1
1000  FOR I=1 TO M
1005     PRINT "SET NUMBER ";P,"X(";I;")=";
1010     INPUT X1(P,I)
1015     PRINT TAB(30): INPUT "STANDARD DEVIATION= ";W(P,I)
```

```
1020    W(P,I)=1/W(P,I)^2
1025 NEXT
1030 GOTO 835
1040 END
1045 INPUT "NUMBER OF CYCLES";Z4
1050 FOR Z5=1 TO Z4
1055    ON ERROR GOTO 1460
1060    ERASE A,R
1065    DIM A(N,N),R(N)
1070    A=0
1075    R=0
1078    ZIP=0
1080    FOR Q=1 TO P
1085       FOR Q1=1 TO M
1090          X(Q1)=X1(Q,Q1)
1095       NEXT
1100       GOSUB 90
1105       FOR Q2=1 TO M
1110          ON Q2 GOSUB 110,120,130,140,150
1115       NEXT
1120       FOR Q3=1 TO N
1125          ON Q3 GOSUB
              210,220,230,240,250,260,270,280,290,300
1130       NEXT
1135       L=0
1140       FOR K=1 TO M
1145          L=L+F1(1,K)^2/W(Q,K)
1150       NEXT
1152       ZIP = ZIP + F*F/L
1155       FOR I=1 TO N
1160          FOR J=1 TO N
1165             A(I,J)=A(I,J)+F1(2,I)*F1(2,J)/L
1175          NEXT
1180          R(I)=R(I)+F1(2,I)*F/L
1185       NEXT
1190    NEXT
1195    GOTO 1470
1200    ON ERROR GOTO 1465
1205    ERASE C1
1210    DIM C1(N)
1215    FOR I=1 TO N
1220       FOR J=1 TO N
1225          C1(I)=C1(I)+A2(I,J)*R(J)
1230       NEXT
1235       C(I)=C(I)-C1(I)
1240    NEXT
1245    PRINT:PRINT "THE NEW VALUES OF THE PARAMETERS
        ARE:":PRINT
1250    FOR I=1 TO N
1255       PRINT "
           C(";I;")=";CSNG(C(I)),"STD=";SQR(A2(I,I))
1260    NEXT
```

```
1262    PRINT "      LEAST SQUARES SUM = ";ZIP
1265    PRINT :PRINT
1295 NEXT
1296 PRINT CHR$(7):INPUT"MORE CYCLES? (YES=1, NO=0)";CYCLES
1298 IF CYCLES=1 THEN GOTO 1045
1299 GOSUB 7000
1300 PRINT: PRINT:PRINT "CHOOSE ANOTHER UDK"
1303 PRINT:PRINT "FOR ASSISTANCE, PRESS F9."
1305 END
1310 PRINT:IF O=0 THEN 1335
1311 PRINT "NOW ENTER THE CONSTANTS B(o).": PRINT
1315 FOR I=1 TO O
1320    PRINT "INPUT CONSTANT VALUE OF B(";I;")";
1325    INPUT B(I)
1330 NEXT.
1335 CLS: PRINT "THE CALCULATION WILL NOW BEGIN.  IT MAY
     TAKE A FEW SECONDS.":PRINT
1337 PRINT "FOR STARTERS, CHOOSE 2 CYCLES OF SUCCESSIVE
     APPROXIMATIONS":PRINT:PRINT
1340 GOTO 1045
1350 CLS:LPRINT :PRINT
1355 FOR J=1 TO N
1360    LPRINT "C(";J;")=";CSNG(C(J));" +/-
        ";CSNG(SQR(A2(J,J)))
1361 NEXT
1362 FOR I=1 TO O
1363    LPRINT "B(";I")=";CSNG(B(I))
1365 NEXT
1370 LPRINT
1373 LPRINT "SET";TAB(9);"F";TAB(24);"X(ODD)"
     TAB(38);"SIGMA";TAB(54);"X(EVEN)";TAB(68);"SIGMA"
1375 FOR J=1 TO P:FOR I=1 TO M
1377       X(I)=X1(J,I)
1380    NEXT
1385    GOSUB 90
1400    LPRINT J;TAB(8);CSNG(F);:FOR I=1 TO M-1 STEP
           2:LPRINTTAB(24);CSNG(X1(J,I));TAB(38); 1/SQR(W
           (J,I));TAB(54);CSNG(X1
           (J,I+1));TAB(68);1/SQR(W(J,I+1)):NEXT
1405    IF I=M THEN LPRINT TAB(24);CSNG(X1(J,I));
        TAB(38);1/SQR(W(J,I))
1410 NEXT
1411 LPRINT:LPRINT "COVARIANCES BETWEEN:":LPRINT
     "C(I)","C(J)","D(I,J)"
1412 FOR I=1 TO N:FOR J=1 TO N:LPRINT
          "C(";I;")","C(";J;")",CSNG(A2(I,J)):NEXT :NEXT
1415 PRINT CHR$(7);"CHOOSE ANOTHER UDK"
1418 PRINT:PRINT "FOR ASSISTANCE, PRESS F9."
1419 LPRINT "[ERROR OF FIT]/[EXPTL ERROR] =
     ";SQR(ZIP/(P - N))
1420 LLIST 90-100
1421 ' line 1420 returns system to command level
```

```
1422 CLS: OPEN "DATA" FOR INPUT AS #1: INPUT #1,H,N,O,I,M:
     CLOSE #1
1424 IF M=0 THEN GOSUB 330
1425 CLS:PRINT TAB(20);"1. ENTER DATA SETS":PRINT:PRINT
     TAB(20);"2. LIST DATA SETS":PRINT :PRINT TAB(20);"3.
     ADD DATA SETS":PRINT :PRINT TAB(20);"4. DELETE
     DATASETS":PRINT
1428 PRINT TAB(20); "5. SAVE DATA SETS AND LEAST SQUARES
     CALCULATION":PRINT :PRINT TAB(20); "6. LOAD DATA SETS
     FROM DISK AND LEAST SQUARES CALC.":PRINT
1429 PRINT TAB(20);"7. SAVE DATA SETS.":PRINT  TAB(25);"GO
     TO HELP SCREEN TO CHOOSE ANOTHER UDK":PRINT :PRINT
     TAB(20); "8. LOAD DATA SETS FROM DISK"
1430 INPUT"ENTER THE NUMBER OF YOUR CHOICE"; CHOICE:ON
     CHOICE GOTO 730,835,990,890,1431,2000,1433,2000
1431 L=1: GOTO 4000
1433 L=2: GOTO 4000
1435 IF ERR=5 THEN RESUME 595
1440 IF ERR=5 THEN RESUME 605
1445 IF ERR=5 THEN RESUME 615
1450 IF ERR=5 THEN RESUME 755
1455 IF ERR=5 THEN RESUME 765
1460 IF ERR=5 THEN RESUME 1065
1465 IF ERR=5 THEN RESUME 1210
1470 FOR I=1 TO N:FOR J=1 TO N
1480       A2(I,J)=1-ABS(SGN(I-J))
1490 NEXT :NEXT
1495 FOR I=1 TO N:FOR J=1 TO N:A1(I,J)=A(I,J):NEXT :NEXT
1500 FOR I=1 TO N-1
1510    IF A1(1,1)<>0 AND ABS(A1(I,I)/A1(1,1))>.000001,
        THEN 1540
1520    PRINT "VALUE OF A(";I;I;") TOO SMALL TO WORK WITH"
1530    STOP
1540    FOR J=I+1 TO N
1550       TX=A1(J,I)/A1(I,I)
1560       FOR K=1 TO N
1570          A1(J,K)=A1(J,K)-TX*A1(I,K)
1580          A2(J,K)=A2(J,K)-TX*A2(I,K)
1590 NEXT :NEXT :NEXT
1600 FOR I=N TO 1 STEP -1
1610    FOR K=1 TO N
1620       FOR J=I+1 TO N
1630          A2(I,K)=A2(I,K)-A1(I,J)*A2(J,K)
1640       NEXT
1650       A2(I,K)=A2(I,K)/A1(I,I)
1660 NEXT :NEXT
1670 GOTO 1200
1800 NEXT
1810 NEXT
1820 CLOSE #2: RETURN
2000 CLS
2010 PRINT "If you preserved your data in your own file,
```

```
     enter the filename using the same format."
2020 PRINT "If your data sets are in the default file
     DATASETS, just press <CR>."
2030 INPUT "Enter the filename";FILE$:IF FILE$="" THEN
     FILE$="DATASETS"
2075 ON ERROR GOTO 3000
2076 ERASE W
2077 ON ERROR GOTO 3010
2078 ERASE X1
2080 CLOSE:I=0:L=0
2090 OPEN FILE$ FOR INPUT AS #2
2100 INPUT #2,P
2105 DIM W(P,M),X1(P,M)
2110 FOR I = 1 TO P
2120    FOR J = 1 TO M
2130       INPUT #2, X1(I,J)
2140    NEXT
2150 NEXT
2160 FOR I = 1 TO P
2170    FOR J = 1 TO M
2180       INPUT #2, W(I,J)
2190    NEXT
2200 NEXT
2210 CLOSE #2: GOTO 835
3000 IF ERR=5 THEN RESUME 2077
3010 IF ERR=5 THEN RESUME 2080
4000 CLS:PRINT "Unless you specify a filename, data will be
     saved in the file DATASETS, which":PRINT "will result
     in their being erased the next time new data are
     entered.":PRINT
4001 PRINT "If you wish to preserve your data more
     permanently, specify a filename.":PRINT "Use your
     initials (3 max) and the date, e.g. WVS2-28-85.":PRINT
     "Note the use of hyphens and NO SPACES."
4002 PRINT:PRINT  "To use DATASETS, just press <CR>."
4003 INPUT "Enter your filename";FILE$:IF FILE$="" THEN
     FILE$="DATASETS"
4005 OPEN FILE$ FOR OUTPUT AS #2
4010 WRITE #2,P
4020 FOR I = 1 TO P
4030    FOR J = 1 TO M
4040       WRITE #2, X1(I,J)
4050    NEXT
4060 NEXT
4070 FOR I = 1 TO P
4080    FOR J = 1 TO M
4090       WRITE #2, W(I,J)
4100    NEXT
4110 NEXT
4120 CLOSE #2: CLS: ON L GOTO 955,10000
4130 END
7000 FOR I=1 TO N
```

```
7010     FOR J=1 TO N
7020        PRINT "COVARIANCE BETWEEN C(";I;") AND C(";J;")
            IS ";CSNG(A2(I,J))
7030     NEXT
7040 NEXT
7050 RETURN
8000 CLS: PRINT "PRE-PROGRAMMED FUNCTIONS.    To load, type
     MERGE ";CHR$(34);"EJ";CHR$(34);" [J=1,2,..].":PRINT
     "Use QUOTES as shown.  Press <CR>.":PRINT
8020 PRINT "E1      X(2) = C(1)*X(1) + C(2)"
8030 PRINT "E2      X(2) = C(1) + C(2)*X(1) + C(3)*X(1)*X(1)"
8040 PRINT "E3      ln [B(1)-X(2)] = C(1) + C(2)*X(1)"
8050 PRINT "E4      ln [C(3)-X(2)] = C(1) + C(2)*X(1)"
8060 PRINT "E5      X(2) = C(1)*X(1)"
8065 PRINT "E6      X(3) = C(1)*X(1) + C(2)*X(1)*X(1) +
     C(3)*X(2)"
8070 PRINT "E7      GOZ = C(1)*X(1)+C(2)*X(2)+C(3)* X(3)+C(4
     )*X(4)"
8071 PRINT "        X(5) = GOZ/(1+C(5)*GOZ)"
8073 PRINT "E8      X(2) = C(1)*X(1)/(1+C(2)*X(1)) +
     C(3)*X(1)^2 "
8075 PRINT "E9      X(2) = C(1)*X(1)/(1+C(2)*X(1)) +
     C(3)*X(1)^2 + C(4)*X(1)"
8077 PRINT "E10     Cg Correction Function (3 parameters)"
8080 PRINT "E11     Modified Cg Correction Function (2
     parameters)"
8085 PRINT "E12     Modified Cg Correction Function (1
     parameter)"
8086 PRINT "E14     CALCULATION OF GAMMA AND MU"
8087 PRINT "E15     X(2) = C(1)*X(1)+C(2)*X(1)^2"
8088 PRINT "E16     X(3) =
     C(1)*X(1)*(1-C(3)*X(1))+C(2)*X(2)*(1-C(3)*X(2))"
8190 PRINT:PRINT "After disk activity stops, press F2 to RUN
     the merged program."
8200 DELETE 90-309
10000 CLS: PRINT  "F1    DISPLAY 'F' AND THE PARTIAL
      DERIVATIVES.":PRINT
10010 PRINT "F2    RUN PROGRAM AND INITIALIZE":PRINT :PRINT
      "F3    ENTER THE FUNCTION F AND ITS
      DERIVATIVES.":PRINT
10015 PRINT "F4    LOAD PRE-PROGRAMMED FUNCTIONS.":PRINT
10020 PRINT "F5    CONTINUE.":PRINT
10040 PRINT "F6    DATA ENTRY, DISPLAY, AND DELETION.":PRINT
10050 PRINT "F7    LEAST SQUARES CALCULATION.":PRINT
10060 PRINT "F8    PRINT RESULTS.":PRINT
10070 PRINT "F9    HELP SCREEN.":PRINT^ZNT "F7    LEAST
      SQUARES CALCULATION.":PRINT
```

B. AMBIENT TEMPERATURE PREPARATION OF TiS_2

The following procedures were performed for preparing TiS_2 from $TiCl_4$ and Li_2S in THF at ambient temperature followed by crystal growth with sulfur transport at high temperature.

REAGENTS:

titanium tetrachloride	(Alfa-Ventron)
lithium sulfide	(Alfa-Ventron)
tetrahydrofuran	(Aldrich)
pyridine	(Aldrich)
sulfur	(Alfa-Ventron)

1. A solution of 10 g of $TiCl_4$ in 400 mL of THF was made up in a glove-box.
2. While stirring the solution at room temperature 4.86 g of Li_2S was added slowly. The solution darkened.
3. The reaction was practically complete in 1 h, but was allowed to proceed for several hours.
4. The resulting dark-brown solid was filtered and washed with 50 mL of THF. The product weighed 38% more than stoichiometric TiS_2. This is more likely $TiS_2 \cdot THF$.
5. The product was soaked in excess pyridine (to replace the THF) for one week.
6. The pyridine was removed from the product by heating at 90 °C under vacuum for two days.
7. The product was sealed in a Vycor tube with a small amount of sulfur and heated to a temperature of 600 °C for four days with slow cooling to ambient temperature.

C. CURVE SMOOTHING

Curve smoothing is the replacement of a curve, or of a sequence of points by another that is in some sense more regular, and yet whose ordinates, for any abscissa, are changed as little as possible. The irregularities in a sequence of points may be due to errors in measurement. If theory requires the theoretically correct points to lie on a given curve, one may apply some method of curve fitting, e.g., least-squares. If not (as in the case of a spectrum), one may arbitrarily select a simple function, possibly a polynomial, and fit it by least-squares. If the purpose is merely to obtain a smooth graph, this may be drawn visually.

REFERENCES

1. Janz, G J. and Tomkins, R. P. T., ***Nonaqueous Electrolytes Handbook***, Academic Press, New York, Vol. I, 1972; Vol. II, 1973.

2. Coetzee, J. F. and Ritchie, C. D., Eds., ***Solute-Solvent Interactions***, Marcel Dekker, New, York, Vol. I, 1969; Vol. II, 1976.

3. Covington, A. K. and Dickinson, T., Eds., ***Physical Chemistry of Organic Solvent Systems***, Plenum Press, New York, 1973.

4. Kolthoff, I. M. and Elving, P. J., Eds., ***Treatise on Analytical Chemistry***, Part I, Vol 1, Chap. 12, and Part I, Vol. 2, Chap. 19, 2nd ed., Wiley-Interscience, New York, 1978-1979.

5. Popovych, O. and Tomkins, R. P. T., ***Nonaqueous Solution Chemistry***, Wiley-Interscience, New York, 1981.

6. Mann, C. K. and Barnes, K. K., ***Electrochemical Reactions in Nonaqueous Systems***, Marcel Dekker, New York, 1970.

7. Riddick, J. A. and Bunger, W. B., ***Techniques of Chemistry***, Vol. II, ***Organic Solvents***, (A. Weissberger, series Ed.), 3rd ed., Wiley-Interscience, New York, 1970.

8. Lagowski, J. J., Ed., ***The Chemistry of Non-Aqueous Solvents***, Vols. I-V, Academic Press, New York, 1966-1978.

9. Gordon, J. E., ***The Organic Chemistry of Electrolyte Solutions***, Wiley, New York, 1975.

10. Mamantov, G., Ed., ***Characterization of Solutes in Nonaqueous Solvents***, Plenum Press, New York, 1978.

11. Selim, R. and Bro, P., *J. Electrochem. Soc.*, 121, 1467, 1974.

12. Rauh, R. D. and Brummer, S. B., *Electrochim. Acta.*, 22, 75, 1977.

13. Jorne, J. and Tobias, C. W., *J. Appl. Electrochem.*, 5, 279, 1975.

14. Koch, V. R. and Brummer, S. B., *Electrochim. Acta.*, 23, 55, 1978.

15. Koch, V.R. and Brummer, S.B., *J. Electrochem. Soc.*, 125, 1375, 1978.

16. Goldman, J.L., Mank, R.M., Young, J.H., and Koch, V.R., *J. Electrochem. Soc.*, 127, 1461, 1980.

17. Koch, V.R. and Young, J.H., *J. Electrochem. Soc.*, 125, 1371, 1978.

18. Stull, D.R., Westrum, E.F., Jr., and Sinke, G.C., ***The Chemical Thermodynamics of Organic Compounds***, Wiley, New York, 1969.

19. Rossini, F.D., Wagman, D.D., Evans, W.H., Levine, S., and Jaffe, I., ***Selected Values of Chemical Thermodynamic Properties***, National Bureau of Standards Circular 500, Part I, U.S. Government Printing Office, Washington, 1952.

20. Kendrinskii, I.A., Morosov, S.V., Sukhova, G.I., and Sukhova, L.A., *Sov. Electrochém.*, 12, 1094, 1977.

21. Peled, E., in ***Lithium Batteries***, Gabano, J-P., Ed., Academic Press, New York, 1983.

22. Abraham, K.M. and Brummer, S.B., in ***Lithium Batteries***, Gabano, J-P., Ed., Academic Press, New York, 1983.

23. Besenhard, J.O. and Eichinger, G., *J. Electroanal. Chem.*, 60, 1, 1976.

24. Abraham, K.M., *J. Power Sources*, 7, 13, 1982.

25. Koch, V.R., *J. Power Sources*, 6, 357, 1981.

26. Brummer, S.B., ***Proceedings of the Workshop on Lithium Nonaqueous Battery Electrochemistry***, Vol. 80-7, pp. 130-142, The Electrochemical Society, Pennington NJ, 1980.

27. Brummer, S.B., Koch, V.R., and Rauh, R.D., in ***Materials for Advanced Batteries***, murphy, D.W., Broadhead, J., and Steele, B.C.H., Eds., Plenum Press, New York, 1980.

28. Dampier, F.W. and Brummer, S.B., *Electrochim. Acta.*, 22, 1339, 1977.

29. Brummer, S.B., Dampier, F.W., Koch, V.R., Rauh, R.D., Reise, T.F. and Young, J.H., *Final Report by EIC Laboratories, Inc., on NSF-RANN grant AER75-03779*, 1978.

30. Koch, V.R., *J. Electrochem. Soc.*, 126, 181, 1979.

31. Koch, V.R., *U.S. Patent*, 4,118,550, (1978).

32. Koch, V.R., and Young, J.H., *Science*, 204, 499, 1979.

33. Shen, D., Yen, S.P.S., Khanna, S.K. and Somoano, R.B., ***Proceedings of The Symposium on Lithium Batteries***, Ventkatasetty, H.V., Ed., The Electrochemical Society, Pennington, NJ, 1981.

34. Newman, G.H., Francis, R.W., Gaines, L.H. and Rao, B.M.L., *J. Electrochem. Soc.*, 127, 2025, 1980.

35. Klemman, L.P. and Newman, G.H., ***Proceedings of the Symposium on Lithium Batteries***, Venkatasetty, H.V., Ed., The Electrochemical Society, Pennington, NJ, 1981.

36. Koch, V.R., Goldman, J.L., Mattos, C.J. and Mulvaney, M., *J. Electrochem. Soc.*, 129, 1, 1982.

37. Yen, S.P.S., Shen, D., Vasquez, R.P., Grunthaner, F.J. and Somoano, R.B., *J. Electrochem. Soc.*, 128, 1434, 1981.

38. Koch, V.R., *J. Power Sources*, 9, 247, 1983.

39. ***Fluorochemical Acid Salt FC124***, Product Information Bulletin, 3M Corporation, 1979.

40. Horowitz, H.H., Haberman, J.I., Klemann, L.P., Newman, G.H., Stogryn, E.L. and Whitney, T.A., ***Proceedings of the Symposium on Lithium Batteries***, Ventkatasetty, H.V., Ed., The Electrochemical Society, Pennington, NJ, 1981.

41. Whittingham, M.S., *Prog. Solid State Chem.*, 12, 41, 1978.

42. Markowitz, M.M., Hawley, W.N., Boryta, D.A. and Harris, R.F., *J. Chem. Eng. Data*, 6, 325, 1961.

43. Blomgren, G.E., in ***Lithium Batteries***, Gabano, J-P., Ed., Academic Press, New York, 1983.

44. Jasinski, R., ***High Energy Batteries***, Plenum Press, New York, 1967.

45. Newman, G. H., ***Proceedings of the workshop on Lithium Nonaqueous Battery Electrochemistry***, p. 200, The Electrochemical Society, Pennington, NJ, 1980.

46. Klemann, L. P., and Newman, G. H., *J. Electrochem. Soc.*, 128, 13, 1981.

47. Klemann, L. P., Newman, G. H., Whitney, T. A., Stogryn, E. L., and Faracasiu, D., ***Proceedings of the Symposium on Lithium Batteries***, Ventkatasetty, H. V., Ed., The Electrochemical Society, Pennington, NJ, 1981.

48. Newman, G. H. and Klemann, L. P., ***Proceedings of the Symposium on Lithium Batteries***, Ventkatasetty, H. V., Ed., The Electrochemical Society, Pennington, NJ, 1981.

49. Klemann, L. P., Newman, G. H., and Stogryn, E. L., ***Proceedings of the 29th Power Sources Symposium***, 1980.

50. Greenwood, N. N. and Earnshaw, A., ***Chemistry of the Elements***, Pergammon Press, New York, 1984.

51. Johnson, J. W., Thompson, A. H., and Brody, J. F., ***Proceedings of the Symposium on Lithium Batteries***, Ventkatasetty, H. V., Ed., The Electrochemical Society, Pennington, NJ, 1981.

52. Johnson, J. W. and Whittingham, M. S., *J. Electrochem. Soc.* 127, 1653, 1980.

53. Johnson, J. W. and Thompson, A. H., *J. Electrochem. Soc.*, 128, 932, 1981.

54. Koch, V. R., Goldman, J. L., Mattos, C. J., and Mulvaney, M., *J. Electrochem. Soc.*, 129, 1, 1982.

55. Desjardins, C. D., Cadger, T. G., Salter, R. S., Donaldson, G., and Casey, E. J., *J. Electrochem. Soc.*, 132, 529, 1985.

56. Auborn, J. J. and Ciemiecki, K. T., ***Extended Abstracts of the Battery Division***, The Electrochemical Society, Fall Meeting 1983, Abstract No. 68.

57. Guzman, J., Garrido, L., and Riande, E., *Macromolecules*, 17, 2005, 1984.

58. Kronenberg, M.L., U.S. Patent No. 3,996,069 (1976).

59. Abraham, K.M., Foos, J.S. and Goldman, J.L., *J. Electrochem. Soc.*, 131, 2197, 1984.

60. Morrison, R.T. and Boyd, R.N., ***Organic Chemistry***, 3rd ed., Allyn and Bacon, New York, 1973, pp. 554.

61. Robertson, A., *Nature*, 162, 153, 1948; *Angew. Chemie*, 61, 344, 1949.

62. Furniss, B.S., Hannaford, A.J., Rogers, V., Smith, P.W.G. and Tatchell, A.R., ***Vogel's Textbook of Practical Organic Chemistry***, Longman Press, New York, 1978.

63. Manly, D.G., U.S. Patent No. 3,021,342 (1962).

64. Perrin, D.D., Armarego, W.L.F. and Perrin, D.R., ***Purification of Laboratory Chemicals***, 2nd ed., Pergammon Press, 1980.

65. Whittingham, M.S., *Prog. Sol. St. Chem.*, 12, 41, 1978.

66. Willard, H.H., Merritt, L.L., Dean, J.A. and Settle, F.A., ***Instrumental Methods of Analysis***, 6th ed., Wadsworth, Belmont, CA, 1981.

67. Pearson, B.D. and Ollerenshaw, J.E., *Chemistry and Industry*, 390, 1966.

68. Keyworth, D.A., *Talanta*, 8, 461, 1961.

69. Forbes, J.W., *Anal. Chem.*, 34, 1125, 1962.

70. Abrams, S.T. and Smith, V.N., *Anal. Chem.*, 34, 1129, 1962.

71. Burfield, D.R., Lee, K-H. and Smithers, R.H., *J. Organic Chem.*, 42, 18, 1977.

72. Tobishima, S. and Yamaji, A., *Electrochim. Acta.*, 28, 1067, 1983.

73. Hinton, J.F. and Amis, E.S., *Chem. Rev.*, 67, 367, 1967.

74. Lindman, B. and Forsen, S., in ***NMR and the Periodic Table***, Harris, R.K., and Mann, B.E., Eds., Academic Press, New York, 1978.

75. Braunstein, J. and Robbins, G.D., *J. Chem. Ed.*, 48, 53, 1971.

76. Parker, C.H., *J. Am. Chem. Soc.*, 45, 1366, 1923.

77. Jones, G. and Bollinger, G.M., *J. Am. Chem. Soc.*, 51, 2407, 1929.

78. Prue, J.E., *J. Phys. Chem.*, 67, 1152, 1963.

79. Ives, D.J.G. and Janz, G.J., ***Reference Electrodes: Theory and Practice***, Academic Press, New York, 1961.

80. Jones, G. and Bradshaw, B.C., *J. Am. Chem. Soc.*, 55, 1780, 1933.

81. Juhaz, E. and Marsh, K.N., *Pure Appl. Chem.*, 53, 1841, 1981.

82. Marsh, K.N., *J. Soln. Chem.*, 9, 10, 1980.

83. Justice, J-C., *J. Chim. Phys. Phys. Chim. Biol.*, 65, 353, 1968.

84. Robinson, R.A. and Stokes, R.H., ***Electrolyte Solutions***, Butterworths, London, 1959.

85. Stokes, R.H., *J. Phys. Chem.*, 65, 1277, 1961.

86. Bickson, R.L. and Smith, S.G., *J. Phys. Chem.*, 68, 1875, 1961.

87. Popov, A.I., *Pure Appl. Chem.*, 41, 275, 1975.

88. Cahen, Y.M., Handy, P.R., Roach, E.T. and Popov, A.I., *J. Phys. Chem.*, 79, 80, 1975.

89. Maciel, G.E., Hancock, J.K., Lafferty, L.F., Mueller, P.A. and Musker, W.K., *Inorg. Chem.*, 5, 554, 1966.

90. Fuoss, R.M. and Accascina, F., ***Electrolytic Conductance***, Interscience, New York, 1959.

91. Onsager, L., *Z. Physik*, 27, 388, 1926.

92. Onsager, L., *Z. Physik*, 28, 277, 1927.

93. Fuoss, R.M., Onsager, L. and Skinner, J.F., *J. Phys. Chem.*, 69, 2581, 1965.

94. Pitts, E., *Proc. Roy. Soc.* 217A, 43, 1953.

95. Fuoss, R.M. and Hsia, L.L., *Proc. Nat. Acad. Sci.*, 57, 1550, 1967.

96. Justice, J-C., *Electrochim. Acta.*, 16, 701, 1971.

98. Yao, N-P. and Bennion, D.N., *UCLA Rep. 69-30, DA Contract No. DA-44-009-AMC-1661(T)*, 1969.

99. Yao, N-P. and Bennion, D.N., *J. Electrochem. Soc.*, 118, 1097, 1971.

100. Jagodzinski, P. and Petrucci, S., *J. Phys. Chem.*, 78, 917, 1974.

101. Wentworth, W.E., *J. Chem. Educ.*, 42, 96, 1965.

102. Deming, W.E., ***Statistical Adjustment of Data***, Wiley, New York, 1943.

103. Popov, A.I. and Skelly, N.E., *J. Am. Chem. Soc.*, 76, 5309, 1954.

104. Delsignore, M., Maaser, H.E. and Pettricci, S., *J. Phys. Chem.*, 88, 2405, 1984.

105. Whittingham, M.S., *Science*, 192, 1126, 1976.

106. Levy, F., Ed., ***Physics and Chemistry of Materials with Layered Structures***, vols. 1-6, Reidel, Amsterdam, 1978-1979.

107. Rudorff, W., *Angew. Chem.*, 71, 487, 1959.

108. Rudorff, W. and Sick, H.H., *Angew. Chem.*, 71, 127, 1959.

109. Rudorff, W. *Chimica*, 19, 489, 1965.

110. Whittingham, M.S., and Dines, M.B., *J. Electrochem. Soc.*, 124, 315, 1977.

111. Whittingham, M.S., *J. Chem. Soc. Chem. Comm.*, 328, 1974.

112. Winn, D.A., Shemilt, J.M. and Steele, B.C.H., *Mat. Res. Bull.*, 9, 1597, 1974.

113. Whittingham, M.S., *J. Electrochem. Soc.*, 123, 315, 1976.

114. Silbernagel, B.G. and Whittingham, M.S., in ***Solid Electrolytes***, van Gool, W., Ed., Academic Press, New York, 1977.

115. Gibson, J.G. and Sudworth, J.L., ***Specific Energies of Galvanic Reactions and Related Thermodynamic Data***, Chapman and Hall, New York, 1978.

116. Hansen, P., ***Physical Metallurgy***, Cambridge University Press, London, 1978.

117. Whittingham, M.S., U.S. Patent No. 4,007,005, 1976.

118. Thompson, A.H., Gamble, F.R. and Symon, C.R., *Mat. Res. Bull.*, 10, 368, 1975.

119. Ebelman, J., *J. Appl. Chim. Phys.*, 20, 390, 1967.

120. Chianelli, R.R. and Dines, M.B., *Inorg. Chem.*, 17, 2758, 1978.

121. Whittingham, M.S. and Gamble, F.R., *Mat. Res. Bull.*, 10, 368, 1975.

122. Winn, D.A., Shemilt, J.M. and Steele, B.C.H., *Mat. Res. Bull.*, 11, 550, 1976.

123. Brown, R.J. and Forsythe, J.B., ***The Crystal Structure of Solids***, Arnold Press, London, 1973.

124. Jolly, W.L., ***The Synthesis and Characterization of Inorganic Compounds***, Prentice Hall, 1970.

125. Stout, G.H. and Jensen, L.H., ***X-Ray Structure Determination***, MacMillan, New York, 1968.

126. Lipson, H. and Cochran, W., ***The Determination of Crystal Structures***, Bell, London, 1966.

127. Wykoff, R.W.G., ***Crystal Structures***, Interscience, New York.

128. Wilson, A.J.C., Ed., ***Structure Reports***, Oosthoek, Utrecht.

129. Thompson, A.H., Symon, C.R. and Gamble, F.R., *Mat. Res. Bull.*, 10, 915, 1975.

130. Benard, J. and Jeannin, Y., *Adv. in Chem.*, 39, 191, 1963.

131. Chianelli, R.R., Scanlon, J.C. and Thompson, A.H., *Mat. Res. Bull.*, 10, 1379, 1979.

132. Whittingham, M.S. and Jacobsen, T. Eds., ***Intercalation Chemistry***, Academic Press, New York, 1982.

133. Vaccaro, A.J., Palanisamy, T., Kerr, R.L. and Maloy, J.T., *J. Electrochem. Soc.*, 129, 677, 1982.

134. Vaccaro, A.J., Palanisamy, T., Kerr, R.L. and Maloy, J.T., *J. Electrochem. Soc.*, 129, 682, 1982.

135. Stickney, J.L., Rosasco, S.D., Schardt, B.C., Solomon, T., Hubbard, A.T. and Parkinson, B.A., *Surface Science*, 136, 15, 1984.

136. Dalard, F., Deroo, D. and Mauger, R., *J. Power Sources*, 9, 321, 1983.

137. Frazer, E.J. and Phang, S., *J. Power Sources*, 10, 23, 1983.

138. Thompson, A.H., *J. Electrochem. Soc.* 126, 608, 1979.

139. Thompson, A.H., *Phys. Rev. Lett.*, 40, 1511, 1978.

140. Thompson, A.H., in ***Fast Ion Transport in Solids***, Proc. Internat. Conf. Lake Geneva, Wisc., Vashistra, P., et al., Eds., 1979.

141. Bockris, J.O'M. and Reddy, A.K.N., ***Modern Electrochemistry***, Plenum Press, New York, 1970.

142. Silbernagel, B.G. and Whittingham, M.S., *J. Chem. Phys.*, 64, 3670, 1976.

143. Murphy, D.W., Disalvo, F.J., Hull, G.W. and Wasczcak, J.W., *Inorg. Chem.*, 15, 17, 1976.

144. Whittingham, M.S., in ***Progress in Solid-State Chemistry***, vol.12, Rosenblatt, G.M. and Worrell, W.L., Eds., 1978.

145. Basu, S. and Worrell, W.L., in ***Fast Ion Transport in Solids***, Proc. Internat. Conf. Lake Geneva, Wisc., Vashistra, P. et al., Eds., 1979.

146. Silbernagel, B.G., *Solid State Comm.*, 17, 361, 1975.

147. Atlung, S., West, K. and Jacobsen, T., *J. Electrochem. Soc.*, 126, 1311, 1979.

148. Jacobsen, T., West, K. and Atlung, S., *J. Electrochim. Acta.*, 27, 1007, 1982.

149. Dunnett, J.S., Geary, D. and Menzies, I.A., *Electrochim. Acta.*, 25, 729, 1980.

150. Jasinski, R.J., ***High Energy Batteries***, Plenum Press, New York, 1967.

151. Popov, A.I. and Maxey, B.W., *J. Am. Chem. Soc.*, 89, 2230, 1967.

152. Maxey, B.W. and Popov, A.I., *J. Am. Chem. Soc.*, 91, 20, 1969.

153. Edgell, W.F., Watts, A.T., Lyford, J. and Risen, W.M., *J. Am. Chem. Soc.*, 88, 1815, 1966.